

Aus der
Klinik für Allgemeine-, Viszerale- und Transplantationschirurgie
Klinik der Ludwig-Maximilians-Universität München

Direktor: Prof. Dr. med. Jens Werner

**Deciphering the roles of LGR6 in WNT and EMT signaling
in pancreatic cancer**

Dissertation
zum Erwerb des Doktorgrades der Medizin
an der Medizinischen Fakultät der
Ludwig – Maximilians – Universität zu München

vorgelegt von
Jing Wang
aus Changzhi, Shanxi, China

2019

Mit Genehmigung der Medizinischen Fakultät
der Universität München

Berichterstatter: Prof. Dr. med. Jens Werner

Mitberichterstatter: Prof. Dr. Stefan Böck
Prof. Dr. Thomas Knösel

Mitbetreuung durch den
promovierten Mitarbeiter: Prof. Dr. Alexandr V. Bazhin
Dr. med. Matthias Ilmer

Dekan: Prof. Dr. med. dent. Reinhard HICKEL

Tag der mündlichen Prüfung: 27.06.2019



LUDWIG-
MAXIMILIANS-
UNIVERSITÄT
MÜNCHEN

Dean's Office
Medical Faculty



Affidavit

Wang Jing

Surname, first name

Street

Zip code, town

Country

I hereby declare, that the submitted thesis entitled
Deciphering the roles of LGR6 in WNT and EMT signaling in pancreatic cancer

is my own work. I have only used the sources indicated and have not made unauthorised use of services of a third party. Where the work of others has been quoted or reproduced, the source is always given.

I further declare that the submitted thesis or parts thereof have not been presented as part of an examination degree to any other university.

Munich, 27.06.2019
Place, date

Jing Wang
Signature doctoral candidate

I. Table of Contents

I. Table of Contents	1
II. List of Abbreviations	3
1. Introduction	6
1.1 Pancreatic cancer	6
1.2 The WNT signaling pathway	10
1.3 The canonical WNT signal pathway	11
1.4 WNT proteins	14
1.5 WNT receptors	14
1.5.1 Frizzled and LRP5/6 receptors	14
1.5.2 Non-conventional receptors	16
1.6 Secreted agonists in WNT signaling	16
1.7 Secreted extracellular antagonist	16
1.8 R-spondin proteins	17
1.8.1 RSPO structural features	17
1.8.2 RSPO functions during embryogenesis	18
1.8.3 Mechanisms of RSPO-mediated enhancement of WNT signaling	19
1.9 LGR receptors	19
1.9.1 LGR receptor structures	20
1.9.2 LGR4/5/6 receptor functions	20
1.10 Epithelial-mesenchymal transition (EMT) and WNT signaling	22
1.11 WNT signaling and disease	23
1.12 Aim of the study	24
2. Materials and Methods	25
2.1 Materials	25
2.1.1 Consumables	25
2.1.2 Chemicals	26
2.1.3 Antibodies	28
2.1.4 Recombinant Proteins and inhibitors	29
2.1.5 Commercial Assays	30
2.1.6 Primers	30
2.1.7 Apparatus	31
2.1.8 Software	32
2.1.9 Buffers and Solutions	33
2.2 Methods	37
2.2.1 Cell culture	37
2.2.2 Gemcitabine-resistance cells Culture	38
2.2.3 GSEA	38
2.2.4 RNA extraction, reverse transcription and qPCR	38
2.2.4.1 RNA isolation	38

2.2.4.2 cDNA production.....	39
2.2.4.3 Real time PCR.....	40
2.2.5 Agarose Gel Electrophoresis	41
2.2.6 Western blot and Co-IP	41
2.2.6.1 Western Bolt.....	41
2.2.6.2 Co-IP.....	42
2.2.7 Sphere-formation assay.....	43
2.2.8 Colony-formation assay.....	43
2.2.9 siRNA transfection.....	44
2.2.10 Immunofluorescence staining.....	45
2.2.11 Flow cytometry.....	45
2.2.12 Cell viability assay.....	46
2.2.13 Statistical analysis.....	46
3. Results	47
3.1 Prediction of LGR6 as a WNT target gene.....	47
3.2 Activation of canonical WNT signaling mediates LGR6 expression ..	49
3.3 Inhibition of the WNT signal pathway decreases LGR6 expression ..	53
3.4 Prediction of LGR6 as an indicator of EMT	56
3.5 LGR6 expression varies in typical epithelial and mesenchymal PDAC cell Lines	58
3.6 LGR6 may participate in cell adhesion in epithelial PDAC cell lines ..	62
3.7 EMT induction changes LGR6 expression.....	65
3.8 LGR6 depletion correlates with reduced cancer stemness.....	68
3.9 LGR6 expression in gemcitabine-resistant PDAC cells.....	70
3.10 LGR6 expression is a poor prognostic marker in pancreatic cancer	76
4. Discussion	77
4.1 LGR6 is a novel WNT target gene in PDAC	77
4.2 LGR6 participates in cell adhesion and EMT in PDAC	79
4.3 LGR6 is involved in cancer stemness in PDAC.....	81
5. Conclusions and future directions.....	84
6. Summary.....	85
III. References	87
IV. Acknowledgment.....	97

II. List of Abbreviations

%	Percentage
°C	Degree Celsius
µg	Microgram
µl	Microliter
µm	Micrometer
APS	Ammonium persulfate
APC	Adenomatous polyposis coli
BSA	Bovine serum albumin
Ca ²⁺	Calcium
CAMKII	Calmodulin-dependent protein kinase II
CFA	Colony formation assay
CK1	Casein kinase1
CRD	Cysteine-rich domain
CSCs	Cancer stem cells
DAG	1,2 Diacylglycerol
DAPI	4',6-Diamidino-2-phenylindole
DKK	Dickkopf protein
DMSO	Dimethylsulfoxid
DVL	Disheveled
E-cadherin	Epithelial cadherin
ECD	Extracellular domain
ECL	Enhanced chemiluminescence
ECM	Extracellular matrix
EGF	Epidermal growth factor
EGFR	Epidermal growth factor receptor
EMT	Epithelial-mesenchymal transition

ES	Enrichment scores
ER	Endoplasmic reticulum
FACS	Fluorescence-activated cell sorting
FBS	Fetal bovine serum
FGF	Fibroblast growth factor
FSHR	Follicle-stimulating hormone receptor
FZD	Frizzled
GPCR	G protein-coupled receptor
GSEA	Gene set enrichment analysis
GSK-3 β	Glycogen synthase kinase-3 β
GR	Gemcitabine resistance
HGF	Hepatocyte growth factor
IF	Immunofluorescence
IP	Immunoprecipitation
IP3	Inositol 1,4,5-triphosphate
JNK	c-Jun-N-terminal kinase
LGR4/5/6	Leucine-rich repeats containing G protein-coupled receptor 4/5/6
LHR	Luteinizing hormone receptor
LRR	Leucine-rich repeats
min	Minute
ml	Milliliter
mm	Millimeter
MET	Mesenchymal–epithelial transition
MMTV	Mouse mammary tumor virus
MSigDB	Molecular Signature Database
N-cadherin	Neural cadherin
PBS	Phosphate-buffered saline

PCR	Polymerase chain reaction
PDAC	Pancreatic ductal adenocarcinoma
PFA	Paraformaldehyde
PKA	Protein kinase A
PKC	Protein kinase C
PLC	Phospholipase C
PSC	Pancreatic stellate cell
RNF43	Ring finger protein 43
RSPO	R-spondin
SDS	Sodium dodecyl sulfate
Ser	Serine
SFA	Sphere-formation assay
sFRP	Secreted frizzled related protein
TBS	Tris-buffered saline
TBST	Tris-buffered saline with Tween 20
TCF/LEF	T-cell factor / lymphoid enhancer factor
TCGA	The Cancer Genome Atlas
TGF β	Transforming growth factor β
Thr	Threonine
TSHR	Thyroid-stimulating hormone receptor
TSR-1	Thrombospondin type 1 repeat
UV	Ultraviolet
WB	Western blot
WIF-1	WNT inhibitory protein-1
WIF	WNT inhibitory factor domain
ZEB1	Zinc finger E-box-binding homeobox 1
ZNRF3	Zinc and ring finger 3

Deciphering the roles of LGR6 in WNT and EMT signaling in pancreatic cancer

1. Introduction

1.1 Pancreatic cancer

The pancreas is both an endocrine gland and a digestive organ. The endocrine islets consist of α - and β -cells with the former producing glucagon and the latter secreting insulin for glucose regulation. Other cell types include δ -cells which produce somatostatin, ϵ -cells which generate ghrelin, and γ [or PP]-cells for pancreatic polypeptide secretion [1]. The exocrine part contains acinar cells and ductal cells and the former produce bicarbonate and digestive enzymes including trypsinogen, lipase as well as amylase. The intralobular ducts accumulate the secretions, transport them first to the main pancreatic duct and then to the duodenum for digestion and absorption of carbohydrate, proteins, and lipids [2]. Besides, stromal components support the architecture of the pancreas including pancreatic stellate cells (PSC), inflammatory cells, acellular extracellular matrix (ECM) as well as nerves. In case of pancreatic cancer, desmoplasia even account for more than 50% of the tumor volume [3].

Pancreatic ductal adenocarcinomas (PDAC) is the most common epithelial malignancy of the pancreas with an extremely poor prognosis [4]. Geographically, the incidence and mortality are higher in developed countries compared to developing countries as shown in Figure 1. It is estimated that 367.000 new pancreatic cancer cases were diagnosed worldwide, while 359.000 people died from it in 2015 [5]. Currently, PDAC is the fourth most common cause for cancer-related death in developed countries with

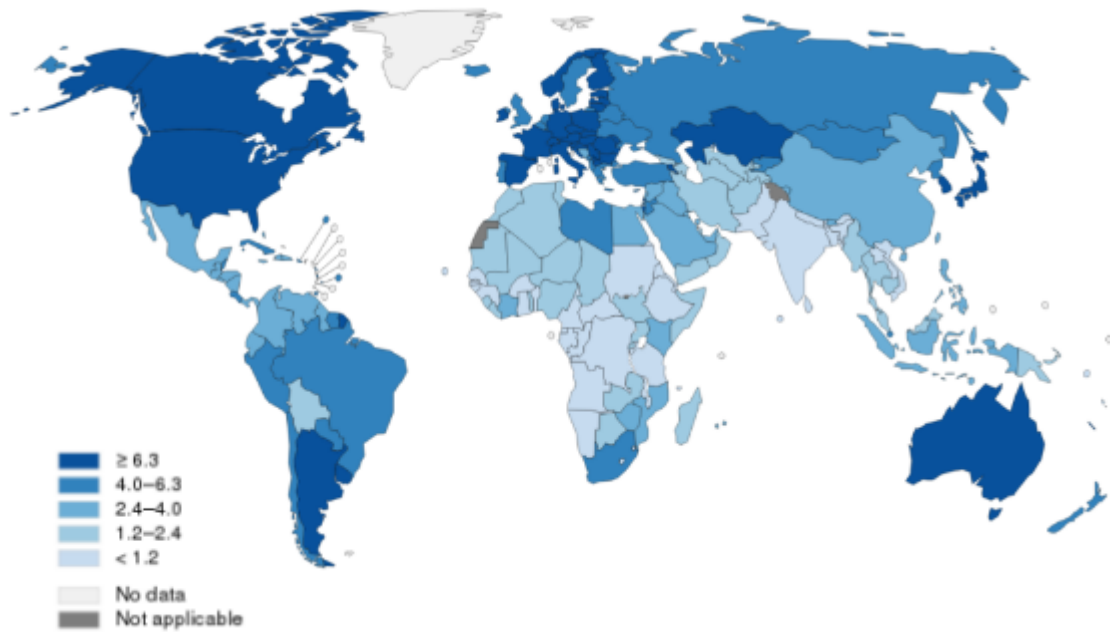
an overall 5-year survival rate of approximately 7% [6] and it is expected to become second over the next couple of decades because of an increasing incidence and limited treatment improvements [7].

Pancreatic cancer is usually diagnosed at late stages due to nonspecific symptoms as well as no sensitive and specific screening techniques or tumor markers [8]. PDAC is frequently seen with local invasive growth into nerve and vascular structures. Most patients were diagnosed at a rather late stage with only 15-20% of patients being eligible for surgery [9]. PDAC is complicated by early recurrence, metastasis, and resistance to chemotherapy and radiotherapy [10]. All the characteristics attribute PDAC to one of the most aggressive cancer types.

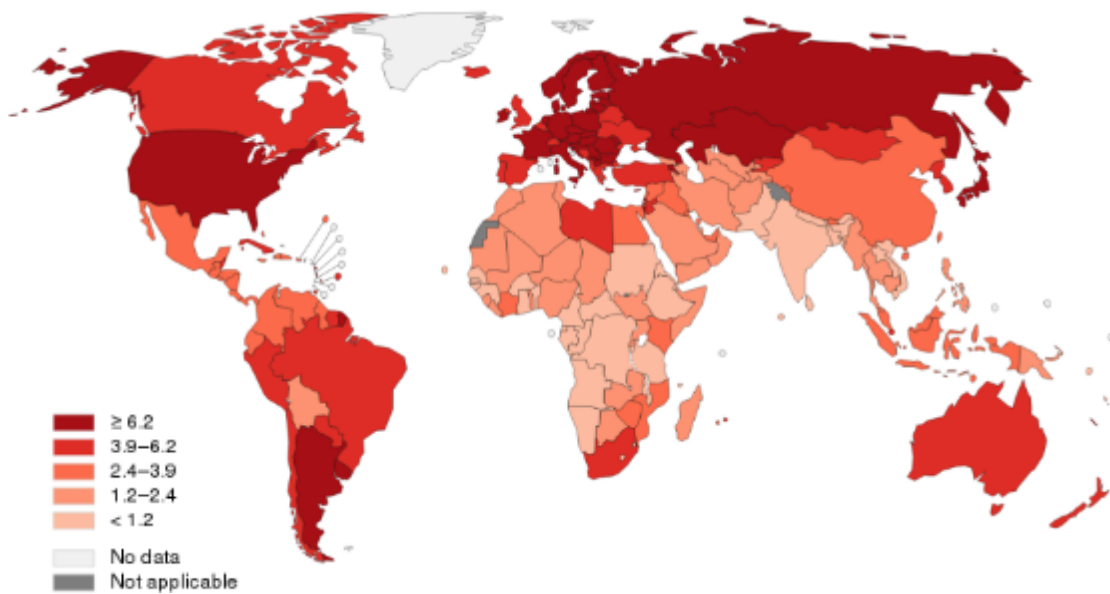
Although notable improvements have been achieved for other malignancies, the prognosis of PDAC remains poor. Risk factors include age, a determinant factor for pancreatic cancer with a peak incidence in the 7th and 8th decade of patients. Other risk factors include smoking, alcohol consumption, chronic pancreatitis, obesity, and low physical activity [4]. Besides, mutations in specific genes are associated with pancreatic carcinogenesis from intraepithelial neoplastic lesions to invasive carcinoma. The most common genes include *KRAS* of which activating mutations occur in more than 90% of cases, while inactivating mutations of *CDKN2A*, *TP53* as well as *SMAD4* are present in 50-80% of tumors [11]. In addition, multiple signaling molecules and aberrations contribute to the development of pancreatic cancer by impacting tumor cells as well as surrounding stromal cells. Signaling pathways activated by transforming growth factor (TGF- β) can regulate cell cycle progression [12], promote epithelial to mesenchymal transition (EMT) stimulating a more invasive phenotype [13], activate PSCs and induce subsequent PSCs-secreted collagen [14]. HEDGEHOG signaling ligand sonic hedgehog (Shh) is overexpressed in pancreatic cancer stem cells (CSCs) [15]. CSCs are cancer cells which possess the primary characteristics

self-renewal and differentiation, but also capabilities such as tumor recapitulation and propagation, therapy resistance, and metastasis formation [16]. The high level of Shh inhibits tumor cell apoptosis by phosphatidylinositol 3-kinase (PI3K) signaling activation as well as Bcl-2 and Bcl-XL stabilization [17]. Besides, Shh increases proliferation potentially by cell cycle regulators cyclin D1 and p21 [17]. HEDGEHOG signaling plays a significant role in stroma directly increasing desmoplasia deposition, which influences the efficiency of drug delivery, potentially even causing chemo-resistance [18, 19]. NOTCH signaling is primarily activated during embryogenesis, however, it is reactivated in some PDAC cases to promote pancreatic cancer pathogenesis [12]. Epidermal growth factor receptor (EGFR) family EGFR signaling may also be important in PDAC tumorigenesis.

Likewise, the canonical WNT signaling pathway plays a major role during pancreas development [20, 21]. Although aberrant WNT/ β -catenin signaling has been implicated in tumorigenesis in multiple organs [22-24], it is not commonly seen in PDAC [25, 26]. However, researchers have shown that an elevated β -catenin accumulation in some pancreatic adenocarcinomas and WNT signaling activation correlates with PDAC development [27, 28]. Rather than functioning independently in pancreatic carcinogenesis and maintenance, most signaling pathways are cross-linked, contributing to pancreatic cancer initiation and progression.



Incidence Age-standardized Rates (ASR) in pancreatic cancer



Mortality Age-standardized Rates (ASR) in pancreatic cancer

Figure 1: Estimated Age-standardized Rates (ASR) of incidence and mortality of pancreatic cancer worldwide for both sexes in 2012. North American and Europe are areas with highest incidence and mortality ASR, while South-central Asia and middle Africa have the lowest incidence and mortality ASR in pancreatic cancer. Data from GLOBOCAN 2012 (IARC) www.globocan.iarc.fr

1.2 The WNT signaling pathway

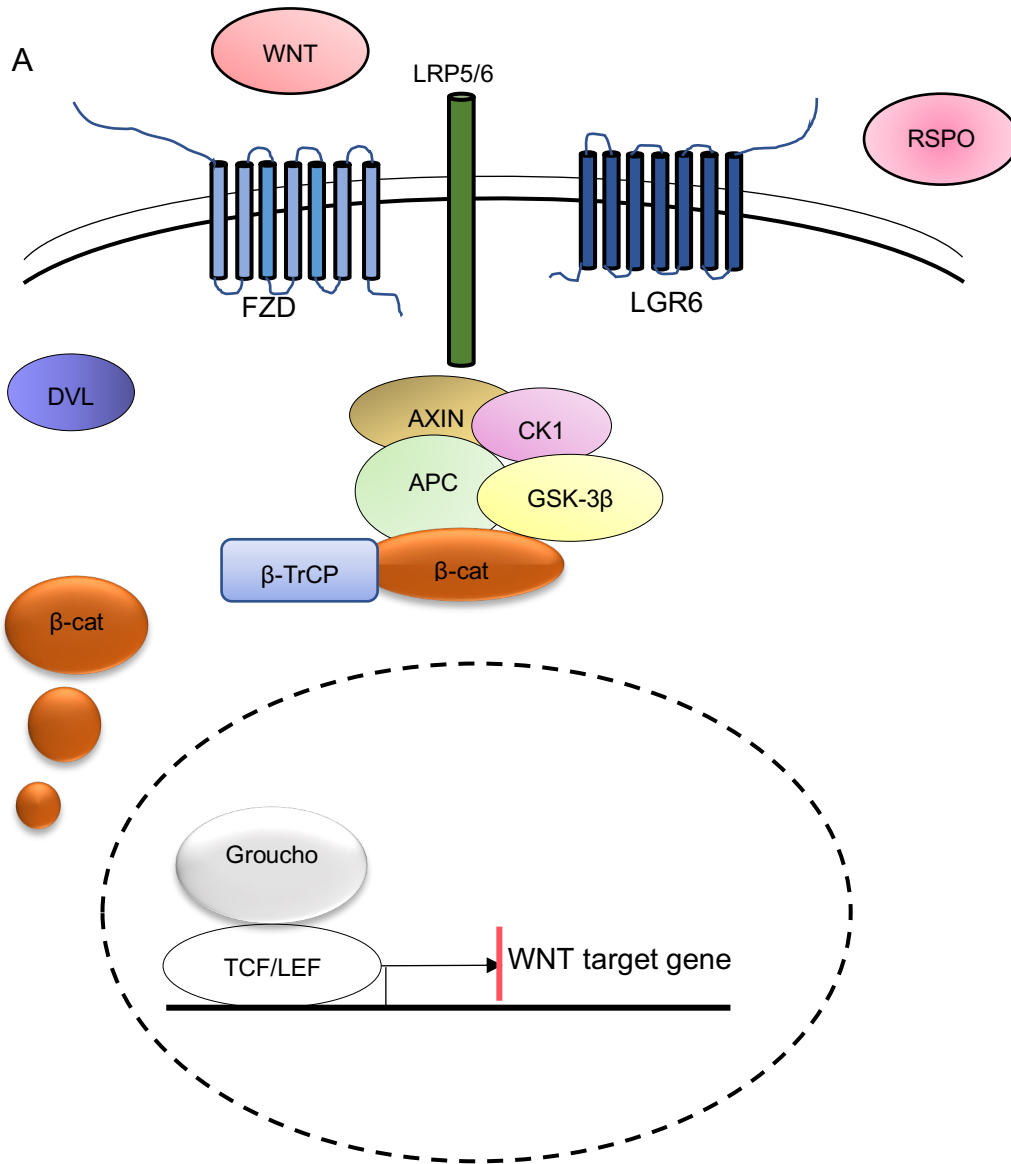
The first mammalian WNT1 gene, also known as Int-1, was identified by Nusse and his colleagues more than 30 years ago. WNT1 was activated when mouse mammary tumor virus (MMTV) integrated its proviral DNA at a specific region of the host genome [29]. After years of study, the WNT signaling pathway was found to be highly conserved among species [30]. The accurate regulation of WNT signaling is essential for embryonic processes as well as tissue homeostasis. WNT signaling mediates cell behaviors such as proliferation, differentiation, self-renewal, cell polarity, and movement [31, 32]. Considering the essential roles during the life span, alterations in WNT signaling are associated with diverse diseases including developmental defects and cancer. As early as 1991, the adenomatous polyposis coli (APC) gene was found to be involved in familial adenomatous polyposis [33, 34]. Subsequently, additional WNT pathway components and the connections with the disease were studied.

The WNT pathway is divided into canonical (β -catenin dependent) and non-canonical (β -independent) pathways [35]. The non-canonical WNT signaling is subdivided into a planar cell polarity (PCP) pathway and a WNT/ Ca^{2+} pathway. They are activated by c-Jun-N-terminal kinase (JNK) and calcium (Ca^{2+}), respectively [31, 36-38]. The PCP pathway mediates tissue morphogenesis during development process and synchronous polarity [39, 40]. The WNT/ Ca^{2+} signaling is essential for developmental processes. It is triggered by phospholipase C (PLC), leading to inositol 1,4,5-triphosphate (IP3) and 1,2 diacylglycerol (DAG) formation, which further results in elevated intracellular Ca^{2+} concentration [39-41]. High Ca^{2+} dose induces the activation of protein kinase C (PKC), a calmodulin-dependent protein kinase II (CAMKII) as well as the nuclear factor activated T cells (NFAT) [40]. Of all the WNT pathways, the canonical pathway is by far the best investigated and understood and is the topic of the thesis.

1.3 The canonical WNT signal pathway

The WNT/ β -catenin pathway controls various processes ranging from embryonic development to adult tissue homeostasis. Without the presence of WNT ligands, the destruction complex comprised of casein kinase1 (CK1), glycogen synthase kinase 3 (GSK-3 β), AXIN, and adenomatous polyposis coli (APC) labels β -catenin for degradation. β -catenin is a key mediator of the WNT/ β -catenin pathway. It is phosphorylated by CK1 at Ser45, which further facilitates the subsequent phosphorylation by GSK-3 β at Ser33, Ser37, and Thr41. The phosphorylation leads to β -catenin ubiquitination through the β -TrCP/Skp pathway and degradation by the proteasome [42, 43] (Figure 2A).

In the presence of WNT ligands, WNT/ β -catenin signaling gets activated by WNT ligands binding to their co-receptors frizzled (FZD) and LRP5/6, further leading to the activation of disheveled (DVL). DVL then removes GSK-3 β from the destruction complex inactivating the APC/AXIN/GSK-3 β /CK1. The inactivation of the destruction complex results in the accumulation of β -catenin in the cytoplasm with subsequent translocation into the nucleus. Protein kinase A (PKA) can phosphorylate β -catenin at Ser675 to induce its accumulation in the nucleus [44]. β -catenin then forms a trimeric complex with TCF/LEF (T-cell factor / lymphoid enhancer factor) transcription factors to regulate WNT target gene expression [45] (Figure 2B).



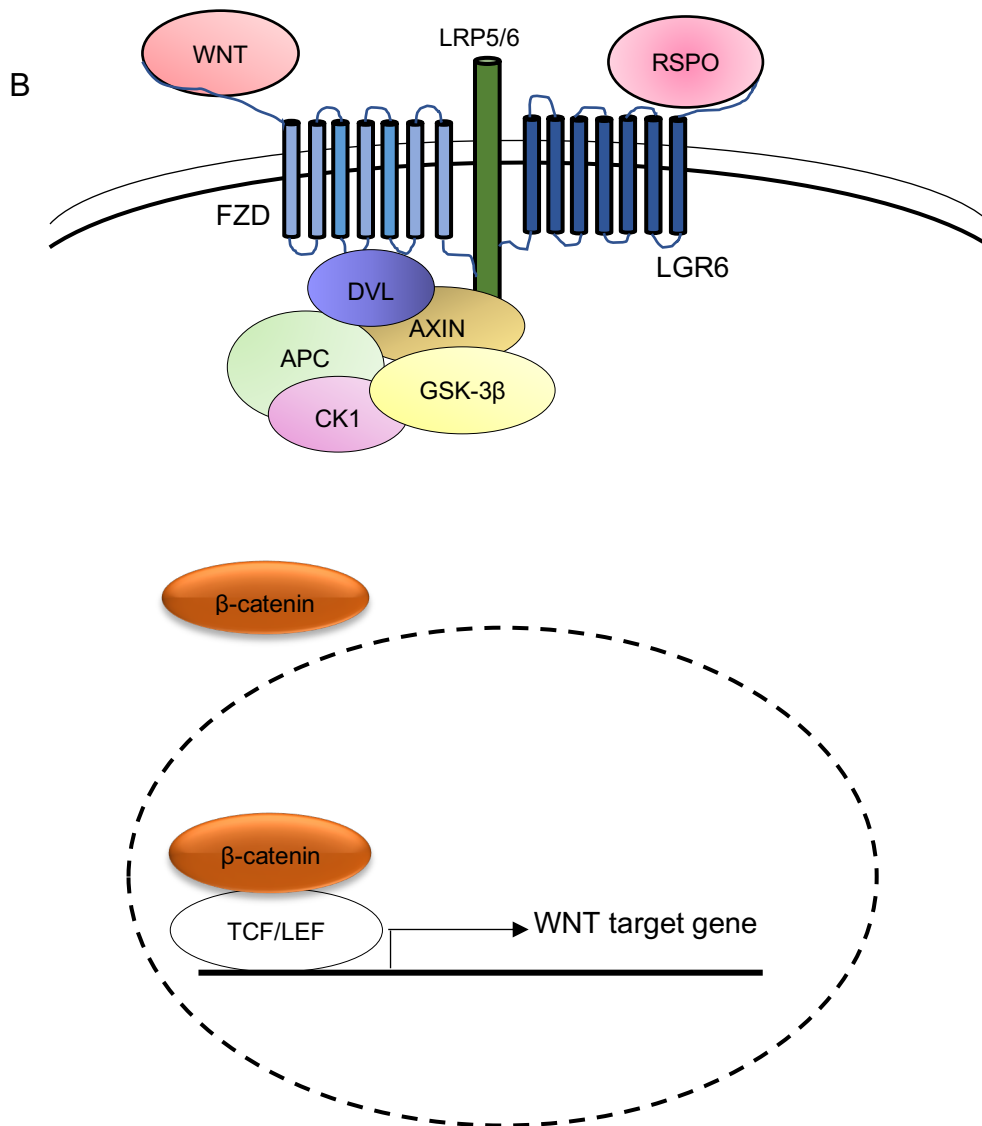


Figure 2: Schematic illustration of the canonical WNT signaling pathway. (A) In the absence of WNT ligands, cytoplasmic β -catenin is targeted for degradation. The destruction complex contains two scaffolding proteins (APC and AXIN1/2) and two kinases (CK1 and GSK-3 β). APC and AXIN bind to β -catenin and the kinases sequentially phosphorylate β -catenin at its Ser and Thr residues. Phosphorylated β -catenin becomes a substrate of the ubiquitin E3 ligase β -TrCP and is subsequently degraded in the proteasome. Besides, Groucho proteins act as transcriptional repressors to take up the nuclear DNA-binding proteins of the TCF/LEF family. (B) With the presence of WNT ligands, canonical WNT signaling is triggered by the interaction of secreted WNT proteins with its co-receptor FZD and LRP5 or LRP6. The binding of ligands and receptors inhibits the destruction complex leading to β -catenin accumulation in the cytoplasm. β -catenin then translocates into the nucleus where it associates with the TCF/LEF family and induces WNT target gene expression.

1.4 WNT proteins

WNT proteins are a family of secreted paracrine glycoproteins with a molecular weight of about 40kDa [46]. It has been discovered that at least 19 human WNT proteins share common structural characteristics [31]. WNT3a was the first successful purification of a canonical WNT protein [47] and is believed to be implicated in both developmental physiological processes and carcinogenesis [48, 49]. Researchers found that lipid-modification of WNT protein may be necessary for WNT secretion as well as efficient WNT signaling [47, 50]. One reason is that one domain of the WNT protein that interacts with its FZD receptor contains the palmitoleic acid [51]. Palmitoleic acid associates with the FZD extracellular cysteine-rich domain (CRD) for WNT signaling transduction. Another reason concerns the requirement of porcupine for WNT protein palmitoylation and maturation in the endoplasmic reticulum (ER) [52]. Porcupine is a multi-pass transmembrane O-acyltransferase in the ER and a highly conserved component in the WNT signal pathway in WNT-producing cells [53]. The loss of porcupine leads to the failure of WNT3a translocation from the ER to Golgi [52, 54]. In addition, seven-transmembrane WNTless (Wls) protein is essential for further WNT protein transportation and secretion [55]. Wls can recognize the specific amino residues lipidation, facilitate cellular trafficking as well as its translocation from the Golgi to the plasma membrane for secretion [53].

1.5 WNT receptors

1.5.1 Frizzled and LRP5/6 receptors

The binding of WNT proteins to a heterodimeric receptor complex comprised of FZD and LRP5/6 is the first step to trigger the WNT signaling cascade [53]. The FZD family

was first discovered as receptors to the WNT cascade in 1996 [56, 57]. Until now, researchers have found 10 distinct family members (FZD1 to FZD10) [58]. All the FZD receptors share a similar structure, a seven-transmembrane domain with an extracellular CRD at its N-terminal as a platform for binding ligands [51, 59]. The direct association of WNT ligands with the CRD domain fully triggers downstream WNT signaling by the recruitment of DVL proteins at the membrane [60-62]. The FZD receptors belong to a large family of G protein-coupled receptor (GPCR) [63] and it was expected that G-protein is functionally associated with the interaction of a FZD receptor and DVL. However, no direct association of heterotrimeric G proteins and FZD receptors was observed in WNT signal transduction as shown in typical GPCR signaling [64]. Still, it remains to be shown that G-proteins take roles in the activation of WNT signaling [64-66].

As FZD could activate both the non-canonical and canonical WNT cascades [61, 67], the involvement of co-receptors LRP5/6 determines the activation of the canonical WNT signaling only [68]. LRP5/6, a single-pass transmembrane molecule, functions to mediate the WNT signal pathway. The signal transduction from extracellular to intracellular is achieved by the WNT/FZD/LRP5/6 signalosomes [69-71]. The phosphorylation of LRP by kinases CK1 and GSK-3 β activate the engagement of LRP6 to AXIN [72-74]. AXIN is a negative regulator in the WNT signal pathway and is kept at a low level in the cells. The more AXIN binds to LRP5/6, the less AXIN participates in the β -catenin degradation complex. Thereby, AXIN provides a stoichiometric rather than a catalytic mechanism to mediate WNT signal transduction. In addition, protein kinase A (PKA), G-protein coupled kinases (Grk5/6) and certain cyclin-dependent protein kinases participate to LRP phosphorylation [75].

1.5.2 Non-conventional receptors

Besides FZD and LRP, other receptors including ROR2, RYK and PTK7, have been identified as WNT ligands binding receptors to mediate WNT signaling. For instance, WNT ligands bind to the CRD domain of ROR2 to mediate WNT signaling [76, 77]. WNT inhibitory protein-1 (WIF-1) binds to WNT inhibitory factor domain (WIF) to down-regulate the WNT cascade [78]. However, the exact contribution of alternative receptors to the WNT signaling process is still unknown.

1.6 Secreted agonists in WNT signaling

In addition to WNT ligands, other proteins may either directly or indirectly activate FZD or LRP5/6 receptors, resulting in increased β -catenin stability. For example, Norrin and R-spondin (the RSPO protein family, consisting of four members) are two types of agonists that regulate the WNT signal pathway through the FZD/LRP complex. Norrin acts as a direct ligand to the frizzled4/LRP5 complex. Co-expression of Norrin, frizzled4, and LRP5 strongly activated WNT signaling [79].

1.7 Secreted extracellular antagonist

WNT activity is regulated extensively by modulators at the receptor-ligand level [80], such as frizzled related proteins (sFRPs), WNT inhibitory factor-1 (WIF-1), the Dickkopf protein family (DKK). The effect of sFRPs is to inhibit WNT signaling either by binding to certain WNT ligands to prevent the association with FZD receptors or by binding to FZD receptors to inhibit the formation of functional complexes of WNT/FZD [81-83]. WIF-1 is to decrease WNT activity by binding to WNT protein to block formation of the

WNT/FZD/LRP5/6 complex [78, 84]. DKK family prevent by association with LRP5/6 to inhibit WNT/FZD/LRP complex [85, 86].

1.8 R-spondin proteins

The R-spondin (RSPO) proteins are secreted agonists of the canonical WNT signaling pathway. They are a recently identified family consisting of 4 secreted cysteine-rich proteins. RSPO1 was first discovered in 2001, followed by RSPO2 and RSPO3 in 2004, whereas RSPO4 was the last ligand identified in 2006 [87-90]. RSPO homologs are only present in vertebrate species, not in invertebrates [91].

1.8.1 RSPO structural features

RSPO belong to the thrombospondin type 1 repeat (TSR-1) superfamily [92]. Human mature RSPOs share 40%-60% sequence homology, harboring two cysteine-rich Furin-like domains at the N-terminal and a central TSR-1 domain [91, 92]. The former domains are also present in growth factor receptors of epidermal growth factor (EGF), hepatocyte growth factor (HGF), insulin as well as neurotrophic factor [93]. The cysteine residues found in two Furin-like domains are essential and sufficient to enhance WNT signaling [89, 91, 94]. Three classes of transmembrane proteins have been discovered interacting with RSPO as shown in Figure 3. The TSR-1 domain may be used for proteoglycans and/or glycosaminoglycan engagement. One Furin-like domain binds to cell surface transmembrane E3 ubiquitin ligases, zinc and ring finger 3 (ZNR3) and/or its homologs ring finger 43 (RNF43), and another Furin-like domain bind to Leucine-rich repeat containing G protein-coupled receptor 4/5/6 (LGR4/5/6). The role of RSPOs to enhance WNT signaling might imply the significance of RSPOs

in WNT-dependent developmental processes.

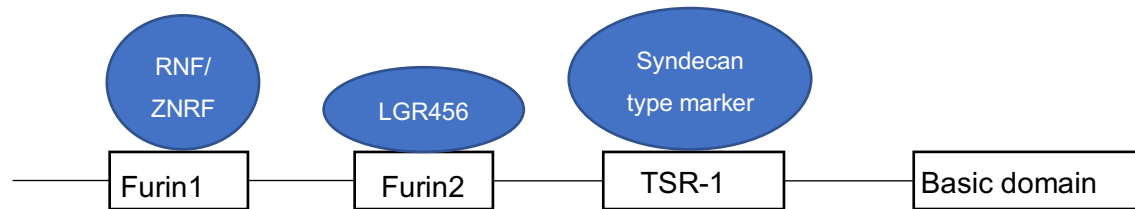


Figure 3: The general structure of RSPO and their binding sites. Schematic illustration shows the protein domain architecture of RSPO with two cysteine-rich Furin-like domains (left), a thrombospondin protein 1 domain and basic amino acids.

1.8.2 RSPO functions during embryogenesis

RSPO play different roles in developmental processes. RSPO1 determines the phenotypic sex phenotype of human and mice. RSPO1 mutations result in a rare syndrome with XX sex reversal, palmoplantar hyperkeratosis and high possibility to develop skin carcinoma [95]. Moreover, RSPO1 plays a key role in the development of the reproductive system [96, 97]. RSPO2 is necessary for organ development of limbs, lungs, and hair follicles. RSPO2 mutations lead to limb and lung defects associated with weakened canonical WNT signaling [98-101]. Besides, RSPO2 is responsible for hair follicle development in domestic dogs [102]. RSPO3 is involved in embryonic vasculogenesis and angiogenesis, with an insufficient penetration of blood vessels in RSPO3 knockout animals in placenta [103]. Finally, RSPO4 is involved in human nail development [104]. It was found that RSPO4 mutations associated with congenital anonychia, a rare autosomal recessive condition with the lack of all fingernails and toenails [105].

1.8.3 Mechanisms of RSPO-mediated enhancement of WNT signaling

Enhancement of the WNT signal pathway by RSPO proteins was first discovered in early frog embryos by Kazanskaya and colleagues [89]. One possible mechanism concerns the direct association between the RSPO-LGR and the WNT/FZD/LRP5/6 complex revealed by mass spectrometric approach [106]. Another possible explanation implicates its interaction with the transmembrane E3 ubiquitin ligases ZNRF3/RNF43 [107]. ZNRF3/RNF43 are negative feedback regulators in WNT signaling [107, 108]. Upon the binding of RSPOs to LGR5, ZNRF3/RNF43 are removed from the cell surface, which decreases the ubiquitination of FZD and LRP6 and subsequently potentiates WNT signaling [107]. Collectively, the recruitment and engagement of RSPO to the LGR4/5/6 receptors facilitate the interaction of RSPO with ZNRF3/RNF43. This process leads to the elimination of ZNRF3/RNF43, consequently keeping the presence of FZD receptors and promoting WNT signaling.

1.9 LGR receptors

Studies have uncovered new members of the GPCR superfamily with Leucine-rich repeats (LRR) associating with RSPO to potentiate canonical WNT signal pathway. Those receptors include LGR4/GPR48 and LGR5/GPR49 which were first discovered in 1998, and LGR6 in 2000 [109, 110]. LGR6 shares 54% similarity with LGR5, and LGR4 is less similar to its homologs with 46% similarity to LGR5 and 44% similarity to LGR6. Secreted WNT agonists RSPO1-4 were identified as endogenous ligands to the LGR4/5/6 receptors. The high affinity of LGR4/5/6 receptors to RSPO can strongly enhance the WNT/ β -catenin signal pathway by increasing phosphorylation of LRP5/6 and β -catenin stabilization [106, 111]. Thus, LGR4/5/6 receptors are special GPCRs that regulate WNT/ β -catenin signaling.

1.9.1 LGR receptor structures

The LGR family proteins are G-protein coupled receptors and are characterized by a large extracellular domain (ECD) with multiple LRR [106, 111]. The LGR family is further divided into three main groups (A,B,C) according to the amount of LRR and LDLa (low-density lipoprotein receptor class A) [112]. Type A receptors include LGR1, the follicle-stimulating hormone receptor (FSHR), LGR2, the luteinizing hormone receptor (LHR), and LGR3, the thyroid-stimulating hormone receptor (TSHR). All type A receptors harbor seven to nine LRRs as well as a long Hinge region joining the LRR region to the 7TM domain. Type C receptors include LGR7 and LGR8, which have a shorter Hinge region and a LDLa motif. The engagement of type A/C receptors and ligands leads to G-protein-coupled intracellular cAMP production [113]. The type B receptor family of LGR4/5/6 is a unique G-protein coupled 7-transmembrane protein with a large ECD containing LRR at the N-terminal LGR protein. It is characterized by the presence of 16-18 LRRs within the ectodomain.

1.9.2 LGR4/5/6 receptor functions

LGR4 is widely expressed in multiple organs such as cartilage, heart, kidney, adrenal gland, reproductive tracts, hair follicles, eyes, and nervous system cells. Thus, its appearance is broad, not limited to rare stem cell [101]. LGR4 is essential in development, as its ablation in embryos showed embryonic lethality [114]. Developmental defects in LGR4 knockout mice displayed in multiple organs. The affected tissues are accompanied with impaired ductal branching and elongation as well as reduced proliferation of epithelial cells [115]. Moreover, LGR4 potentially participates in colon cancer because elevated levels of LGR4 were detected in most colon tumors [115].

LGR5 is considered a WNT target gene. It labels stem cells of tissues with high rates of self-renewing, including small intestine and colon [116], stomach [117], and hair follicles [118]. LGR5 expression is not restricted to the above mentioned tissues, but also detected in kidney [119], pancreas [120], liver [121], and the mammary gland [122]. Epithelial cells of the small intestine and colon are derived from LGR5⁺ cells, a finding discovered by lineage tracing approaches [116]. Additionally, LGR5⁺ cells can fully differentiate into intestinal [123], stomach [117], and mammary gland organoids [124]. LGR5 is a gene with increased expression in tumors of colorectal, ovarian and hepatic tissues, possibly due to mutational activation of canonical WNT signaling in such cancers [125-128].

LGR6 labels multipotent stem cells in multiple organs. In the cochlea, dynamic LGR6 expression was detected during its developmental process [129]. LGR6 labels rare cells in basal and luminal compartments of the mammary gland in mice [130]. Those LGR6⁺ cells expand clonally during puberty and regain proliferative ability during pregnancy [130]. LGR6 marks stem cells in both anterior and posterior taste buds of the tongue [131]. In the lung, LGR6 labels a rare stem cell population that co-expresses integrin $\alpha 6$ and its homologue LGR5 [132]. LGR6 was found to be expressed in certain cells of the hair follicle. Interestingly, the transplantation of LGR6⁺ cells seems to generate new follicles as well as new epidermis [107]. Regarding the role of LGR6 in cancer, loss-of-function mutation of LGR6 in colorectal cancer leads to a failure in binding RSPOs with subsequently reduced WNT enhancement [133]. LGR6 mutations are involved in tumor development in mammary glands by inducing luminal cell expansion [130]. A study showed that the LGR6 promoter is hypermethylated in around 20% of sporadic colorectal cancers [134]. So far, LGR6 is considered to be a marker of adult stem cells and a potential marker for CSCs [108]. LGR6, together with LGR4 and LGR5, is an amplifier of WNT signaling and is involved in stem cell maintaining.

1.10 Epithelial-mesenchymal transition (EMT) and WNT signaling

Epithelial–mesenchymal transition (EMT) is a process by which epithelial cells transdifferentiate into mesenchymal cells. The reverse process was named mesenchymal–epithelial transition (MET). It is regulated by transcription factors, including zinc finger E-box-binding homeobox 1 (ZEB1), SNAIL family, SNAIL1 and SNAIL2, and basic helix–loop–helix (bHLH) family member TWIST [135-138]. During the process, epithelial cells undergo a morphological change by losing tight junctions and polarity to mesenchymal phenotype characterized by spindle-shaped phenotype, less cell adhesion and increased motility [139, 140]. EMT is detected by the expression of vimentin and neural cadherin (N-cadherin), as well as the repression of epithelial cadherin (E-cadherin) [141, 142]. EMT plays important roles in development processes fundamental to various steps of embryogenesis and it is reactivated in cases of wound healing, fibrosis, and cancer progression [139, 143, 144]. Moreover, EMT is involved in cancer stemness generation by enabling dedifferentiation processes of non-CSCs into CSCs. The plasticity of EMT endows cancer cells with the ability to switch between the mesenchymal CSCs phenotype and its more differentiated epithelial phenotype [145]. Moreover, EMT induction facilitates CSCs dissociating from the primary site and colonizing as a secondary tumor through the reverse process of MET [146-148]. Therefore, EMT is a critical mechanism during cancer progression and novel therapeutic approaches are of interest to confine cancer cells to the site of the primary tumor in order to prevent metastatic spread.

WNT signaling is involved in EMT, because β -catenin also plays a role in adherence junctions. In this dual role, β -catenin acts on the one hand as a key effector in canonical WNT signaling and on the other hand, with E-cadherin and α -catenin to mediate cell adhesion [149, 150]. Of note, E-cadherin is a negative regulator of WNT signaling by recruiting β -catenin to adherent junctions. The loss of E-cadherin leads to

accumulation of β -catenin in the nucleus, activating WNT signaling [151-153]. Upon high WNT activity, the direct activation of SNAIL2 or indirect activation of ZEB1 can induce EMT, suggesting a feedforward loop of dedifferentiation of cancer cells.

1.11 WNT signaling and disease

Studies initially focused on the role of WNT signaling in the regulation of cellular proliferation, differentiation, and stem cell maintenance. As shown above, WNT signaling overlaps between developmental and oncological processes. Therefore, research shifted to the role of WNT signaling in disease. APC gene mutations were discovered in case of family adenomatous polyposis, as the loss of APC function leads to inappropriate β -catenin accumulation. In that case, additional mutations such as KRAS and TP53 would lead to progression of adenomateous polyps to malignancy [154].

Besides, aberrant WNT activation has been implicated in PDAC progression and the maintenance of CSCs [27, 155]. In analysis of 136 human PDAC tissues, nuclear or cytoplasmic accumulation of β -catenin was detected in the majority of PDAC samples [28]. Moreover, WNT signaling is supposed to play roles in pancreatic carcinogenesis as levels of cytoplasmic and nuclear β -catenin expression associate with the grade of PanIN and invasive PDAC [156]. Ilmer and colleagues found rare PDAC cell subpopulations with high intrinsic WNT activity that possessed properties of CSCs. RSPO2 is capable to enhance WNT signaling, attributing cells with cancer stemness traits [157]. Specific traits of CSCs include chemo-resistance, EMT and remote metastatic potential [158]. Research demonstrated that altered WNT signaling correlated with poor prognosis in PDAC patients, indicating that WNT signaling is a predictor of patients outcome and may serve as potential therapeutic targets [159].

1.12 Aim of the study

As explained above, LGR6 is a receptor of RSPO thereby potentially enhancing canonical WNT signaling activity. LGR6 is known to mark stem cells of taste buds, lung, skin as well as rare mammary gland cells. As its homolog LGR5 was proved to be a WNT target gene, this study aims to decipher the role of LGR6 in WNT signaling, apart from functions as a receptor of RSPO in PDAC. Considering the overlap between WNT signaling and EMT, we also investigated the potential role of LGR6 in EMT.

2. Materials and Methods

2.1 Materials

2.1.1 Consumables

Consumables	Source
6-well plates Nunclon™ delta surface	Thermo Fisher Scientific, Roskilde, Denmark
12-well plates Nunclon™ delta surface	Thermo Fisher Scientific, Roskilde, Denmark
24-well plates Nunclon™ delta surface	Thermo Fisher Scientific, Roskilde, Denmark
96-well plates	Sarstedt, Nümbrecht, Germany
5ml pipette	Costar, Maine, USA
10ml pipette	Costar, Maine, USA
25ml pipette	Costar, Maine, USA
1.5ml tips	Eppendorf, Hamburg, Germany
2.0ml tips	Eppendorf, Hamburg, Germany
15ml tube	TPP, Trasadingen, Switzerland
50ml tube	Falcon, Reynosa, Mexico
Blot paper	Bio-Rad, California, USA
Cell culture flask T25 Nunclon™ delta surface	Thermo Fisher Scientific, Roskilde, Denmark
Cell culture flask T75 Nunclon™ delta surface	Thermo Fisher Scientific, Roskilde, Denmark
Cell culture flask T125 Nunclon™ delta surface	Thermo Fisher Scientific, Roskilde, Denmark
Cell scraper	TPP, Trasadingen, Switzerland
FACS tubes	Falcon, New York, USA
Filters 0.25uM	Sartorius stedim, Goettingen, Germany

Filters 0.45uM	Sartorius stedim, Goettingen, Germany
Film ECL	GE healthcare, USA
Glass cover slips Menzel Gläser	Thermo Fisher Scientific, Schwerte, Germany
Glass slides	Marienfeld, Lauda-Königshofen, Germany
Hydrophobic pen	Dako, Waldbronn, Germany
Low-attachment 96-well plates	Corning, Krailling, Germany
Nitrocellulose-transfer membrane	LI-COR, USA
Sterile needle	BD Microlance™, Heidelberg, Germany

2.1.2 Chemicals

Chemicals	Source	Identifier
β-Mercaptoethanol	Sigma-Aldrich, Steinheim, Germany	M6250
Agarose	Peqlab Biotechnologie, Erlangen, Germany	35-1020
Ammonium persulfate (APS)	Serva, Heidelberg, Germany	13376.01
BSA	Biomol, Hamburg, Germany	01400.100
Crystal violet	Sigma-Aldrich, Steinheim, Germany	C0775
6X DNA Sample Loading Buffer	Thermo Fisher Scientific, Schwerte, Germany	R0611
DMEM/ F12	Gibco, New York, USA	11330-032
DMSO	Sigma-Aldrich, Karlsruhe, Germany	D2650
DNA-Ladder standard	Invitrogen, California, USA	10787-018
ECL™ Western Blotting Detection System	Amersham Biosciences	RPN2209
70% Ethanol	Apotheke GH, Munich, Germany	

>99% Ethanol	Apotheke GH, Munich, Germany	
FBS	Sigma-Aldrich, Missouri, USA	F7524
Goat serum	Sigma-Aldrich, Missouri, USA	G6767
Gemcitabine	Pharmacy, Munich, Germany	
Glycin	Carl Roth, Karlsruhe, Germany	3187.4
Hoechst	Invitrogen, California, USA	H3570
Hydrogen peroxide 30%	Merck, Darmstadt, Germany	8.22287.1000
IC Fixation buffer	eBiosciences Invitrogen, California, USA	00-8222-49
Isopropanol	Carl Roth, Karlsruhe, Germany	UN1219
Loading buffer 4x	Bio-Rad, California, USA	161-0747
Methanol	Merck, Darmstadt, Germany	1.06009.1000
Milk powder	Carl Roth, Karlsruhe, Germany	T145.2
Methyl cellulose	Sigma-Aldrich, Steinheim, USA	M0387
Mounting Medium	Burlingame, USA	Vectashield H-1000
NaCl	Sigma-Aldrich, Copenhagen, Denmark	71380
PBS	PAN-Biotech, Munich, Germany	P04-36500
30% PolyAcrylamid	Carl Roth, Karlsruhe, Germany	3029.1
4% PFA	Pharmacy, Munich, Germany	
37% PFA	AppliChem, Darmstadt, Germany	A0823
Penicillin-Streptomycin	Lonza, St. Louis, USA	DE17-602E

Permeabilization Buffer 10X	eBiosciences Invitrogen, California, USA	00-8333-56
Phosphatase inhibitor cocktail	Roche, Mannheim, Germany	04906837001
Protein standards	Bio-Rad, California, USA	161-0374
Protease inhibitor cocktail	Roche, Mannheim, Germany	05892791001
RNase-free water	Qiagen, Hilden, Germany	129112
RPMI 1640 Medium	Gibco, New York, USA	21875-034
RIPA lysis buffer 10X	Millipore, Darmstadt, Germany	20-188
SDS	Carl Roth, Karlsruhe, Germany	2326.2
SYBR safe DNA gel stain	Invitrogen, California, USA	S33102
TAE buffer 50x	Serva, Heidelberg, Germany	42549.01
TEMED	Bio-Rad, California, USA	161-0800
Tris Base	Bio-Rad, California, USA	161-0716
Triton-X-100	Sigma-Aldrich, Steinheim, Germany	T8787
Trypan blue	Sigma-Aldrich, Steinheim, Germany	T8154
Trypsin/EDTA	Lonza, St. Louis, USA	BE17-161E
Tween 20	Sigma-Aldrich, Heidelberg, Germany	P1379

2.1.3 Antibodies

Antibodies	Source	Identifier
β -catenin	Cell signaling Technology Frankfurt am Main, Germany	Cat#8480
Phospho- β -catenin (Ser675)	Cell signaling Technology Frankfurt am Main, Germany	Cat#4176

GAPDH	Santa Cruz Biotechnology, Texas, USA	Cat#sc-25778
E-cadherin	BD Biosciences, California, USA	Cat#610181
LGR6	Sigma, Missouri, USA	Cat# HPA008556
LGR6 APC-conjugated	R&D system, Minnesota, USA	Cat# FAB8458A-025
anti-mouse IgG-HRP	Santa Cruz Biotechnology, Texas, USA	Cat# sc-2005
anti-rabbit IgG HRP	Cell signaling Technology Frankfurt am Main, Germany	Cat#7074
anti-rabbit IgG-FITC	Santa Cruz Biotechnology, Texas, USA	Cat#sc-2012
anti-mouse IgG-TR	Santa Cruz Biotechnology, Texas, USA	Cat#sc-2781

2.1.4 Recombinant Proteins and inhibitors

Product	Source	Identifier
B27	Gibco, New York, USA	Cat#12587-010
EGF	ImmunoTools, Friesoythe, Germany	Cat#11343406
FGF- β	ImmunoTools, Friesoythe, Germany	Cat#11343623
IWP2	Selleckchem, Texas, USA	Cat#S7085
RSPO2	Peprtech, New Jersey, USA	Cat#120-43
TGF β 1	ImmunoTools, Friesoythe, Germany	Cat#11343160
U0126	Cell signaling technology, Frankfurt am Main, Germany	Cat#9903S
WNT3a	R&D system, Minnesota, USA	Cat#5036-WN-010

2.1.5 Commercial Assays

Product	Source	Identifier
BCA protein Assay kit	Thermo Fisher Scientific, Germany Schwerte,	Cat#23225
ChIP Assay kit	Merck, Darmstadt, Germany	Cat#17-295
iScript cDNA synthesis kit	Bio-Rad, California, USA	Cat#1708891
Lipofectamine RNAiMAX	Invitrogen, California, USA	Cat#13778-100
RNA isolate kit	Peqlab Biotechnologie, Erlangen, Germany	Cat#12-6834-02
SiPOOLS	siTOOLS Biotech, Munich, Germany	
Sso Fast Eva Green	Bio-Rad, California, USA	Cat#172-5201
WST1	Roche, Mannheim, Germany	Cat#05015944001

2.1.6 Primers

Primers	Source	Identifier
AXIN2	Qiagen, Hilden, Germany	Cat#QT00037639
CDH1	Qiagen, Hilden, Germany	Cat#QT00080143
GAPDH	Qiagen, Hilden, Germany	Cat#QT00079247
ZEB1	Qiagen, Hilden, Germany	Cat#QT00020972
LGR6	Qiagen, Hilden, Germany	Cat#QT00085827

2.1.7 Apparatus

Apparatus	Company
Autoclave	Unisteri, Oberschleißheim, Germany
AxioCam MRC5	ZEISS, Munich, Germany
Centrifuge	Hettich, Ebersberg, Germany
Cool Centrifuge	Eppendorf, Hamburg, Germany
Micro centrifuge	Labtech, Ebersberg, Germany
CO ₂ Incubator	Binder, Tuttlingen, Germany
DNA workstation	Uni Equip, Martinsried, Germany
Drying cabinet	Thermo Fisher Scientific, Schwerte, Germany
Electronic pH meter	Knick Elektronische Messgeräte, Berlin, Germany
FACS Fortessa	BD Biosciences, Heidelberg, Germany
4°C Fridge	Siemens, Munich, Germany
-20°C Fridge	Siemens, Munich, Germany
-80°C Fridge	Siemens, Munich, Germany
Fluorescence Microscope	ZEISS, Munich, Germany
Ice machine	KBS, Mainz, Germany
Liquid Nitrogen tank	MVE Goch, Germany
Hypercassette	Biosciences GE Healthcare, Freiburg, Germany
Image Scanner	Konica Minolta, Feldkirchen, Germany
Lamina flow	Thermo Fisher Scientific, Schwerte, Germany
Microscope	Olympus, Hamburg, Germany
Microwave Oven	Siemens, Munich, Germany
Micro weigh (CHYO)	Micro Precision Calibration, California, USA

Mini-trans blot electrophoretic transfer cell	Bio-Rad, California, USA
Nanodrop 2000	Thermo Fisher Scientific, Schwerte, Germany
Novex PowerEase 500 Power Supply	Invitrogen, California, USA
Pipette controller	Eppendorf, Hamburg, Germany
Power Supply Power Pac 300	Bio-Rad, California, USA
Step one PCR system	Thermo Fisher Scientific, Schwerte, Germany
Shaker	Edmund Bühler, Bodelshausen, Germany
Thermocycler	Eppendorf, Hamburg, Germany
Thermomixer comfort	Eppendorf, Hamburg, Germany
UV illuminator	LTF Labortechnik, Wasserburg, Germany
VersaMax ELISA Microplate Reader	Molecular Devices, California, USA
Vortex Mixer VF2 (Janke & Kunkel)	IKA, North Carolina, USA
Water bath	Memmert, Schwabach, Germany
X cell II TM Blot module	Invitrogen, California, USA

2.1.8 Software

Software	Company
Excel	Microsoft
FACS Diva software	BD
Graphpad 6.0	Prism Version 6.0
ImageJ Version 1.50i	National Institutes of Health,
Step One software v2.3	Applied Biosystems
ZEN software Version 2.0	Carl Zeiss

2.1.9 Buffers and Solutions

Agarose gel electrophoresis

1xTAE Buffer

50x TAE buffer	20ml
H ₂ O	980ml

Western Blot

12% Separating Gel

H ₂ O	4,3ml
1.5M Tris pH8.8	2,5ml
30% PolyAcrylamid	3ml
10% SDS	100µl
10% APS	100µl
TEMED	5µl

Stacking Gel

H ₂ O	2,3ml
1M Tris pH6,8	380µl
PolyAcrylamid	380µl
10% SDS	30µl
10% APS	30µl
TEMED	5µl

10xRunning Buffer

Tris Base	30g
Glycin	144g
SDS	10g
H ₂ O	1L

1xRunning Buffer

10x Running buffer	100ml
H ₂ O	900ml

10x Transfer Buffer

Tris Base	30g
Glycin	144g
H ₂ O	1L

1x Transfer Buffer

10x Transfer Buffer	100ml
Methanol	100ml
H ₂ O	800ml

10xTBS

Tris Base	24g
NaCl	80g
H ₂ O	1L
PH	7,6

1xTBS-T

10xTBS	100ml
H ₂ O	900ml
Tween	1ml

1x Stripping Buffer

Glycin	15g
H ₂ O	1L
Tween	500µl
PH	2.5

Blocking Buffer

Milk	5% w/v
	In TBST

Protein lysis Buffer

RIPA buffer	100ml
Phospho Stop	1 Table
Protease Inhibitor	1 Table

1M Tris-HCl

Tris-base	12.12g
H ₂ O	200ml
PH	6.8

1.5M Tris-HCl

Tris-base	36.34g
H ₂ O	200ml
PH	8.8

Loading buffer

4xloading buffer	900ul
β-Mercaptoethanol	100ul

10%SDS

SDS	10g
H ₂ O	100ml

10%APS

APS	10g
H ₂ O	100ml

Immunofluorescence staining

Peroxidase Block

Methanol	16.7ml
H ₂ O ₂	0.5ml
H ₂ O	3.8ml

Colony formation assay

0.5% Crystal violet solution

Crystal violet	0.5g
Methanol	20ml
H ₂ O	80ml

2.2 Methods

2.2.1 Cell culture

Human pancreatic cancer cell lines AsPC-1, BxPC-3, Capan-2, Miapaca-2, Panc-1 were purchased from ATCC. Cells were cultured in RPMI1640, supplemented with 10% FBS and 1% penicillin/streptomycin. All cells were kept at a humidified atmosphere of 5% CO₂ at 37°C. Cells were maintained as a monolayer, and passaged with trypsin when 80% confluence was reached. All cells were routinely tested for mycoplasma according to internal SOPs every four months and authenticated commercially by IDEX BioResearch once a year (Ludwigsburg, Germany).

2.2.2 Gemcitabine-resistance cells Culture

Gemcitabine resistant cells (GR cells) were obtained by culturing pancreatic cancer cell lines in medium with increasing concentration of gemcitabine. The GR cells were firstly cultured in medium with 5ng/ml gemcitabine, the medium was changed every 3 days. Cells were passaged once reached to 80% confluence and subsequently exposed to a relatively higher concentration of gemcitabine. The process was repeated until resistance population was selected. Each GR cell lines were cultured for more than 6 months.

2.2.3 GSEA

Gene set enrichment analysis (GSEA) was performed following the guidelines published at the Broad Institute web pages (<http://www.broadinstitute.org/gsea/index.jsp>). Gene sets were collected from Molecular Signature Database (MSigDB), Pancreatic cancer patients were selected from TCGA database PAAD LGR6corr. GSEA was performed to identify the correlation of selected gene sets and LGR6 expression in pancreatic cancer patients. Enrichment scores (ES) was calculated by walking through the ranked-ordered gene list, When $ES > 0$, it was considered as “enriched”, showing positive correlation of selected gene sets in PAAD LGR6corr patients.

2.2.4 RNA extraction, reverse transcription and qPCR

2.2.4.1 RNA isolation

Cells were cultured in 12-well plates with or without stimulations. Total RNA from cultured cells was extracted using RNA isolate kit according to manufacturer's instructions. Culture medium was aspirated off and cells were washed with PBS shortly. After 400ul RNA lysis buffer was added into the plates, cells were scratched to facilitate complete lysis. The lysate was collected and transferred into a DNA-removing column placed on a 2.0ml collection tube. The lysate was then centrifuged for 1 min at 1200 x g at room temperature to get flow-through lysate. Afterwards, same amount of 70% ethanol was added into lysate and homogenized well by pipetting. The mixture was later transferred again into a perfect bind-RNA column and centrifuged at 10000 x g for 1 min, the flow-through liquid was discarded. Perfect bind-RNA column containing RNA was kept and washed with wash buffer I and wash buffer II respectively to remove cellular debris and other contaminants, making sure that only RNA was left in the columns. The columns containing RNA was then centrifuged again at 1000 x g for 2 min to dry completely. The column was then placed into a fresh 1.5 ml tube and 30-50µl RNase-free water was added directly to the spin column membrane and incubates for 3 minutes. Tubes were centrifuged for 1 min at 10000 x g to elute RNA. RNA was quantified using Nanodrop 2000, the purity was evaluated by A260/A280 value. RNA samples aliquots were stored at -80 °C.

2.2.4.2 cDNA production

cDNA transcription was performed using cDNA synthesis kit following the manufacturer's instructions. Equal amount of RNA (500ng-1µg) was added into a RNase-free tube, together with variable volume of RNase-free water calculated according to RNA concentration. The total volume of RNA template and RNase-free water was made equal to 15µl. Afterwards, 5µl mixture of 5x iScript reaction mix and iScript reverse transcriptase was added into the reaction tube (Table 1). RNA samples were reverse-transcribed in a thermocycler with the following protocol: Priming, 25 °C

for 5 min, Reverse transcription, 46 °C for 20 min, RT inactivation, 95°C for 1 min and hold at 4°C. cDNA was diluted at 1:10 with RNase-free water before using for RT-PCR.

RNA template	variable
RNase free H ₂ O	variable
5x iScript reaction mix	4µl
iScript reverse transcriptase	1µl
Total	20µl

Table1 Components of cDNA production

2.2.4.3 Real time PCR

PCR was performed using Sso Fast EvaGreen kit, the PCR product was measured based on the fluorescent signal which is related to the DNA amount. Master-mix containing specific primer, Evagreen supermix, RNase-free H₂O, cDNA template was prepared for each reaction (Table 2). All the reactions were mixed thoroughly and placed in a 96-well plate. The plate was centrifuged at 1,000 rpm for 1 min to make sure that all components were at the bottom of the plate. Afterwards, the plate was moved to amplification process on StepOne™ Real-Time PCR System. The amplification processes were as follows: enzyme activation at 95°C for 30 sec, 40 cycles of denaturation at 95°C for 5 sec and annealing at 60°C for 20 sec, followed by melt curve from 65-95°C. Each sample was performed in duplicate and a negative control with sterile RNase free H₂O was used instead of template DNA. Housekeeping gene GAPDH was used to normalize the variation of cDNA. The change of RNA expression was calculated by $2^{-\Delta Ct} = 2^{-(Ct_{\text{gene of interest}} - Ct_{\text{internal control}})}$.

Primer	1 μ l
cDNA template	2 μ l
Evagreen supermix	10 μ l
RNase free H ₂ O	7 μ l

Table 2. Master-mix of Eva Green-qPCR

2.2.5 Agarose Gel Electrophoresis

1.5 g of agarose powder was measured and mixed with 100 mL 1xTAE buffer. The mixture was then melted in a microwave for about 5 min until the agarose completely dissolved. Agarose solution was cooled down to about 70°C and 10 μ l SYBR dye was added and mixed. Melted agarose solution was poured into the casting tray and the combs were placed in the gel casting tray to wait until it is solid. Once solidified, agarose gel was placed into the electrophoresis chamber filled with 1xTAE buffer. Combs were carefully removed; DNA ladder standard and samples were carefully loaded. The running process is 100V, 200mA for 1h. When gel is ready, DNA fragments were visualized under ultraviolet (UV) light.

2.2.6 Western blot and Co-IP

2.2.6.1 Western Bolt

Cells were seeded into 6-well plates with or without stimulation. After incubation, cells were washed twice with cold PBS and then lysed with RIPA lysis buffer containing protease inhibitor and phosphatase inhibitor cocktails. Cell monolayers were scratched with a cell scraper and the lysate was collected into a tube. After incubation on ice for

20min, the cell extracts were centrifuged at 12000 rpm for 20 min at 4°C to get protein lysate. The supernatant containing total protein was removed into a new tube and the protein concentration was measured with BCA protein assay kit according to manufacturer's instructions. The protein concentration in samples obtained was calculated with reference to BSA standard curve. Samples containing 30ug protein were mixed with 4xloading buffer and heated at 95°C for 5 min. The whole protein was then separated by 12% SDS-PAGE gel and transferred onto nitrocellulose membranes. Later, the membranes were blocked with 5% non-fat milk in TBST for 1h at room temperature. Afterwards, membrane was probed with primary antibodies overnight at 4° C, washed with TBST for three times, and then second-antibody incubation for 1h at room temperature and washed again. GAPDH was used to verify the amount of protein loaded. The membrane was exposed using enhanced chemiluminescence (ECL) reaction system. Amersham Hyperfilms were used to detect Chemiluminescent signals. The films were scanned and quantified by Image J.

2.2.6.2 Co-IP

1*10⁶ cells were seeded on dishes with or without stimulation. Old medium was replaced with 10ml fresh medium supplement with 270ul formaldehyde. After incubation for 10min at 37°C, medium was abandoned and dishes were washed twice with PBS containing protease inhibitors. Cells were collected into a tube and centrifuged at 2000 rpm at 4°C for 4 mins to get cell pellets. Afterwards, cell pellets were resuspended with 200ul SDS lysis buffer containing protease inhibitors and incubated on ice for 10 min. Next, lysate was sonicated and centrifuged again at 13,000 rpm at 4°C for 10 min. The supernatant was removed into a new tube and then diluted with dilution buffer at 1:10. Subsequently, 2ml of diluted supernatant with 75ul Salmon Sperm DNA/Protein A Agarose-50% slurry incubated for 30 min at 4°C on a shaker. The mixture was centrifuged again and supernatant was removed into a new tube.

Primary antibody was added into the supernatant and incubated at 4°C overnight. Afterwards, 60ul of salmon sperm DNA/Protein A Agarose was added and incubated at 4°C on a shaker for 1h. The mixture was centrifuged again gently to get pellets. Then, pellets were washed with low salt immune complex wash buffer, high salt immune complex wash buffer and LiCl immune wash buffer at 4°C on a shake respectively. Pellets were washed again with TE buffer at room temperature for twice. After centrifugation, the complex pellets were resuspended at 50ul TE buffer, and then 1x loading buffer was added, mixed and heated at 95°C for 10min. At last, samples were collected for subsequent Western Blot.

2.2.7 Sphere-formation assay

Stimulated or transfected cells were digested and resuspended as signal cell suspension. After counting and calculation, 1000 cells in 100ul were resuspended in CSC medium. The CSC medium was supplemented with 1XB27, 1% penicillin/streptomycin, recombinant human epidermal growth factor (EGF) 10ng/ml and recombinant human fibroblast growth factor (FGF) 20ng/ml in DMEM/F12. Besides, 1% methylcellulose was added into medium to prevent cell-cell aggregation. Cells were seeded slowly into low attachment 96-well plates to avoid bubbles. Medium was changed every 3-4 days with or without stimulators as indicated in the text. After 12-15 days incubation at 37°C, spheres with more than 50 cells were counted. Images were taken by a microscope.

2.2.8 Colony-formation assay

Cells were digested and resuspended as signal cell suspension. 1000 cell were

counted and seeded into 6-well plates in complete RPMI1640 medium containing stimulators as indicated in the text. The cells were incubated at 37°C, 5% CO₂ for 7-10 days. After incubation, medium was removed and the plates were washed with PBS shortly. Afterwards, cells were fixed with 4% PFA for 20 min on a shaker, and washed again with PBS. Colonies were stained with 0.5% crystal violet for 10 mins on a shaker, and washed again. Clusters with approximately 50 cells or more were considered as a colony.

2.2.9 siRNA transfection

Cells were seeded into 24-well plates with about 60% confluence in RPMI1640 with 10% FBS only. After incubation overnight, the old medium was removed, and 400ul medium without FBS and P/S was added into plates. Next, LGR6 siPOOL dilution was prepared by adding 10µl of 0.15µM LGR6 siPOOL stock solution into 40µl medium, negative control was prepared the same way. RNAiMAX dilution was made by pipetting 1µl RNAiMAX into 49µl medium. Afterwards, either LGR6 siPOOL dilution and RNAiMAX dilution, or negative control siRNA dilution and RNAiMAX dilution were combined at a ratio of 1:1 and mixed well by pipetting up and down. After incubation for 10 min at room temperature to allow transfection complex formation, the mixture was added drop-wise into the cell culture plate. The plate was gently shaken and kept in incubator at 37°C, 5% CO₂ for 24h or 48h. RNA was isolated 48h after transfection. RT-PCR was performed to test the efficiency of transfection. For sphere formation assay and colony formation assay, the cells were collected 24h after transfection.

2.2.10 Immunofluorescence staining

2.5*10⁵ cells in 2ml RPMI 1640 media with 10% FBS were seeded on coverslips in 6-well plates. After stimulation, the slides were washed with PBS shortly and then fixed with 4% PFA for 20 mins. It was followed by endogenous peroxidase blocking buffer for 10 min on a shaker, and washed with PBST for 5 mins. Afterwards, the cells were permeabilized with 0.1% Triton X-100/PBS for 10 min on a shaker, followed by 5 min wash with PBST. After blocking with 5% goat serum for 1h at room temperature, the cells were incubated with primary antibody at 4°C overnight. Afterwards, the cells were washed again and incubated with followed second antibody incubation at room temperature for 1h in dark. Nucleus were counterstained with Hoechst (1:10.000 in PBS) for 5 min and followed by washing for 5 min. Lastly, slides were mounted in Fluorescence Mounting Medium and evaluated by fluorescence microscope with specific filter to select individual fluorescence. Images were captured by software ZEN2.0.

2.2.11 Flow cytometry

Cells with or without stimulation were trypsinized, washed and collected into a tube. For membrane-bound LGR6 analysis, cells were incubated with human LGR6 APC-conjugated antibody for 30 min at room temperature and washed with PBS, after centrifugation at 500g for 5 min, cell pellet was suspended with PBS again. For cytoplasmic LGR6, cells were washed with PBS and centrifuged at 500g for 5 min, the supernatant was removed and cells were fixed with 100ul IC fixation buffer for 30 min at 4°C, afterwards were washed with 1 ml permeabilization buffer at 500g for 5 min for twice. Next, cells were incubated with LGR6 antibody for 30min at room temperature. After washing again with permeabilization buffer and PBS respectively, cells were

analyzed by BD LSR Fortessa. Negative control was prepared in the same procedures, but without antibody incubation.

2.2.12 Cell viability assay

Cell viability on gemcitabine was analyzed by WST1 assay. 5000 cells were seeded into 96-well plates and attached overnight. Medium was changed with or without gemcitabine the following day. Cells were cultured at incubator for 72h at 37°C, 5% CO₂. The medium was removed and WST1 solution was added according to manufacturer's protocol. 10ul WST1 in 100ul medium was added into each well of plates, a negative control was made as a reference. After incubation for 1-2h, OD value was quantified by measuring the absorbance at 450nm and references at 620nm on a plate reader. The relative cell viability was calculated by Excel.

2.2.13 Statistical analysis

Statistical analysis was performed by GraphPad Prism. Data are represented as mean \pm SEM. Comparisons was made by t test. P <0.05 was considered as statistically significant.

3. Results

3.1 Prediction of LGR6 as a WNT target gene

Gene Set Enrichment Analysis (GSEA) is a powerful software to identify gene expression data sharing biological functions or mechanisms in pathways and processes. We applied GSEA to uncover the correlation of WNT signaling associated gene sets in MSigDB with LGR6 expression in pancreatic cancer patients. Gene sets including HERBST_WNT_TARGETS_GENOMICS (64 gene sets), HERBST_WNT_TARGETS_UP (122 gene sets), NUSSE_WNT_TARGETS_IN_INTESTINE_OR_COLON_CANCER (35 gene sets) were collected. The most WNT-positive correlated gene sets located in high LGR6 expressed samples. Normalized enrichment score and False discovery rate were calculated respectively. NES =1.88, FDR =0.0 in HERBST_WNT_TARGETS_GENOMICS; NES = 1.80, FDR =0.0 in HERBST_WNT_TARGET_UP, NES=1.86, FDR =0.0 in NUSSE_WNT_TARGETS_IN_INTESTINEOR_COLON_CANCER (Figure 3.1).

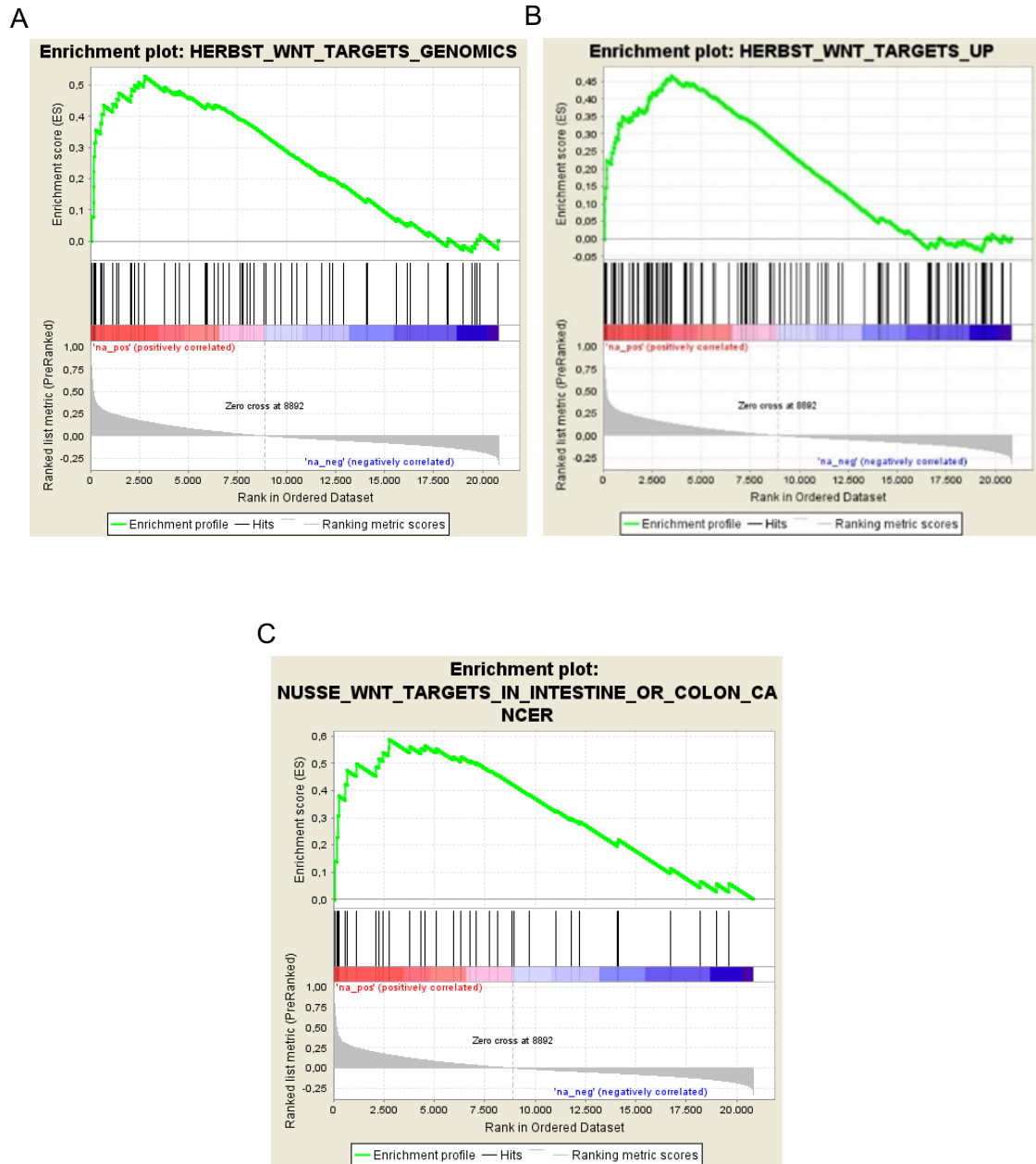


Figure 3.1: GSEA enrichment plots of WNT signaling signature positively correlated with LGR6 expression in pancreatic cancer. (A) Gene set: HERBST_WNT_TARGETS_GENOMICS; (B) Gene set: HERBST_WNT_TARGETS_UP; (C) Gene set: NUSSE_WNT_TARGETS_IN_INTESTINE_OR_COLON_CANCER.

3.2 Activation of canonical WNT signaling mediates LGR6 expression

As reported before, the stimulation of PDAC cells with RSPO2 resulted in an increased WNT activity in high responder cells [157]. To evaluate whether LGR6 expression could be altered by WNT signaling, we activated canonical WNT signaling pathway by treating Panc1 and Capan2 with human recombinant RSPO2, WNT3a or a combination thereof. To confirm whether the WNT signal pathway was activated by such stimulation, qPCR analysis for typical WNT target genes (*AXIN2*) was evaluated. No apparent increase was observed upon RSPO2 stimulation alone in both cell lines, while WNT3a has limited effect on *AXIN2* increase in Panc1 (Figure 3.2.1). The results are in line with the fact that exogenous WNT3a is required for functional effects of RSPO2 to enhance WNT signaling.

Phosphorylation of β -catenin at Ser⁶⁷⁵ leads to its accumulation in the nucleus thereby enhancing transcriptional WNT activity. Therefore, we performed Western blot to analyze the change of phospho- β -catenin-Ser⁶⁷⁵ upon RSPO2 and/or WNT3a stimulation. An increased phospho- β -catenin-Ser⁶⁷⁵ expression level was observed upon RSPO2 and WNT3a stimulation in Panc1, while total β -catenin expression remained the same, demonstrating that the differences of phospho- β -catenin-Ser⁶⁷⁵ is not due to total β -catenin up-regulation. However, no apparent changes were observed in either RSPO2 or WNT3a stimulation of Panc1. Besides, the differences of phospho- β -catenin-Ser⁶⁷⁵ were not significant upon stimulation with RSPO2 and/or WNT3a in Capan2 (Figure 3.2.2).

The activation of WNT signaling can also be detected by the translocation of β -catenin to the nucleus; therefore, we performed immunofluorescence staining to show the distribution of β -catenin in response to above mentioned stimuli. We found that β -catenin was predominantly located at the cell membrane in the untreated group (white

arrow) (Figure 3.2.3). After 24h culture with RSPO2, it showed a limited effect on β -catenin translocation into the nucleus (red arrow). The addition of WNT3a as well as RSPO2 led to a significant increase of nuclear β -catenin, implying an activated WNT signaling.

Afterwards, LGR6 expression was analyzed by Western Blot to see whether its expression correlated with WNT activity. As shown in Figure 3.2.4, LGR6 expression was up-regulated upon simultaneous stimulation with RSPO2 and WNT3a in both Capan2 and Panc1. These observations gave a hint that WNT/ β -catenin activation may correlate with high LGR6 expression.

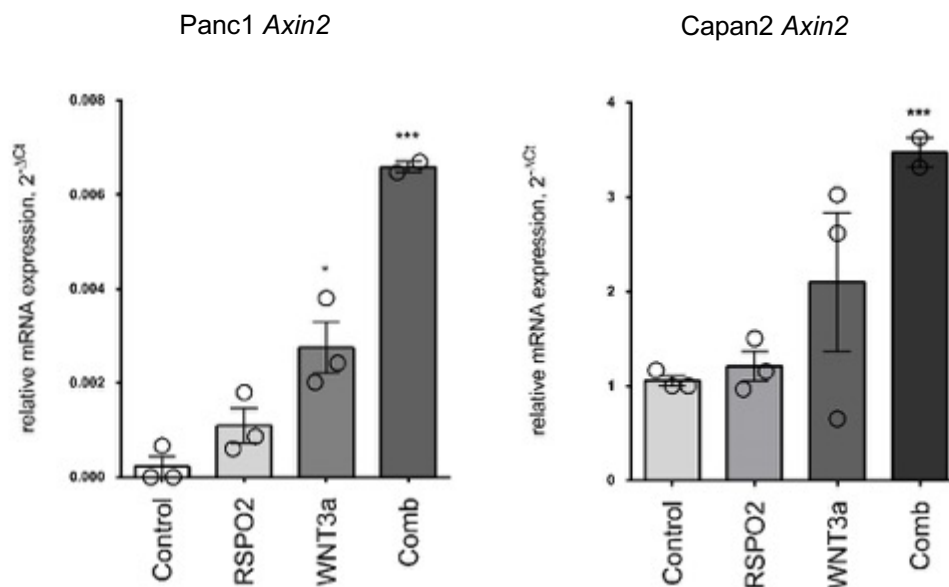


Figure 3.2.1: PCR analysis of AXIN2 mRNA levels upon RSPO2 and/or WNT3a stimulation in Panc1 and Capan2. No significant changes were detected upon RSPO2 stimulation in both cell lines. WNT3a alone increased AXIN2 expression in Panc1. *, $P < 0.05$. The combination of RSPO2 and WNT3a had elevated effects on AXIN2 expression in both cell lines. ***, $P < 0.001$.

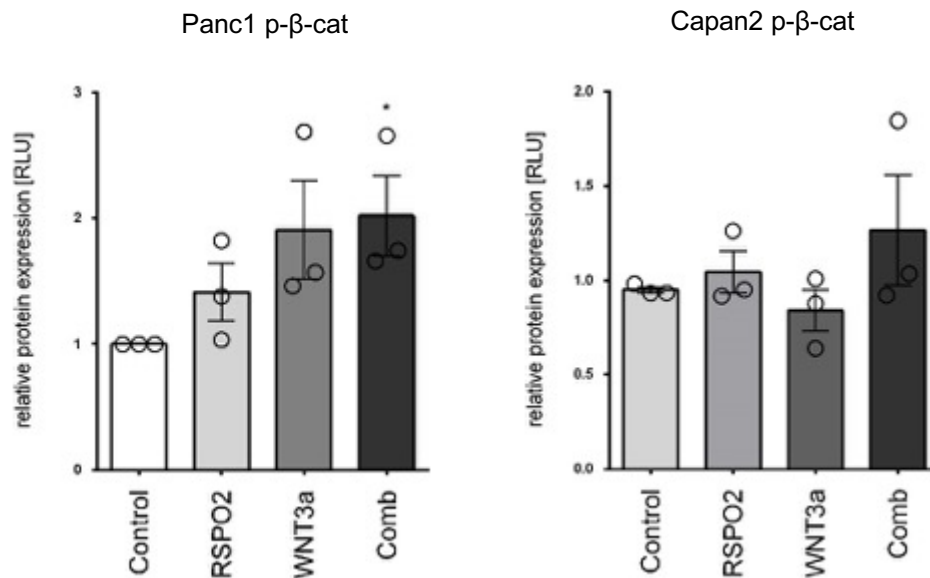
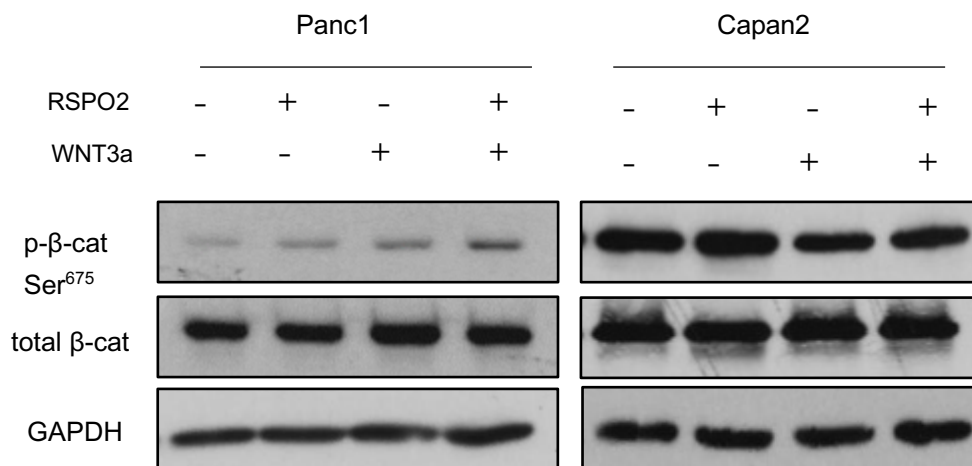
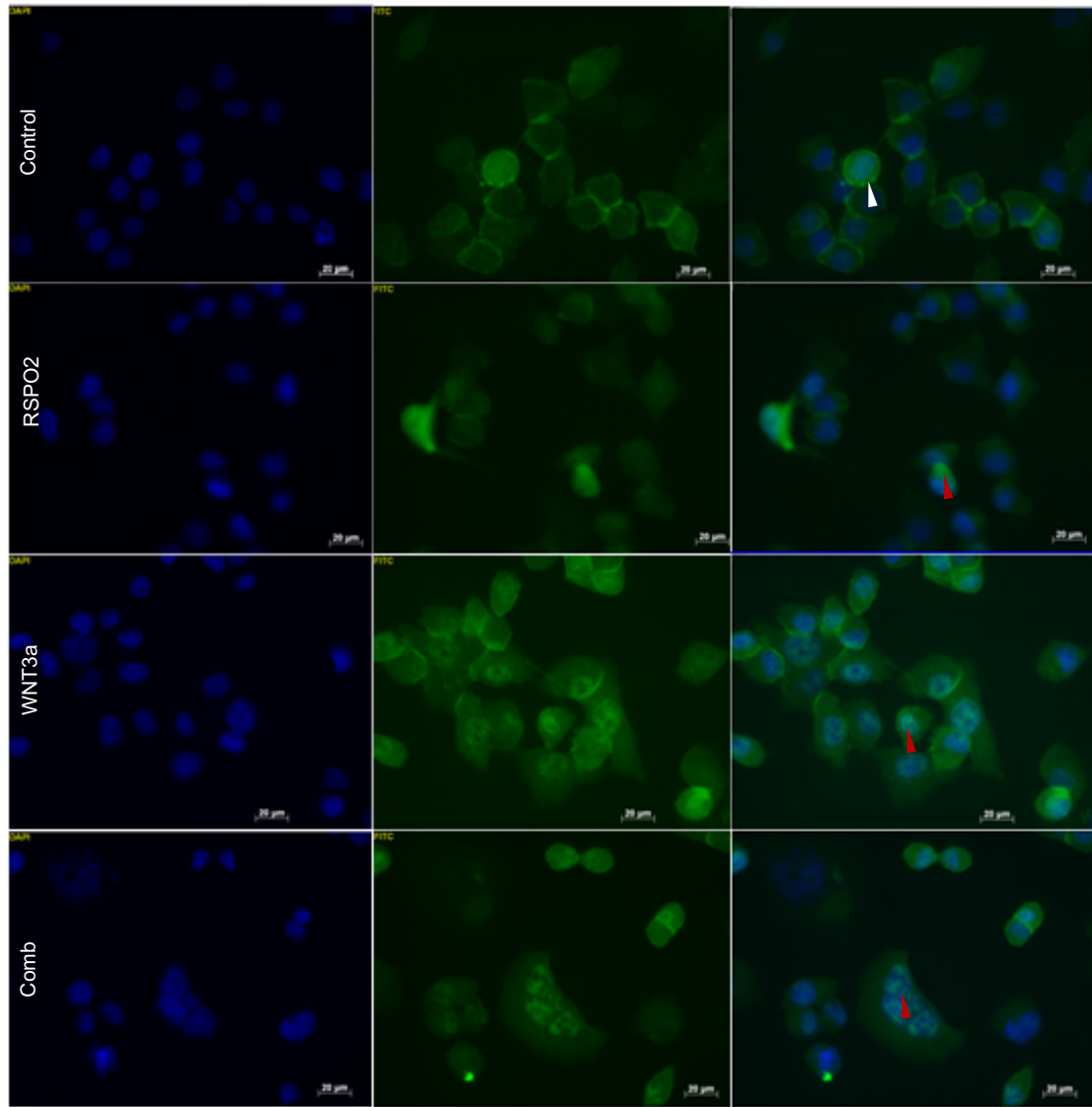


Figure 3.2.2: Western Blot analysis of phospho-β-catenin-Ser⁶⁷⁵ and total β-cat expression after RSPO2 and/or WNT3a stimulation. An increase of phospho-β-catenin Ser⁶⁷⁵ was only seen in Panc1 upon the double stimulation of RSPO2 and WNT3a. *, P<0.05. No significant differences were observed in Capan2. GAPDH was used as loading control. Quantification evaluation was performed by ImageJ.



—20μm

Figure 3.2.3: Immunofluorescence staining of β -catenin in Panc1 after stimulation with RSPO2 and/or WNT3a. Panc1 cells were cultured with or without RSPO2 (20ng/ml)/WNT3a(100ng/ml) and stained for β -catenin (green). Nuclei were counterstained with DAPI (blue). In the absence of RSPO2 and WNT3a, most β -catenin located on cell membrane. In the presence of RSPO2, a limited increase of nuclear β -catenin was seen. While cultured with both RSPO2 and WNT3a, considerable increase of nuclear β -catenin was shown. White arrows, membrane-bound β -catenin; red arrows, cytoplasmic β -catenin. Bar,20μm.

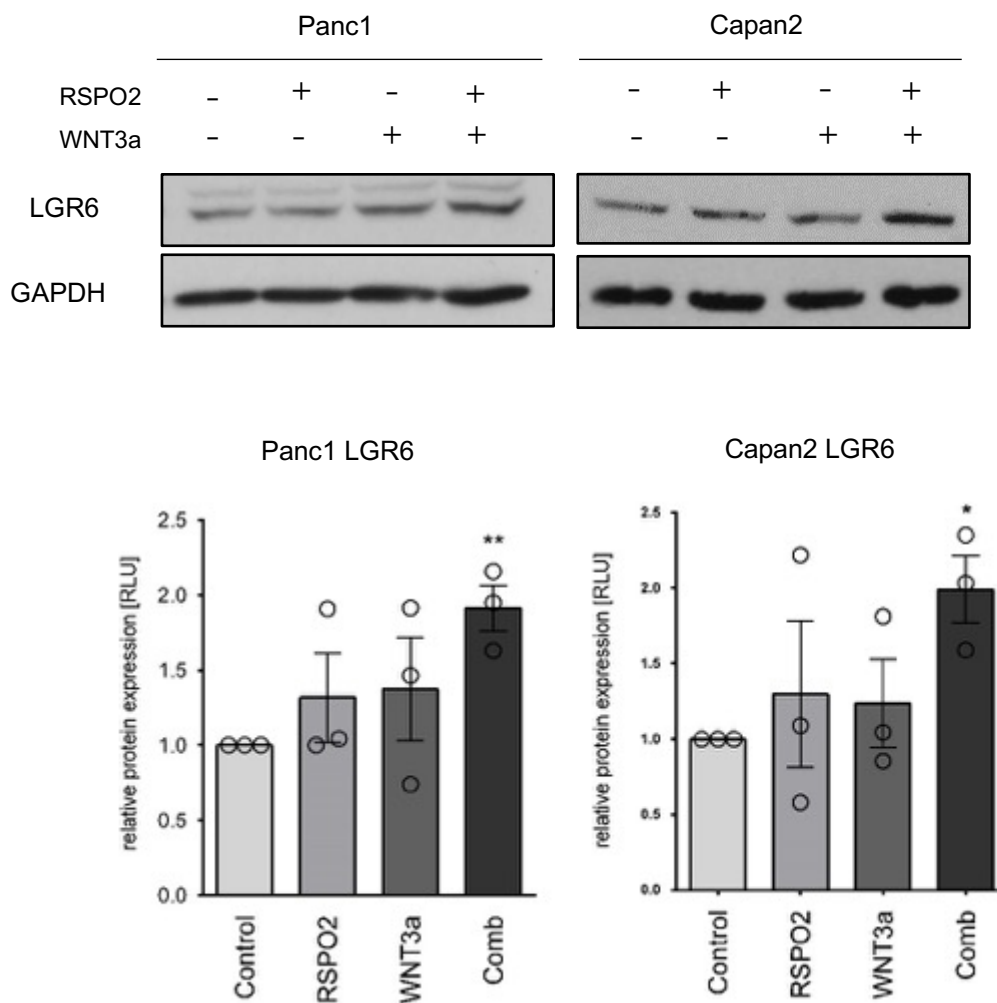


Figure 3.2.4: Western Blot analysis of LGR6 after RSPO2 and/or WNT3a stimulation. An increased LGR6 expression was shown both in Panc1 and Capan2 upon RSPO2 and WNT3a stimulation. **, $P < 0.01$ in Panc1 and *, $P < 0.05$ in Capan2. No significant difference was seen in either RSPO2 or WNT3a stimulation in both cell lines. GAPDH was used as loading control. Quantification evaluation was performed by ImageJ.

3.3 Inhibition of the WNT signal pathway decreases LGR6 expression

To further investigate the regulatory effects of WNT signaling on LGR6 expression, we pharmacologically inhibited the WNT signaling activity by IWP2, a porcupine inhibitor, that negatively regulates canonical WNT signaling. As shown in Figure 3.3.1, the inhibitory effect was represented by down-regulation of the WNT target gene *AXIN2* in

Capan2. Such WNT inactivation by IWP2 was also revealed by decreased phospho- β -catenin-Ser⁶⁷⁵ levels by Western blot (Figure 3.3.2). Besides, qPCR was carried out to investigate whether LGR6 expression in Capan2 changed upon IWP2 treatment. As shown in Figure 3.3.3, down-regulation of the WNT signal pathway by IWP2 lead to a reduced LGR6 expression on mRNA level in Capan2, but not on protein level (Figure 3.3.4). These data suggest inhibition of the WNT signaling might lead to a decrease of LGR6 expression.

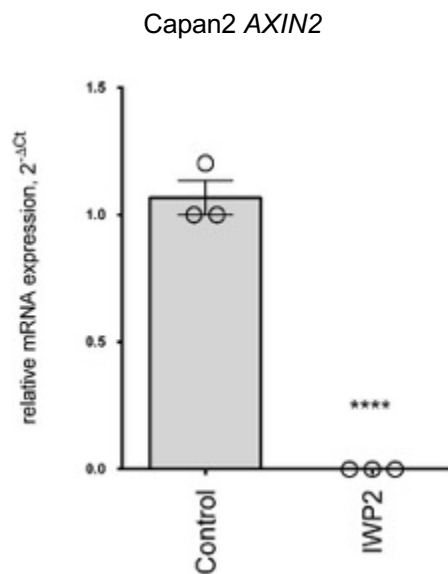


Figure 3.3.1: Effect of IWP2 on *AXIN2* mRNA expression in Capan2. The cells were cultured with 10uM IWP2 for 72h, medium was changed every other day. PCR analysis of *AXIN2* suggests significant decrease in presence of IWP2. ***, $P < 0.001$.

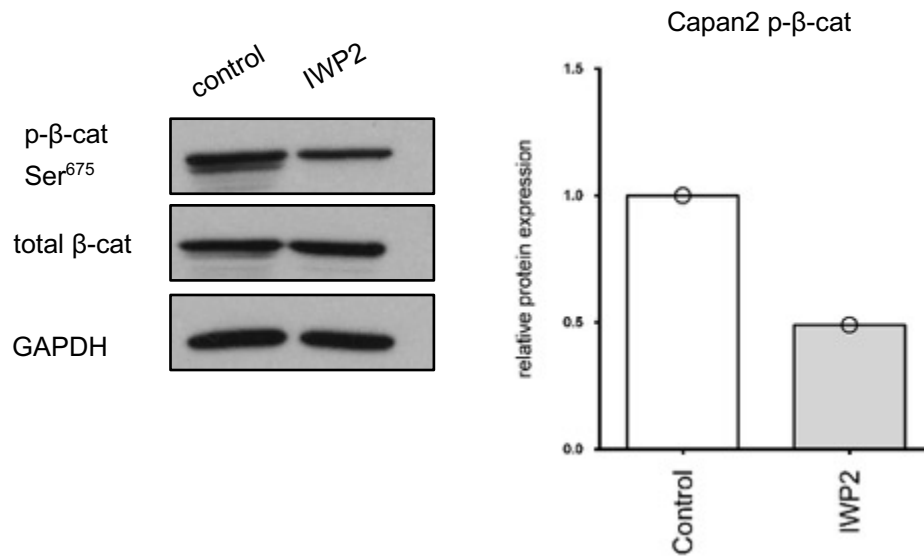


Figure 3.3.2: Evaluation of phospho-β-catenin-Ser675 and total β-cat expression with IWP2 treatment in Capan2. The cells were cultured with 10uM IWP2 for 72h. phospho-β-catenin-Ser675 expression decreased in the presence of IWP2. GAPDH served as loading control. Quantification evaluation was performed by ImageJ.

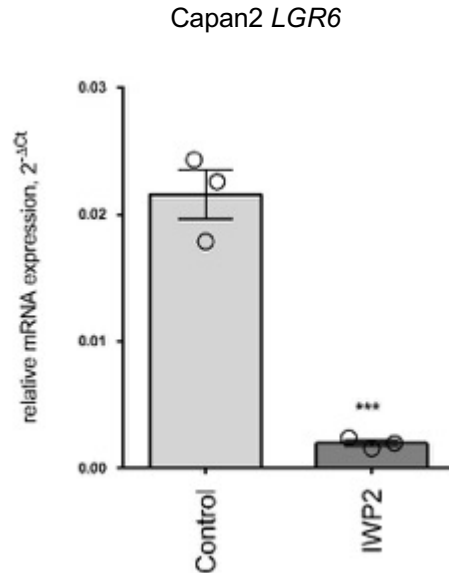


Figure 3.3.3: Effect of IWP2 on *LGR6* mRNA expression in Capan2. The cells were cultured with 10uM IWP2 for 72h, medium was changed every other day. PCR analysis of *LGR6* showed significant decrease in presence of IWP2 ***, P<0.001.

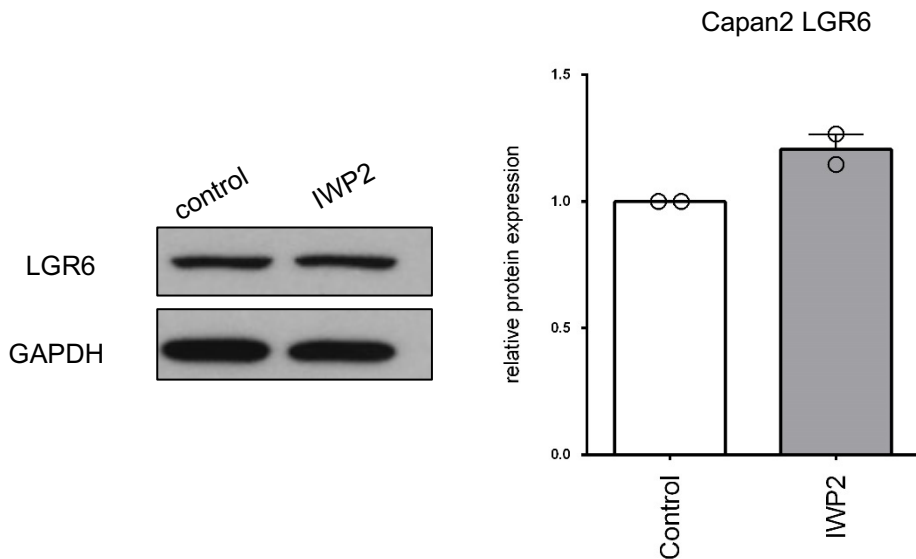


Figure 3.3.4: Western blot analysis of LGR6 expression upon IWP2 treatment in Capan2. The cells were cultured with 10uM IWP2 for 72h, medium was changed every other day. WB analysis of LGR6 detected no significant changes in presence of IWP2. GAPDH was used as loading control. Quantification evaluation was performed by ImageJ.

3.4 Prediction of LGR6 as an indicator of EMT

GSEA was used to investigate whether LGR6 expression correlated with typical epithelial/mesenchymal gene signatures. Accordingly, EMT signature gene sets were chosen from MSigDB including GOTZMANN_EPITHELIAL_TO_MESENCHYMAL_TRANSITION_UP (69 gene sets); JECHLINGER_EPITHELIAL_TO_MESENCHYMAL_TRANSITION_UP (71 gene sets); ANASTASSIOU_CANCER_MESENCHYMAL_TRANSITION_SIGNATURE (64 gene sets); TAUBE_CORE_EPITHELIAL_TO_MESENCHYMAL_TRANSITION_INTERACTOME_GENE-EXPRESSION_SIGNATURE (91 gene sets). GSEA then suggested that high LGR6 expression positively correlated with epithelial features as shown in Figure 3.4.1. NES = -1.29, FDR=0.05 in JECHLINGER_EPITHELIAL_TO_MESENCHYMAL_TRANSITION_UP; NES = -2.58, FDR=0.0 in TAUBE_CORE_EPITHELIAL_TO_MESENCHYMAL_TRANSITION_INTERACTOME_GENE-EXPRESSION_

SIGNATURE; NES =-1.49, FDR=0.01 in GOTZMANN_EPITHELIAL_TO_MESENCHYMAL_TRANSITION_UP; NES=-2.85, FDR=0.0 in ANASTASSIOU_CANCER_MESENCHYMAL_TRANSITION_SIGNATURE. It might indicate that LGR6 correlates with a less aggressive form or phenotype of PDAC.

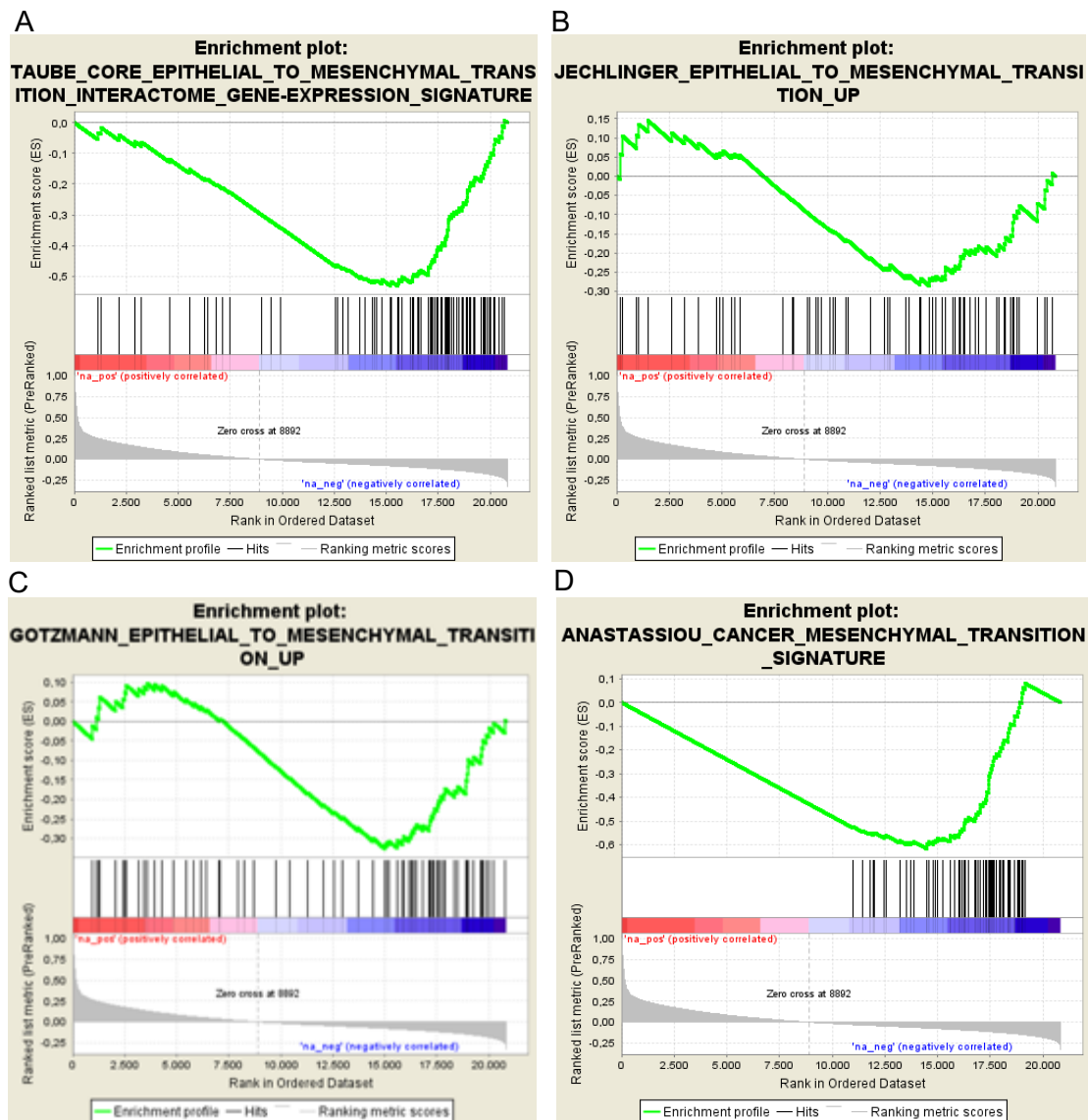


Figure 3.4.1: GSEA enrichment plots of Epithelial signatures negatively correlated with LGR6 expression in pancreatic cancer. (A) Gene set: JECHLINGER_EPITHELIAL_TO_MESENCHYMAL_TRANSITION_UP; (B) Gene set: TAUBE_CORE_EPITHELIAL_TO_MESENCHYMAL_TRANSITION_INTERACTOME_GENE-EXPRESSION_SIGNATURE; (C) Gene set: GOTZMANN_EPITHELIAL_TO_MESENCHYMAL_TRANSITION_UP; (D) Gene set: ANASTASSIOU_CANCER_MESENCHYMAL_TRANSITION_SIGNATURE.

3.5 LGR6 expression varies in typical epithelial and mesenchymal PDAC cell Lines

Pancreatic cancer cell lines were categorized into epithelial and mesenchymal phenotypes according to their morphology as well as expression analysis of the epithelial marker E-cadherin. PDAC cell lines, such as Capan2 and BxPC3, were defined as epithelial due to their strong cell-cell connections and cluster-like appearance. In contrast, MiaPaCa2 and Panc1 possess loose cell-cell connections with a spindle-like phenotype and were therefore considered mesenchymal (Figure 3.5.1). Furthermore, EMT markers were detected using qPCR. *CDH1* was highly expressed in epithelial cell lines, while the transcription factor *ZEB1* was more expressed in mesenchymal cell lines (Figure 3.5.2). Western blot analysis also detected considerable E-cadherin and β -catenin expression in epithelial PDAC cell lines (Figure 3.5.3).

To understand LGR6 expression pattern in the above-defined cell lines, we detected LGR6 expression on both mRNA and protein level. Notably, higher *LGR6* expression levels were detected in epithelial cell lines (BxPC3 and Capan2) compared to mesenchymal cell lines (MiaPaCa2 and Panc1) by both conventional PCR and RT-PCR (Figure 3.5.4). In addition, these findings were corroborated by Western blot showing similar results (Figure 3.5.5). The differential expression of LGR6 in defined epithelial and mesenchymal PDAC cell lines was then analyzed by immunofluorescence staining. Strong LGR6 signals can be seen on the cell membrane in the epithelial cell lines BxPC3 and Capan2, compared to cytoplasmic LGR6 staining in the mesenchymal cell line MiaPaCa2. LGR6 was not detectable in Panc1 (Figure 3.5.6). Distinct distribution pattern of LGR6 in such cell lines suggest LGR6 could correlate with the phenotype of PDAC cell lines.

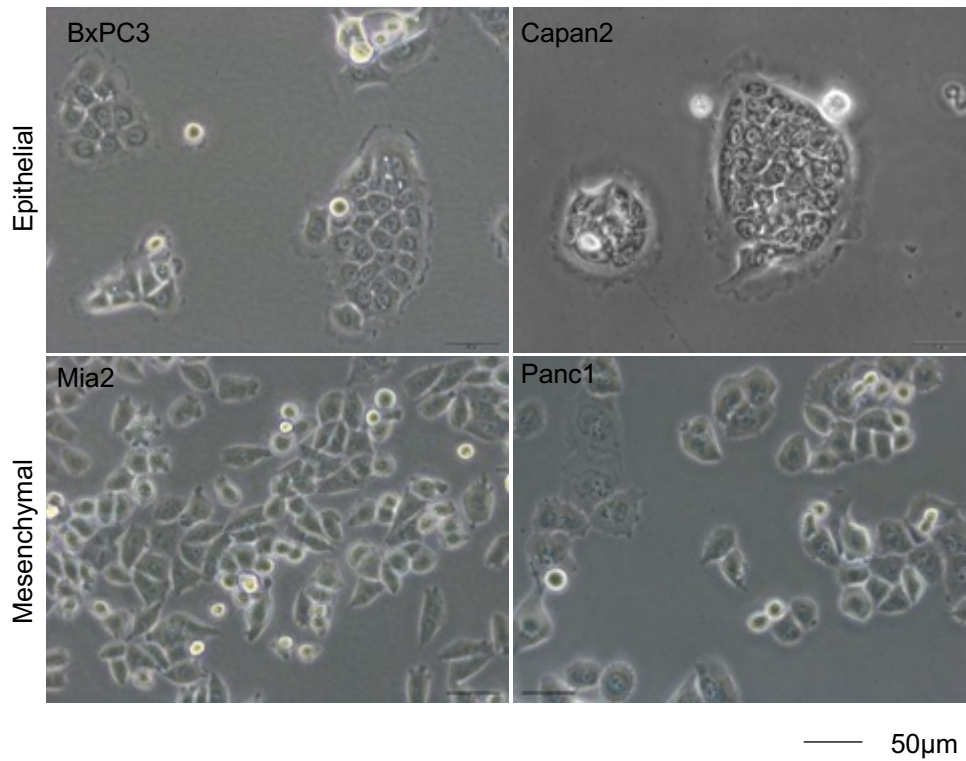


Figure 3.5.1: Morphology of defined epithelial and mesenchymal PDAC cell lines. BxPC3 and Capan2 have strong cell-cell connection, while MiaPaCa2 and Panc1 are spindle like cells with less cell-cell adhesions. Bar, 50µm.

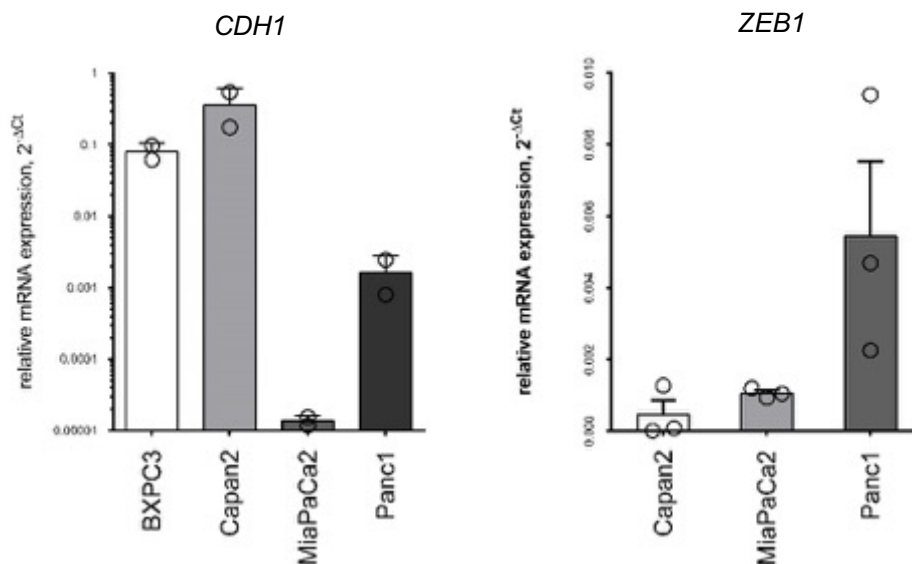


Figure 3.5.2: Evaluation of *CDH1* and *ZEB1* in PDAC cell lines. qPCR was used to assess EMT markers. Epithelial PDAC cell lines BxPC3 and Capan2 have higher *CDH1* and lower *ZEB1* expression levels, while mesenchymal cells express more *ZEB1* and less *CDH1*.

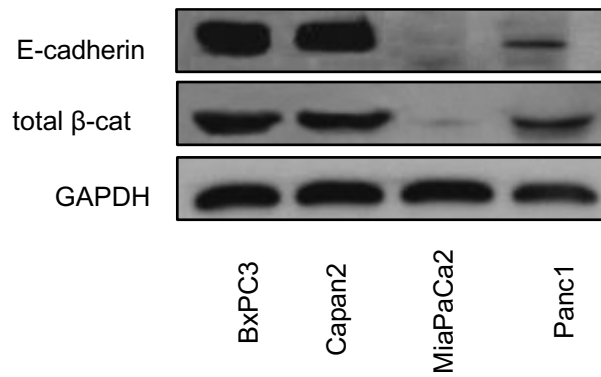


Figure 3.5.3: E-cadherin and β -catenin expression in PDAC cell lines. Western blot analysis showed higher expression of E-cadherin and β -catenin compared to mesenchymal ones. GAPDH was used for loading control. Quantification evaluation was performed by ImageJ.

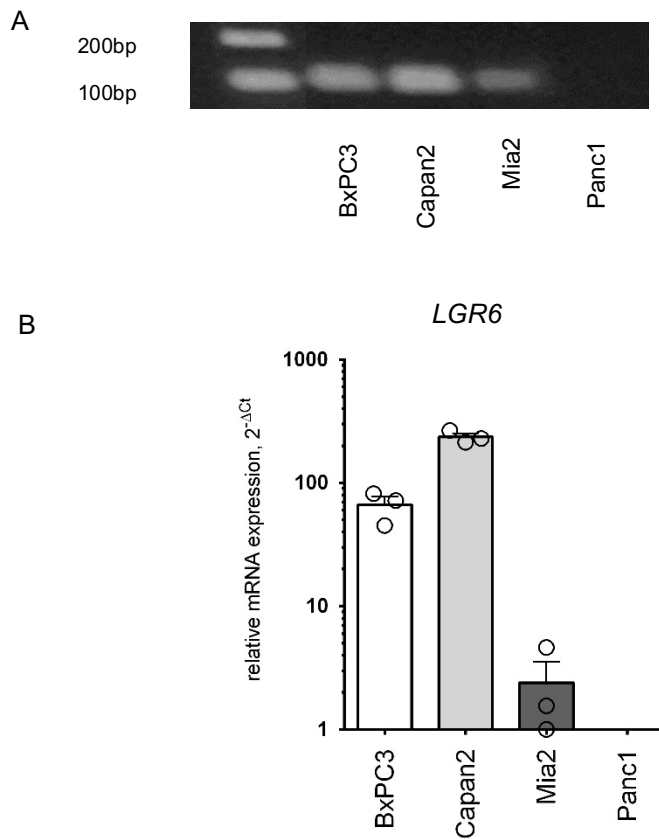


Figure 3.5.4: Evaluation of *LGR6* mRNA expression in PDAC cell lines by PCR. (A) *LGR6* RNA expression levels of PDAC cell lines were accessed by conventional PCR, molecular marker of 100bp and 200bp were set in a 1.5% agarose gel. (B) *LGR6* expression was measured by qPCR. Compared to BxPC3 and Capan2, *LGR6* was expressed to a lower degree in MiaPaCa2 and Panc1.

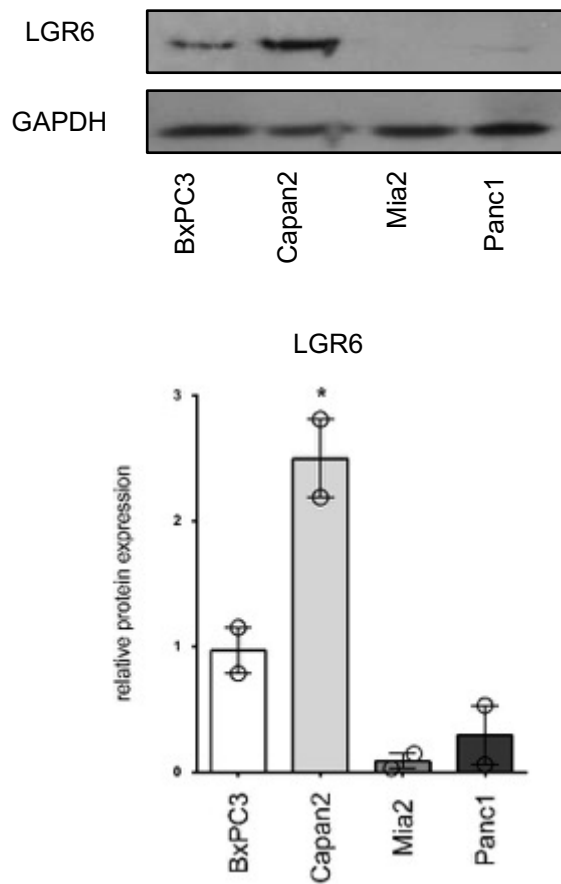


Figure 3.5.5: Western blot analysis of LGR6 expression in PDAC cell lines. LGR6 was highly expressed in BxPC3 and Capan2 compared to MiaPaCa2 and Panc1. GAPDH served as loading control. Quantification evaluation was performed by ImageJ.

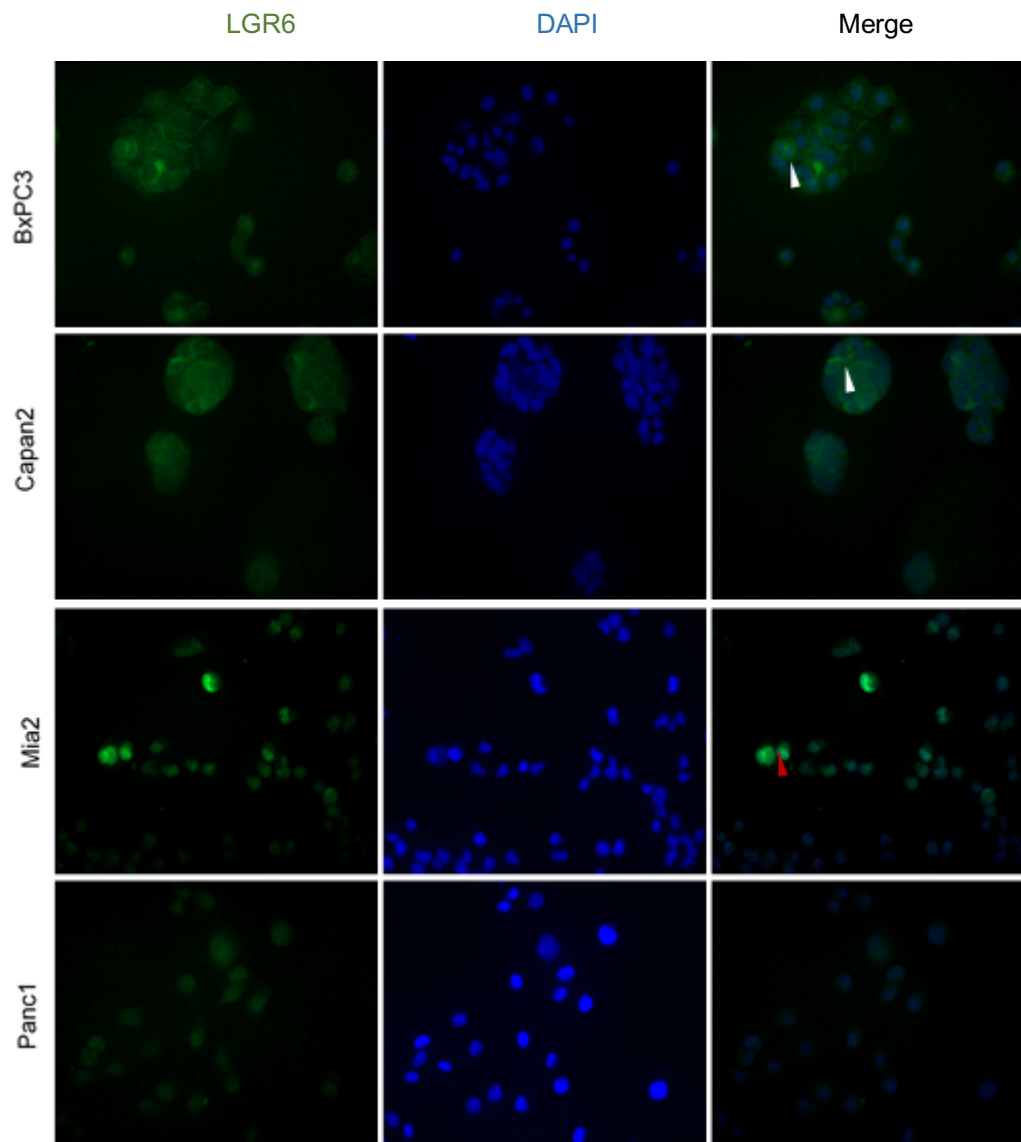


Figure 3.5.6: Immunofluorescence staining of LGR6 in PDAC cell lines. Representative immunofluorescence images showed LGR6 expression pattern in defined epithelial and mesenchymal PDAC cell lines. LGR6 was detected by FITC-labeled antibody (green). Nuclei were counterstained using DAPI (blue). White arrows, membrane-bound LGR6; red arrows, cytoplasmic LGR6.

3.6 LGR6 may participate in cell adhesion in epithelial PDAC cell lines

As LGR6 was preferentially expressed in epithelial PDAC cell lines, we next explored whether there might be a direct correlation between E-cadherin and LGR6. Therefore, Co-IP was conducted to investigate such a connection. Co-IP is a technique to analyze

protein–protein interactions by precipitating intact protein complexes using specific antibodies. By targeting a known protein, it is possible to identify the associated proteins in a presumed complex. E-cadherin was used as a positive control, because of the assembly of E-cadherin/ β -catenin in cell junction stabilization. As shown in Figure 3.6.1, β -catenin was pulled down by E-cadherin in BxPC3 and Capan2, while such connection lacked in Panc1 and MiaPaCa2.

Next, we detected the association of E-cadherin and LGR6 in Capan2 and BxPC3 with or without WNT3a stimulation. WNT3a has limited effect on the association of E-cadherin and β -catenin. However, such connection cannot be seen in MiaPaCa2 and Panc1 (Figure 3.6.2). Furthermore, the results were confirmed by immunofluorescence staining using E-cadherin (red), LGR6 (green) and β -catenin (green) respectively. We observed co-localization of β -catenin, LGR6 and E-cadherin on the cell membrane in Capan2 (Figure 3.6.3). Taken together, these results suggest that LGR6 might participate in the cell adhesion complex of epithelial PDAC cell lines.

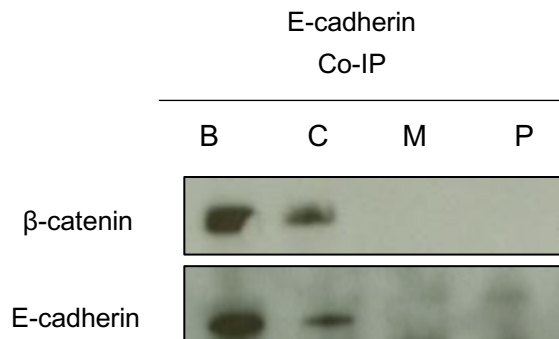


Figure 3.6.1: E-cadherin and β -catenin association. Total cell lysates from BxPC3, Capan2, Panc1, and MiaPaCa2 were collected and immunoprecipitation was carried out to show the association of E-cadherin and β -catenin. Anti-E-cadherin was used to pull-down E-cadherin and associated proteins.

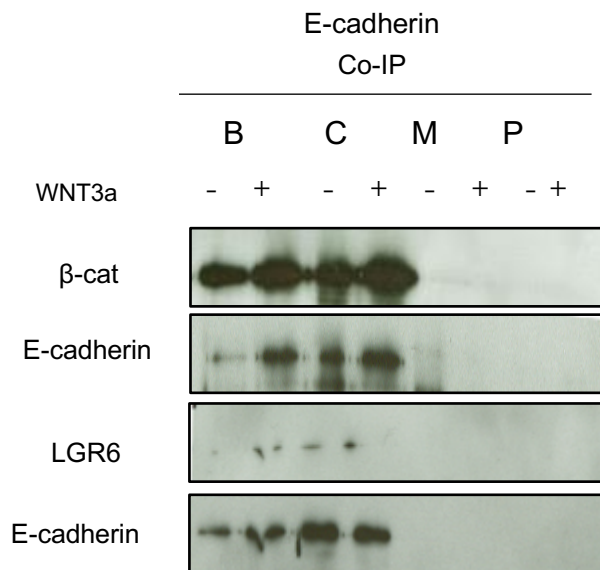


Figure 3.6.2: E-cadherin and LGR6 association. Total cell lysates from BxPC3, Capan2, Panc1, and MiaPaCa2 with/without WNT3a stimulation were collected. The association of E-cadherin and β -catenin was used as positive control. Immunoprecipitation showed an existing association of E-cadherin and LGR6 in Capan2 and BxPC3. WNT3a has limited (positive) effects on this correlation.

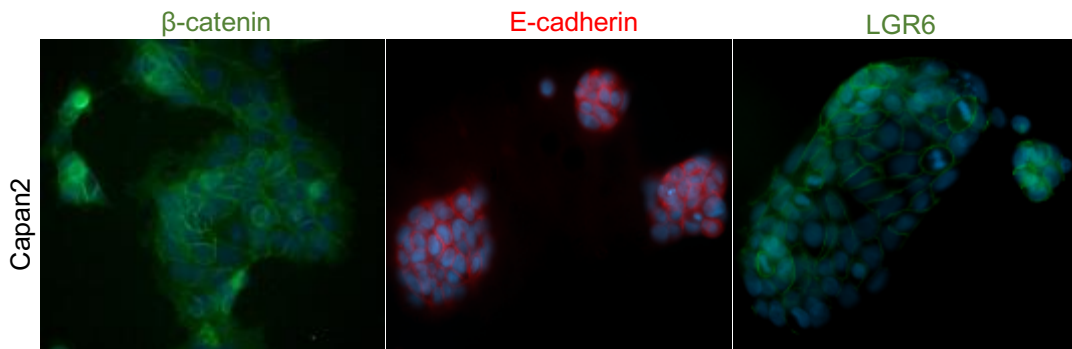


Figure 3.6.3: Co-localization of β -catenin, LGR6 and E-cadherin in Capan2. Immunofluorescence staining showed β -catenin (green), E-cadherin (red) and LGR6 (green) located in the cell membrane in Capan2. Nuclei were counterstained using DAPI (blue).

3.7 EMT induction changes LGR6 expression

We next hypothesized that LGR6 might be associated with EMT based on the noteworthy differences of LGR6 expression among defined epithelial and mesenchymal PDAC cell lines. EMT was therefore induced to examine the influence on LGR6 expression. Upon TGF β stimulation, Panc1 underwent EMT with the morphology of the cells shifting to a more mesenchymal phenotype with spindle-like appearance as shown in Figure 3.7.1. The reverse process of EMT, designated as MET, was achieved by treating cells with the MEK/ERK inhibitor U0126. Cells become tightly adherent compared to normal Panc1 cells. Next, we compared E-cadherin expression as an indicator of EMT induction. Western blot showed significant differences among the three groups. Thereafter, to investigate how changes in EMT could affect LGR6 expression, we used Western blot analysis to evaluate LGR6 expression in response to EMT induction. LGR6 was up-regulated upon TGF β stimulation. No LGR6 expression differences were observed between the control group and the U0126 group as measured. Although no significant differences were seen in AsPC1 upon the same procedure, it showed a similar tendency as detected in Panc1 on both E-cadherin and LGR6 expression (Figure 3.7.2).

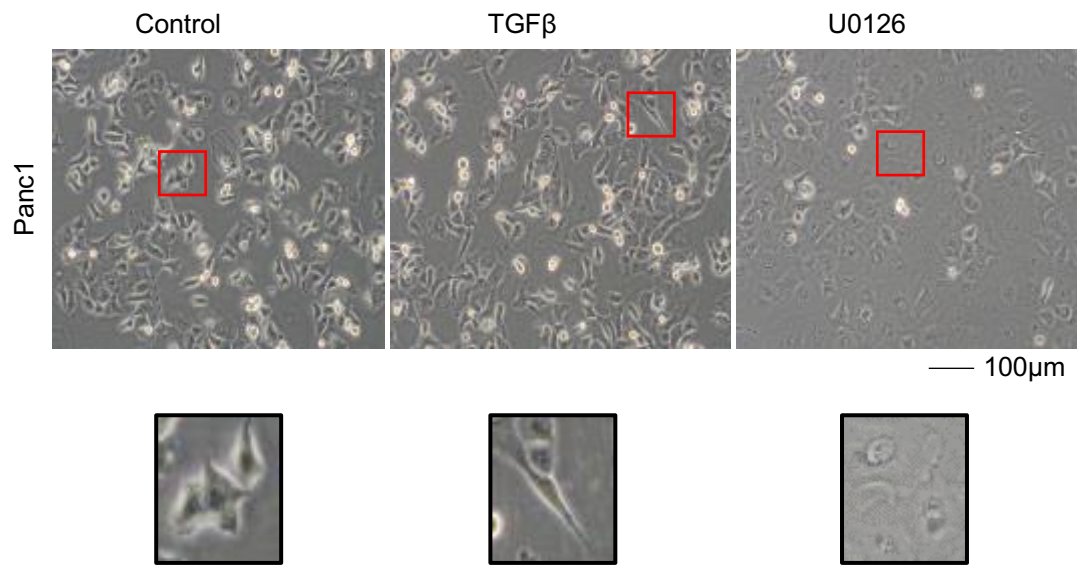


Figure 3.7.1: Morphological changes of Panc1 after EMT induction. The cells were cultured with 10ng/ml TGF β , or 10uM U0126 for 72h, medium was changed every other day. Red box, cells with typical phenotype; black box, magnification of typical phenotype. Bar,100 μ m.

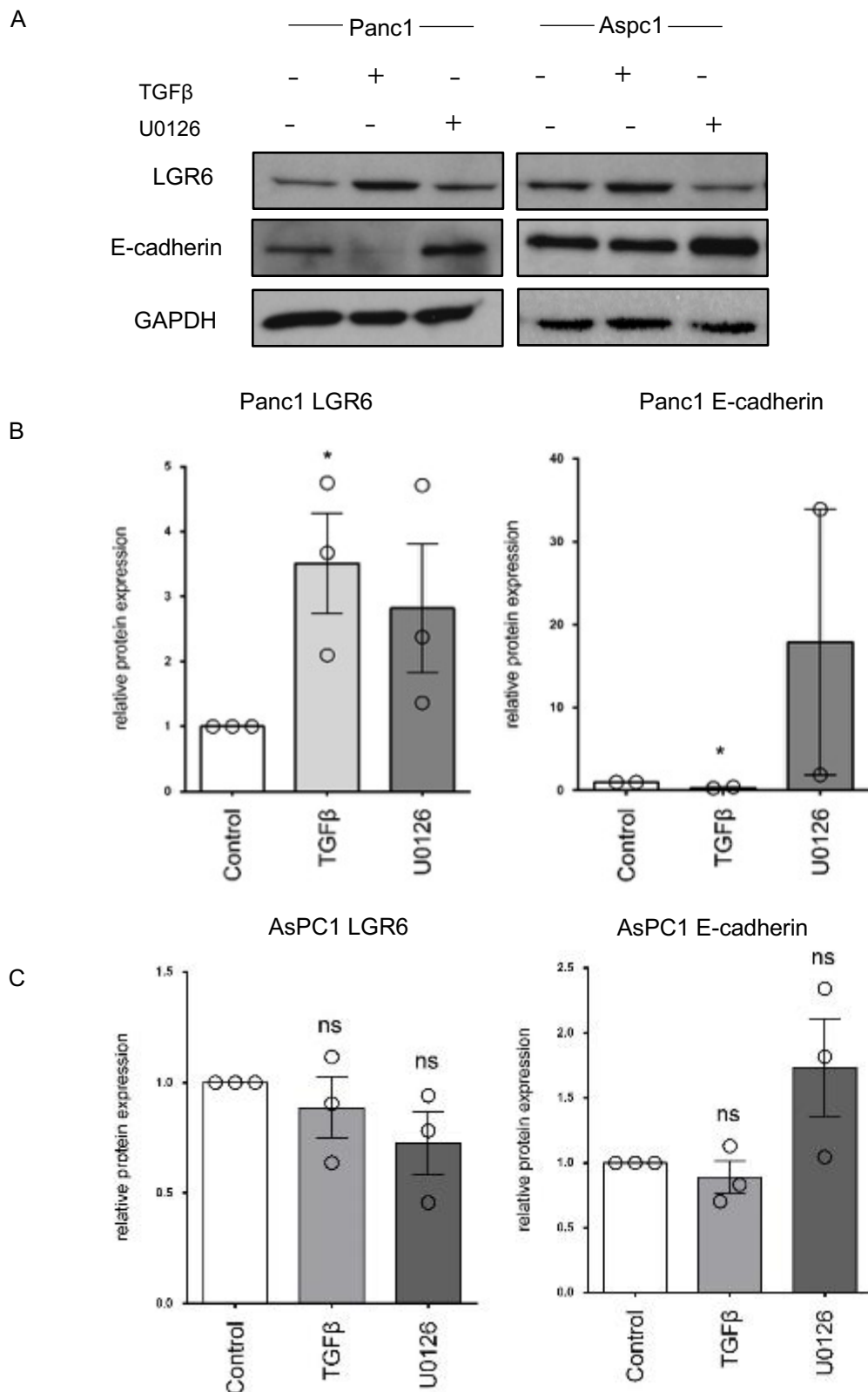


Figure: 3.7.2 Protein analysis of LGR6 and E-cadherin after EMT induction. The cells were cultured with 10ng/ml TGFβ, or 10uM U0126 for 72h, medium was changed every other day. GAPDH was used as loading control.

3.8 LGR6 depletion correlates with reduced cancer stemness

To explore the functional role of LGR6 on cancer cell stemness, we knocked down LGR6 by siRNA transfection in Capan2. The knock down efficiency was evaluated by qPCR, which showed a 90% decrease in mRNA level compared to vector control (Figure 3.8.1). Next, we evaluated the consequence of LGR6 silencing on colony formation ability. As shown in Figure 3.8.2A, the colonies are smaller in the siLGR6-transfected group compared to the vector control. Consistent with this, we conducted sphere-formation assays, a functional surrogate assay for cancer stemness, which showed a significantly decreased effect of LGR6 knock down on the size and numbers of spheroids compared with vector control (Figure 3.8.2B). These data suggest that LGR6 is associated with cancer cell stemness.

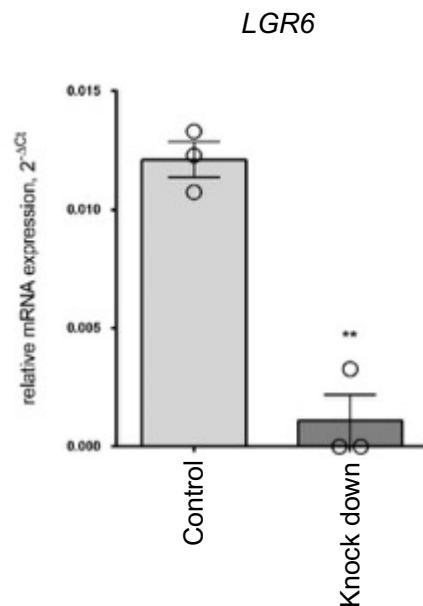
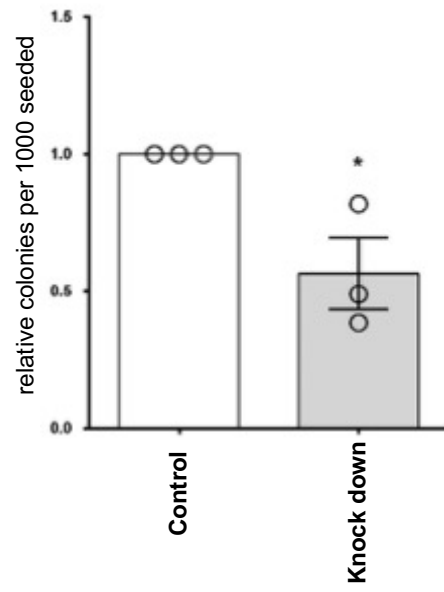
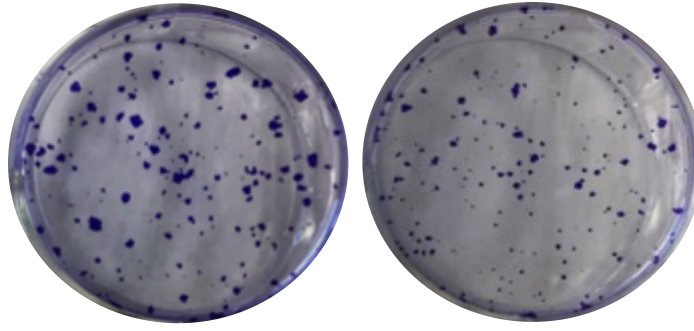


Figure 3.8.1: LGR6 knock down efficiency. Cells were transiently transfected with siRNA or vector control for 48h, RNA was collected and qPCR was performed. **, $P < 0.01$.

A

Control

Knock down



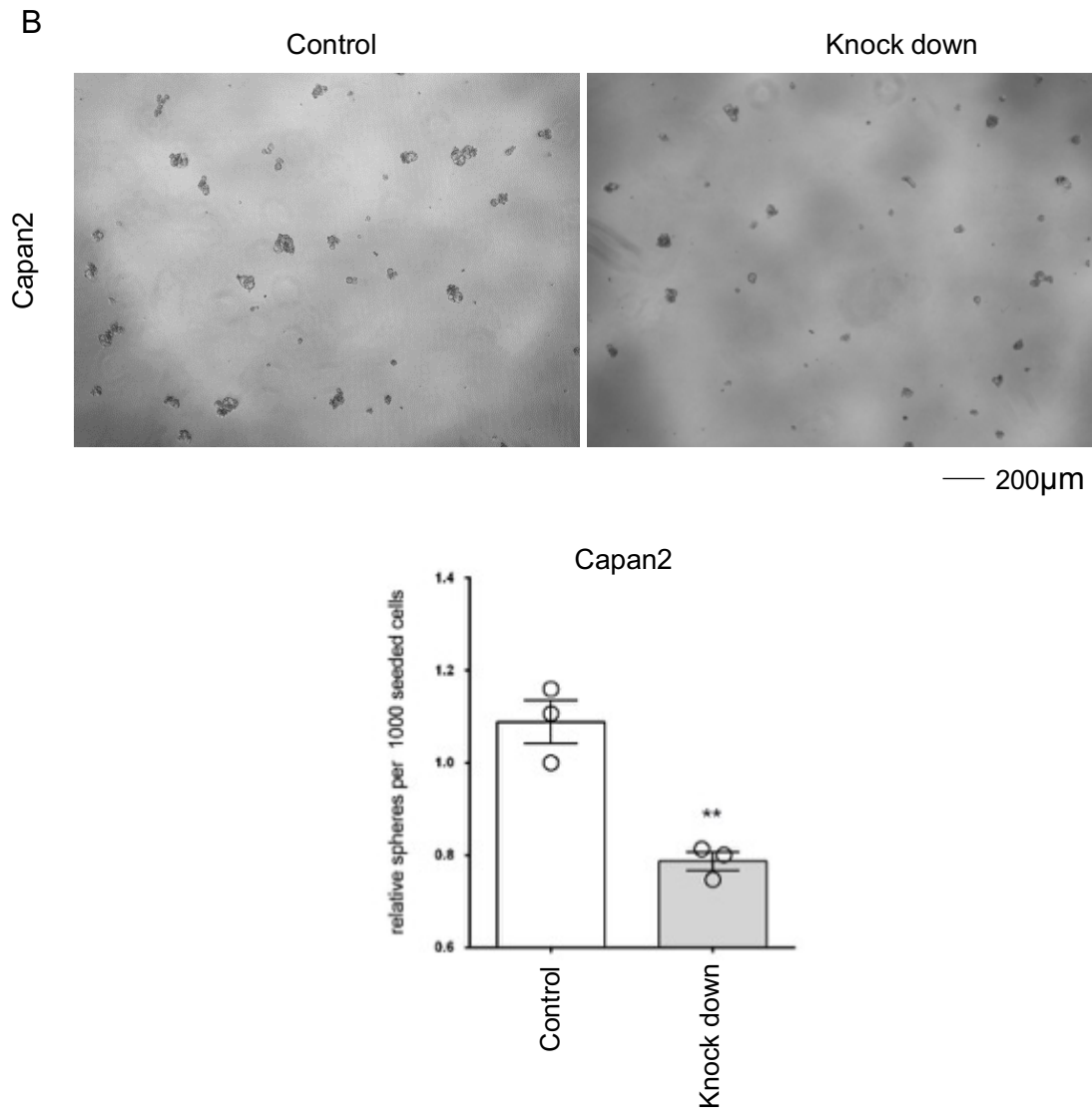


Figure 3.8.2: LGR6 and cancer cell stemness. (A) Colony formation assay of control versus LGR6 knock down in Capan2; (B) Sphere formation assay of Capan2 control versus LGR6 knock down. Quantification of spheroids is shown as normalized to control group. *, $P < 0.05$ **, $P < 0.01$. Bar, 200µm.

3.9 LGR6 expression in gemcitabine-resistant PDAC cells

Gemcitabine is a first-line treatment for pancreatic cancer. Patients usually benefit from chemotherapy based on gemcitabine at the beginning, however, many PDACs will eventually develop resistance. To understand whether LGR6 expression alters in cells

with gemcitabine resistance, we generated gemcitabine-resistant PDAC cells (GR cells) by prolonged exposure to gemcitabine. The morphology of GR cells is distinct from parental cells. GR cells underwent morphological changes including increased pseudopodia formation, reduced cell adhesion, and more elongated, spindle-shaped morphologies compared to their parental cells (Figure 3.9.1). The resistance to gemcitabine was evaluated by WST1 assay, when cells were exposed to various doses of gemcitabine. MiaPaCa2 GR kept a high viability up to 50ug/ml of gemcitabine, while MiaPaCa2 viability was inhibited dramatically at 10ug/ml of gemcitabine (Figure 3.9.2). Besides, the cell viability of Panc1 GR remained at a relatively high state until 1ug/ml gemcitabine, while it dramatically lowered in parental Panc1 when treated with 50ng/ml gemcitabine (Figure 3.9.2).

It was reported that the WNT signaling pathway is involved in doxorubicin-resistant cells [160]. It is generally believed that there is a higher stem cell subpopulation in GR cells, suggesting a higher WNT activity. Therefore, we performed qPCR to detect expression of the WNT target gene *AXIN2* as an indicator of WNT activity. In line with this, *AXIN2* expression is higher in MiaPaCa2 GR cells compared to parental cells. However, no significant changes were detected between Panc1 and Panc1 GR (Figure 3.9.3)

Besides, *LGR6* expression was measured on mRNA level in GR as well as parental cell lines. qPCR showed that *LGR6* expression increased in Panc1 GR compared with Panc1. However, *LGR6* expression in parental and resistant cells in MiaPaCa2 was undetectable (Figure 3.9.4). Furthermore, we compared *LGR6* protein expression between normal cells and GR cells. Consistent with the results above, Western blot analysis showed an elevated *LGR6* expression in Panc1 GR cell compared with parental cells. However, *LGR6* was not detected in any experimental setting in MiaPaCa2 (Figure 3.9.5).

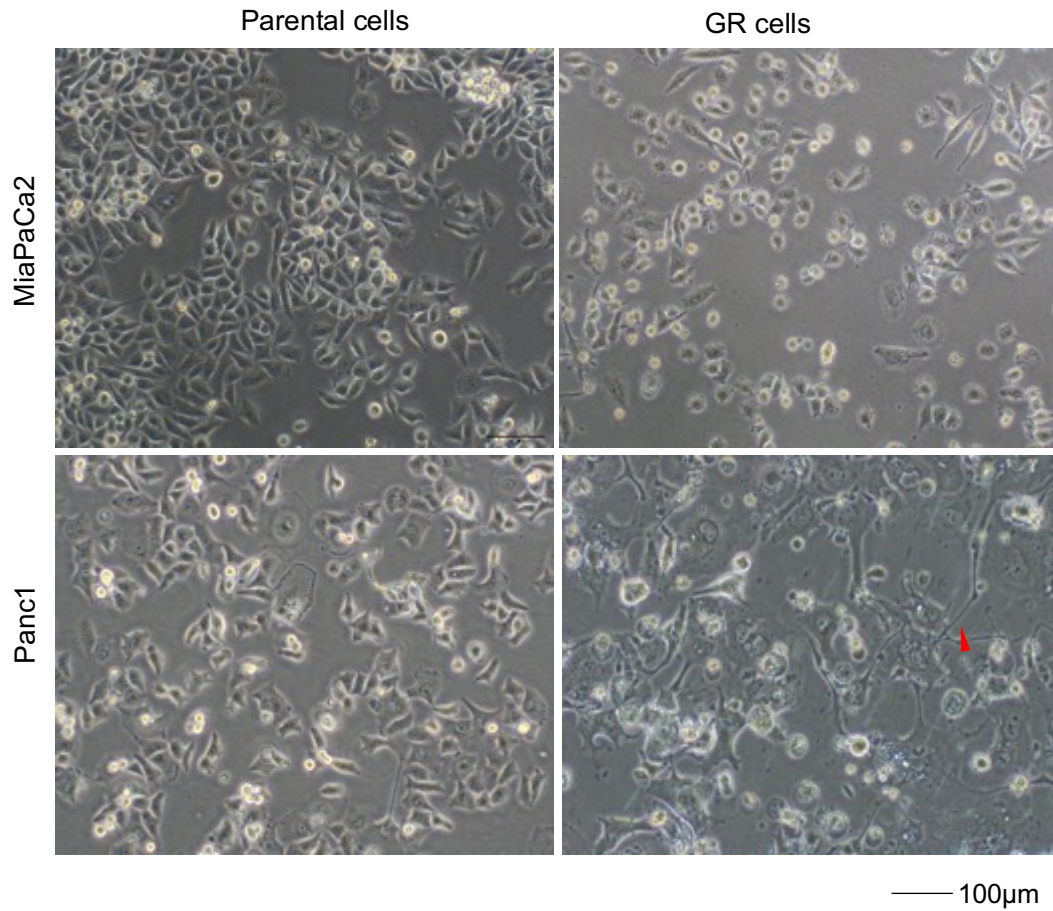


Figure 3.9.1: The morphological changes of GR cells. MiaPaCa2 GR cells changed to spindle or small rounded-shaped with less cell contacts compared to MiaPaCa2; while, Panc1 GR had more pseudopodia (red arrow). Images were taken by phase contrast microscopy. Bar, 100 μm.

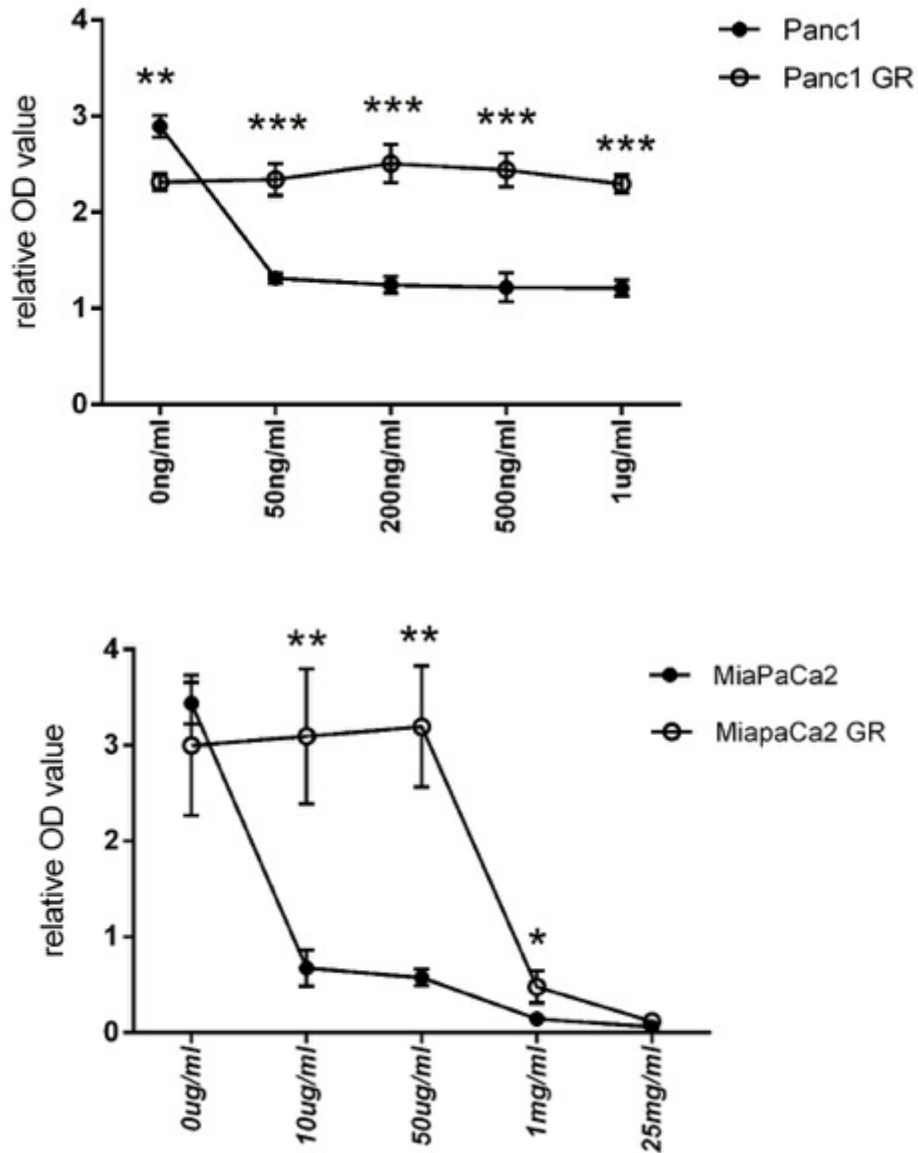


Figure 3.9.2: Gemcitabine resistance of GR cells compared to their parental cell lines. Cells were incubated with increasing dose of gemcitabine for 72h. WST1 assay was used to determine the cell viability. **, P<0.01; ***, P<0,001.

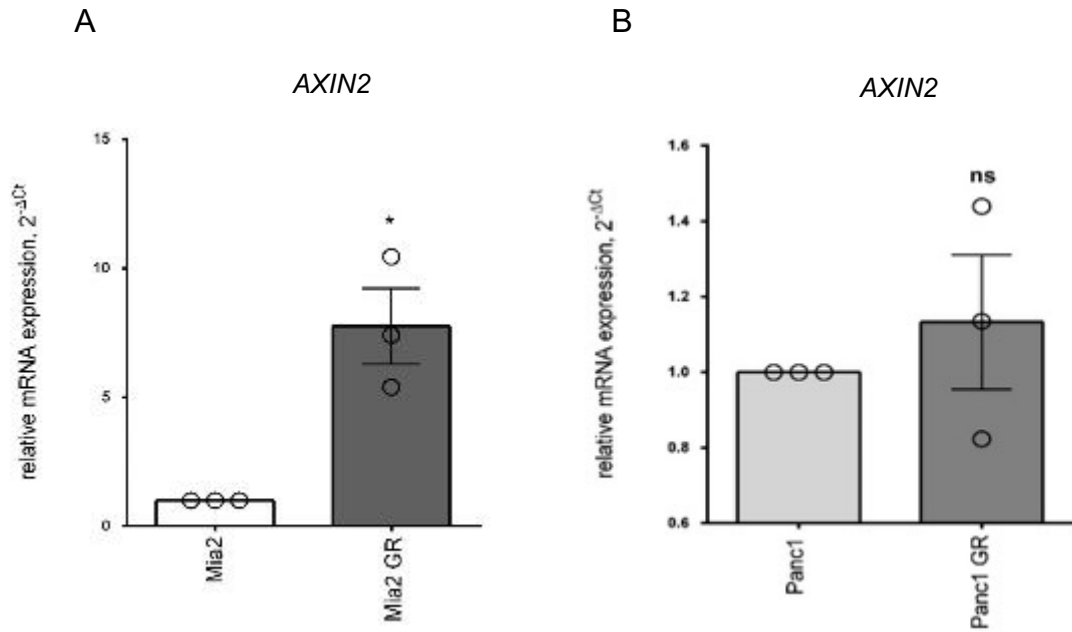


Figure 3.9.3: PCR analysis of *AXIN2* mRNA in normal and GR cells. (A) An elevated *AXIN2* was measured in MiaPaCa2 GR compared to MiaPaCa2. *, $P < 0.05$. (B) No significant changes were detected in Panc1 and Panc1 GR cell.

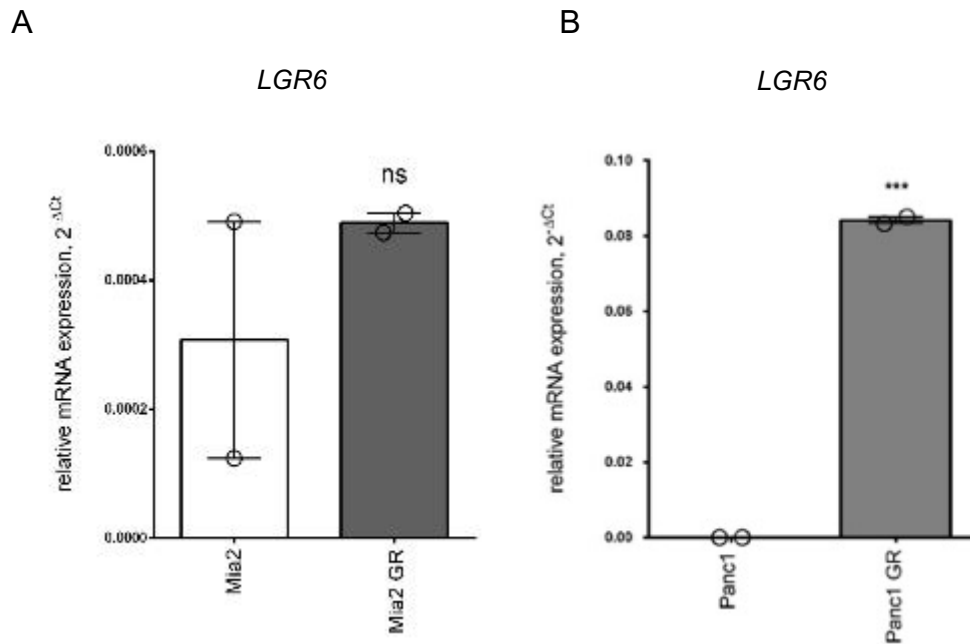


Figure 3.9.4: PCR analysis of *LGR6* mRNA in normal and GR cells. (A) An increased *LGR6* was detected in Panc1 GR, ***, $P < 0.001$. (B) No significant changes were seen in MiaPaCa2 and MiaPaCa2 GR cell.

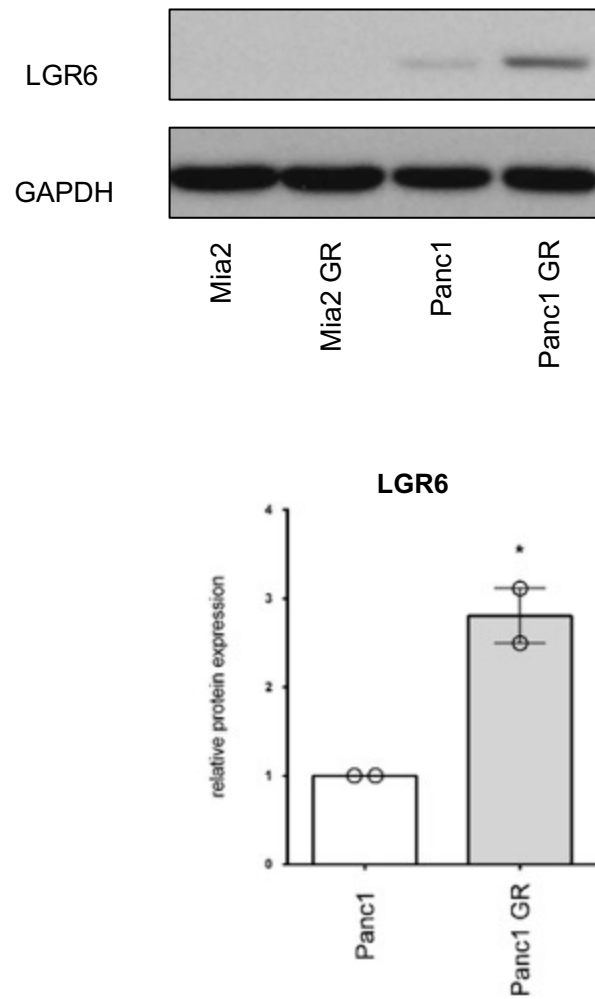


Figure 3.9.5: LGR6 expression in normal and GR cells. Protein from normal cells, gemcitabine-resistant cells were prepared. Increased LGR6 expression was shown in Panc1 GR, *, $P < 0.05$. No LGR6 was seen in MiaPaCa2 and MiaPaCa2 GR. GAPDH was used as loading control.

3.10 LGR6 expression is a poor prognostic marker in pancreatic cancer

Last, we searched The Human Protein Atlas to examine the correlation of LGR6 expression with pancreatic cancer clinical prognosis. It showed that high LGR6 RNA expression in tissues correlates with poor survival in pancreatic cancer patients (Figure 3.10). The result supported LGR6 as a marker of poor outcome in pancreatic cancer.

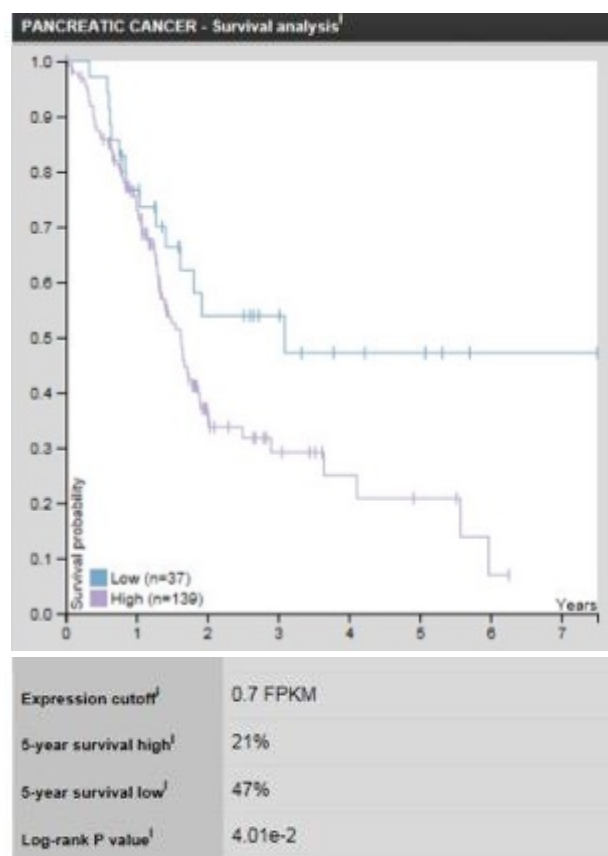


Figure 3.10: Survival analysis of pancreatic cancer patients according to LGR6 expression. 5-year survival is 21% of high LGR6 expression and 47% of low LGR6 expression respectively, cited by The Human Protein Atlas, <https://www.proteinatlas.org/ENSG00000133067-LGR6/pathology/tissue/pancreatic+cancer#Location>.

4. Discussion

4.1 LGR6 is a novel WNT target gene in PDAC

The canonical WNT signaling pathway has long been considered to play essential roles in organ development as well as oncogenesis in multiple cancers. When activated, β -catenin gets released from its destruction complex in the cytosol and translocates to the nucleus where it associates with the TCF/LEF family of transcription factors to induce canonical WNT target gene transcription. The research of WNT signaling target genes has established well-known genes including *AXIN2*, *MYC*, *cyclin D1*, and *LGR5* [116, 161-165]. Van de Wetering et al. first identified LGR5 as a WNT target gene in human colon cancer cell lines harboring WNT-activating mutations [125]. LGR5 has been shown to be a receptor of RSPOs and as such is also involved in enhancing the canonical WNT pathway [106, 116]. The RSPO family is a group of secreted factors that enhance previously activated WNT signaling by binding to the receptors LGR4-6. Evaluation of The Cancer Genome Atlas (TCGA) database showed that copy numbers of the RSPO2 gene are upregulated in PDAC tissues compared with normal pancreas. In line with this, a previous study of Ilmer et al. could show higher levels of RSPO2 in cells with high WNT activity as well as in highly tumorigenic pancreatic CSCs in KPC mouse models [157].

As a homolog of LGR5, we hypothesized that LGR6 might be a WNT target gene in PDAC apart from its role as a receptor of RSPOs to enhance WNT signaling. According to open access data from the TCGA, we found that LGR6 positively correlated with typical published canonical WNT signal pathway signatures. Our previous study showed that WNT signaling could be activated in response to extrinsically added recombinant human WNT3a or RSPO2 and even stronger to their combination in several pancreatic cancer cell lines. WNT3a is a widely used canonical WNT ligand for

stimulation experiments in the field of canonical WNT signaling. RSPO2 is a potent agonist that is able to further increase WNT signal pathway activity in the presence of WNT ligands [106, 111]. In the present study, we used a similar approach to activate WNT signaling by stimulation with RSPO2 and/or WNT3a. The activity was assessed indirectly by detection of *AXIN2* mRNA and β -catenin protein expression. In Panc1, WNT signaling activity was up-regulated in conditions of WNT3a alone as well as combined stimulation with RSPO2 and WNT3a. However, analysis of phospho- β -catenin (Ser⁶⁷⁵) expression showed that the activation was only present with RSPO2 and WNT3a in Panc1. IF confirmed this notion by showing that membrane associated β -catenin translocated into the nucleus upon WNT3a or WNT3a/RSPO2 stimulation. In case of Capan2, the activation was only detectable after stimulation with WNT3a/RSPO2 and assessment by *AXIN2* mRNA expression. No significant differences were observed in Capan2 by phospho- β -catenin (Ser⁶⁷⁵) evaluation. The inconsistency of WNT signaling activity may be due to the different mechanisms of *AXIN2* and β -catenin to regulate WNT signaling. *AXIN2* is a direct target gene of the WNT signaling cascade regulating WNT activity by enhancing the phosphorylation and degradation of β -catenin [162]. β -catenin in contrast is the key mediator of the WNT pathway, which gets released from the destruction complex and enters the nucleus where it converts TCF to a transcriptional activator [166, 167]. We then evaluated *LGR6* expression in activated WNT signaling conditions. It showed that *LGR6* was upregulated on protein level upon stimulation with WNT3a/RSPO2 in both cell lines.

Baseline WNT signaling activity can be inhibited by IWP2. We decided to use Capan2 only because of its high intrinsic WNT signaling activity. WNT signaling activity was evaluated by expression of *AXIN2* and we found a decreased expression in IWP2 treated samples. Endogenous *LGR6* mRNA expression was downregulated upon WNT pathway inactivation, whereas protein analysis did not show the same tendency

at the same time point, presumably because protein stability was too high in order to be able to detect changes on protein level.

In conclusion, we were able to show that LGR6 expression changed according to WNT signaling activity leading to the assumption that the *LGR6* gene itself may be a direct target of the WNT signaling pathway in pancreatic cancer cells. The regulation of LGR6 may therefore constitute a critical part of a positive feedback loop for WNT signaling activity.

4.2 LGR6 participates in cell adhesion and EMT in PDAC

Previous research showed that either overexpression or knockout of LGR5 led to strong changes in cytoskeletal structures and cell adhesion in some colon and liver cancer cell lines without endogenous or exogenous RSPO stimulation [168, 169]. For instance, one study showed that LGR5 silenced colorectal cancer cells tend to be more mesenchymal, while LGR5 overexpression was linked to a more epithelial phenotype [168]. Another study concluded that LGR5 overexpression in hepatocellular carcinoma cells led to changes from a mesenchymal phenotype to a more aggregated phenotype typical for epithelial subtype. Down-regulation of LGR5 shifted cells from an aggregated to a spindle-shaped phenotype [169]. Moreover, overexpression of endocytosis-impaired LGR5 induced cytoskeleton reorganization independent of RSPO activity, a phenotype that was characterized by the presence of elongated filopodia [133]. They further showed that LGR5 overexpression modified the actin cytoskeleton and enhanced cell-cell adhesion. This novel mechanism explained that LGR5 associated with the intracellular scaffold signaling protein IQGAP1, which regulates cytoskeletal dynamics and cell adhesion [170]. Concerning LGR6, its overexpression in HeLa cells was shown to increase cell migration when treated with RSPO1 and WNT3a. Moreover, overactivation of WNT signaling is known to be

correlated with increased cell migration [133]. So far, LGR6 functions in cell adhesion in PDAC are yet to be defined.

In the present study, we used pancreatic cancer cell lines of different morphological appearances to study the role of LGR6 in cell adhesion. For example, Capan2 and BxPC3 possess an epithelial phenotype with intensive cell-cell connections, while MiaPaCa2 and Panc1 are representatives of the mesenchymal phenotype with spindle-shaped morphology and lose cell-cell connections. Therefore, we used Capan2 and BxPC3 as epithelial and MiaPaCa2 and Panc1 as mesenchymal PDAC cell line representatives. This phenomenon raised our interest to investigate how LGR6 was distributed in these cell lines. In order to investigate a potential correlation, we used *Gene Set Enrichment Analysis (GSEA)* and found that LGR6 inversely correlated with EMT signatures in PDAC. Subsequently, we used different approaches (PCR, WB or IF) to look at the LGR6 expression pattern in the above-mentioned four PDAC cell lines. Interestingly, LGR6 is preferentially highly expressed in the epithelial cell lines Capan2 and BxPC3, whereas the mesenchymal cell lines MiaPaCa2 and Panc1 harbored much lower LGR6 expression levels. Furthermore, IF was used to detect intracellular distribution patterns of LGR6 and showed that LGR6 was mostly located on the cell membrane in epithelial cell lines, while less or no expression was detected in mesenchymal cell lines. This led to the assumption that LGR6 expression might be associated with cell adhesion and EMT processes.

To gain further insights into the role of LGR6 in EMT, we induced EMT and MET processes in AsPC1 and Panc1 by stimulation with TGF β and U0126, respectively. Successful EMT induction was achieved according to the morphological change to a more spindle-shaped morphology with decreased E-cadherin expression in Panc1. MET induction by U0126 changed the morphology of Panc1 to an epithelial phenotype with increased E-cadherin expression. According to our hypothesis, WB analysis

detected upregulated LGR6 expression upon EMT induction. To study the mechanism in more detail, Co-IP was performed using E-cadherin as a specific target protein because of its association with β -catenin in cell junction stability. β -catenin was pulled down by E-cadherin in the epithelial PDAC cell lines BxPC3 and Capan2. Interestingly, LGR6 was also pulled down by E-cadherin, which might indicate that LGR6 constitutes a part of the cell adhesion complex directly or indirectly with E-cadherin in epithelial PDAC cell lines. Afterwards, we stimulated PDAC cell lines with WNT3a to investigate whether the WNT signaling can affect LGR6-associated cell adhesion. However, the addition of WNT3a had no significant effects, indicating the irrelevance of WNT signaling in regulating such a process. In summary, we could show that LGR6 might play a role in EMT/MET processes as well as cell attachment activities in PDAC. However, the exact mechanisms will require further investigation.

4.3 LGR6 is involved in cancer stemness in PDAC

Cancer stem cells are believed to initiate and maintain the tumor and to be involved in their metastasis and chemo-resistance. The properties of self-renewal and differentiation have been proposed to be the defining criteria for CSCs. CSCs have been studied in multiple solid neoplasms, including breast cancer, prostate cancer, colon cancer [171] as well as pancreatic cancer [172, 173]. LGR5 was identified as an adult stem cells marker in tissues, including intestine, liver, skin, stomach, and ovarian epithelium [174, 175]. Recently, LGR5 has been shown to define pancreatic CSCs [176] and to be co-expressed with other CSC markers [177]. Regarding LGR6, experiments revealed that LGR6⁺ cells can contribute to the recovery of all skin compartments, including hair follicles. It is considered to act as a marker of adult stem cells in the skin. Additionally, both LGR5⁺ and LGR6⁺ stem cell compartments contribute to epidermal repair in response to acute wounds [178, 179]. In the present

study, we investigated stemness in PDAC by *in vitro* surrogate assays, such as colony formation capacity in 2D and sphere formation capacity in 3D. LGR6 was knocked-down by siRNA transfection with more than 90% efficiency. The numbers of colonies and spheres were smaller in the knock-down group compared with the vector group. Therefore, the deletion of LGR6 might have a negative impact on the growth of spheres and colonies, hinting towards a potential role of LGR6 in maintaining PDAC stemness. Gemcitabine is a standard care of pancreatic cancer [10]. However, patients either have intrinsic or rapidly develop gemcitabine-resistance [180]. Research showed that gemcitabine resistant (GR) cells are more invasive and possessed increased CSC markers suggesting a higher proportion of CSCs [180]. Cells underwent phenotypic changes after gemcitabine treatment to a more mesenchymal phenotype with more aggressive and invasive properties [180]. In our studies, we developed MiaPaCa2 GR and Panc1 GR cells by culturing them with increasing doses of gemcitabine for at least 6 months. The resistance was assessed by WST1 assays, which showed a significantly higher resistance to gemcitabine. Compared with parental cells, Panc1 GR had more pseudopodia. Pseudopodia are membrane protrusions of highly dynamic actin that extend out from the cell edge. They are considered to participate in cell migration and cancer cell invasion [181]. The WNT signal pathway has been reported to affect the outcome of gemcitabine therapy [182]. WNT target gene *MDR1*-encoded P-gp leads to chemo-resistance by expelling anticancer drugs out of cancer cells [183]. Additionally, the WNT-associated gene *Mre11* functions in repairing DNA double-strand breaks (DSBs) to influence gemcitabine resistance [184]. In MiaPaCa2 GR cells, WNT signaling activity was upregulated as shown by *AXIN2* mRNA expression analysis. Although not statistically different, there is a tendency that WNT signaling activity was higher in Panc1 GR. Moreover, LGR6 was overexpressed in Panc1 GR both on mRNA and protein level.

Previous studies showed overexpression of LGR5 in malignant pancreatic tissues compared with non-neoplastic pancreatic tissue [177]. Moreover, patients with more LGR5 positive cells are accompanied with shorter median survival [177]. LGR6 is known as a commonly mutated gene in colon cancers using whole-exon sequencing [185] and highly expressed in gastric cancer compared with their corresponding normal tissue [186]. *In vivo* studies in mice explored that oncogenic mutation in LGR6 expressing cells induced luminal cell expansion and tumor development in mammary glands [130]. In our study, we found that LGR6 correlates with poor prognosis in PDAC. Analyses of The Human Protein Atlas data showed that PDAC patients with high LGR6 RNA expression was associated with poor survival. In conclusion, we showed that LGR6 may be a novel WNT target gene and its expression may be associated with cell adhesion. Besides, we uncovered its potential role in cancer stem cell features as well as in the prediction of PDAC prognosis.

5. Conclusions and future directions

So far, research has reportedly investigated the function of LGR6 in WNT signaling as well as in stem cells. In this study, we showed that LGR6 is involved in WNT signaling activity of PDAC as LGR6 expression changed accordingly to the activity of WNT signaling. The stimulation of the WNT pathway seems to increase LGR6 expression, suggesting a positive self-regulatory loop. Furthermore, LGR6 is elevated in epithelial PDAC cells and appears to be preferentially membrane-bound, suggesting a role in EMT and cell adhesion. Lastly, we uncovered LGR6's potential role in cancer stem cell features and in the prediction of PDAC prognosis.

However, there are a number of limitations to this study. First, we did not generate any LGR6-overexpressing PDAC cell lines. Comparison of LGR6+ cells with LGR6- cells is a direct way to investigate its role in WNT signaling and other features. Second, the gold standard assay to assess WNT signaling activity is the Super TOP/FOP (STF) dual-luciferase system. In this study, WNT signaling activity was assessed by *AXIN2* mRNA and (phosphor) β -catenin protein expression. Third, no mouse models were implemented to translate the results of *in vitro* experiments to *in vivo* conditions. Fourth, we did not assess LGR6 expression results of the TCGA in a different cohort of human PDAC samples.

Together, we provide compelling evidence that LGR6 might be a novel WNT target gene and may participate in cell adhesion and EMT in PDAC. LGR6 may be involved in cancer stemness and could be used as a predictive factor of PDAC patients' outcome. Further research is still needed to dissect the exact mechanism of how LGR6 exerts its effects on the canonical WNT signaling in PDAC as well as EMT under physiological as well as pathological conditions of benign and cancerous pancreatic cells.

6. Summary

The canonical WNT signal pathway has long been considered essential for regulating embryonic processes as well as tissue homeostasis. However, alterations in WNT signaling are also associated with diverse diseases including developmental defects as well as multiple cancers. The R-spondin (RSPO) family is a group of secreted factors that enhance previously activated WNT signaling activity by binding to LGR4/5/6 (leucine-rich repeat containing G-protein coupled receptors 4/5/6). Of note, one of the receptors - LGR5 - is a well-established WNT target gene and (cancer) stem cell marker. So far, little evidence exists about the function of LGR6 in PDAC. Epithelial–mesenchymal transition (EMT) is a process by which epithelial cells transdifferentiate into mesenchymal cells. The overlap between WNT signaling and EMT compelled us to investigate the potential role of LGR6 in EMT.

According to open access data from the TCGA, we found that LGR6 positively correlated with typical published canonical WNT signal pathway signatures. Hence, we further hypothesized that LGR6 could be a novel WNT target gene in PDAC. WNT signaling was activated by stimulation with RSPO2 and/or WNT3a, which subsequently upregulated LGR6 expression in different PDAC cell lines. Moreover, inhibition of baseline WNT signaling activity by IWP2 led to downregulation of endogenous LGR6 expression. Taken together, we were able to show that LGR6 gene itself may be a direct target of the WNT signaling pathway in PDAC cells with LGR6 expression changes according to WNT activity.

LGR6 is involved in regulating EMT processes in PDAC. Gene Set Enrichment Analysis (GSEA) showed that LGR6 was inversely correlated with EMT signatures in PDAC. PDAC cell lines of different morphological appearances were used to assess the distribution of LGR6 expression. We found that epithelial cell lines (BxPC3, Capan2)

possessed a higher LGR6 expression compared to mesenchymal cell lines (MiaPaCa2, Panc1). IF showed that LGR6 was mostly located at the cell membrane in epithelial cell lines, while less or no expression was detected in mesenchymal cell lines. Furthermore, EMT induction was carried out and LGR6 expression was analyzed. We detected upregulated LGR6 expression upon EMT induction in Panc1. Additionally, Co-IP showed that LGR6 may constitute a part of the cell adhesion complex in epithelial PDAC cell lines.

Cancer stemness in PDAC was assessed by surrogate assays *in vitro* including colony formation capacity in 2D and sphere formation capacity in 3D. We investigated the effects of LGR6 knock-down on cancer stemness. The numbers of colonies and spheres were smaller in the knock-down group compared with the vector group. Thus, we concluded that the deletion of LGR6 might have a negative impact on the growth of spheres and colonies. As gemcitabine resistant (GR) cells are more invasive and possessed increased CSC markers suggesting a higher proportion of CSC, we developed MiaPaCa2 GR and Panc1 GR cells by culturing them with increasing doses of gemcitabine for at least six months. LGR6 was detected overexpressed in Panc1 GR both on mRNA and protein level. In addition, we searched The Human Protein Atlas and showed that high LGR6 RNA expression in tissues correlates with poor survival in pancreatic cancer patients. This supported our hypothesis that LGR6 could serve as a marker of poor outcome in pancreatic cancer.

III. References

1. Jennings, R.E., et al., *Human pancreas development*. Development, 2015. **142**(18): p. 3126-37.
2. Hall, J.E. and A.C. Guyton, *Guyton and Hall textbook of medical physiology*. 12th ed. 2011, Philadelphia, Pa.: Saunders/Elsevier. xix, 1091 p.
3. Erkan, M., et al., *The activated stroma index is a novel and independent prognostic marker in pancreatic ductal adenocarcinoma*. Clin Gastroenterol Hepatol, 2008. **6**(10): p. 1155-61.
4. Kleeff, J., et al., *Pancreatic cancer*. Nat Rev Dis Primers, 2016. **2**: p. 16022.
5. Ferlay, J., et al., *Cancer incidence and mortality worldwide: sources, methods and major patterns in GLOBOCAN 2012*. Int J Cancer, 2015. **136**(5): p. E359-86.
6. He, J., et al., *2564 resected periampullary adenocarcinomas at a single institution: trends over three decades*. HPB (Oxford), 2014. **16**(1): p. 83-90.
7. Rahib, L., et al., *Projecting cancer incidence and deaths to 2030: the unexpected burden of thyroid, liver, and pancreas cancers in the United States*. Cancer Res, 2014. **74**(11): p. 2913-21.
8. Siegel, R.L., K.D. Miller, and A. Jemal, *Cancer statistics, 2015*. CA Cancer J Clin, 2015. **65**(1): p. 5-29.
9. Gillen, S., et al., *Preoperative/neoadjuvant therapy in pancreatic cancer: a systematic review and meta-analysis of response and resection percentages*. PLoS Med, 2010. **7**(4): p. e1000267.
10. Kamisawa, T., et al., *Pancreatic cancer*. Lancet, 2016. **388**(10039): p. 73-85.
11. Chang, D.K., S.M. Grimmond, and A.V. Biankin, *Pancreatic cancer genomics*. Curr Opin Genet Dev, 2014. **24**: p. 74-81.
12. McCleary-Wheeler, A.L., R. McWilliams, and M.E. Fernandez-Zapico, *Aberrant signaling pathways in pancreatic cancer: a two compartment view*. Mol Carcinog, 2012. **51**(1): p. 25-39.
13. Ellenrieder, V., et al., *Transforming growth factor beta1 treatment leads to an epithelial-mesenchymal transdifferentiation of pancreatic cancer cells requiring extracellular signal-regulated kinase 2 activation*. Cancer Res, 2001. **61**(10): p. 4222-8.
14. Apte, M.V., et al., *Pancreatic stellate cells are activated by proinflammatory cytokines: implications for pancreatic fibrogenesis*. Gut, 1999. **44**(4): p. 534-41.
15. Lauth, M. and R. Toftgard, *Hedgehog signaling and pancreatic tumor development*. Adv Cancer Res, 2011. **110**: p. 1-17.
16. Illmer, M. and D. Horst, *Pancreatic CSCs and microenvironment*. Genes Cancer, 2015. **6**(9-10): p. 365-6.
17. Morton, J.P., et al., *Sonic hedgehog acts at multiple stages during pancreatic tumorigenesis*. Proc Natl Acad Sci U S A, 2007. **104**(12): p. 5103-8.
18. Apte, M.V., et al., *Desmoplastic reaction in pancreatic cancer: role of pancreatic stellate cells*. Pancreas, 2004. **29**(3): p. 179-87.
19. Olive, K.P., et al., *Inhibition of Hedgehog signaling enhances delivery of chemotherapy in a mouse model of pancreatic cancer*. Science, 2009. **324**(5933): p. 1457-61.

-
20. Wells, J.M., et al., *Wnt/beta-catenin signaling is required for development of the exocrine pancreas*. BMC Dev Biol, 2007. **7**: p. 4.
 21. Papadopoulou, S. and H. Edlund, *Attenuated Wnt signaling perturbs pancreatic growth but not pancreatic function*. Diabetes, 2005. **54**(10): p. 2844-51.
 22. de La Coste, A., et al., *Somatic mutations of the beta-catenin gene are frequent in mouse and human hepatocellular carcinomas*. Proc Natl Acad Sci U S A, 1998. **95**(15): p. 8847-51.
 23. Hugh, T.J., et al., *beta-catenin expression in primary and metastatic colorectal carcinoma*. Int J Cancer, 1999. **82**(4): p. 504-11.
 24. Turashvili, G., et al., *Wnt signaling pathway in mammary gland development and carcinogenesis*. Pathobiology, 2006. **73**(5): p. 213-23.
 25. Abraham, S.C., et al., *Solid-pseudopapillary tumors of the pancreas are genetically distinct from pancreatic ductal adenocarcinomas and almost always harbor beta-catenin mutations*. Am J Pathol, 2002. **160**(4): p. 1361-9.
 26. Gerdes, B., et al., *Analysis of beta-catenin gene mutations in pancreatic tumors*. Digestion, 1999. **60**(6): p. 544-8.
 27. Zeng, G., et al., *Aberrant Wnt/beta-catenin signaling in pancreatic adenocarcinoma*. Neoplasia, 2006. **8**(4): p. 279-89.
 28. Pasca di Magliano, M., et al., *Common activation of canonical Wnt signaling in pancreatic adenocarcinoma*. PLoS One, 2007. **2**(11): p. e1155.
 29. Nusse, R. and H.E. Varmus, *Many tumors induced by the mouse mammary tumor virus contain a provirus integrated in the same region of the host genome*. Cell, 1982. **31**(1): p. 99-109.
 30. Kim, W., M. Kim, and E.H. Jho, *Wnt/beta-catenin signalling: from plasma membrane to nucleus*. Biochem J, 2013. **450**(1): p. 9-21.
 31. Logan, C.Y. and R. Nusse, *The Wnt signaling pathway in development and disease*. Annu Rev Cell Dev Biol, 2004. **20**: p. 781-810.
 32. Cadigan, K.M. and M.L. Waterman, *TCF/LEFs and Wnt signaling in the nucleus*. Cold Spring Harb Perspect Biol, 2012. **4**(11).
 33. Kinzler, K.W., et al., *Identification of FAP locus genes from chromosome 5q21*. Science, 1991. **253**(5020): p. 661-5.
 34. Nishisho, I., et al., *Mutations of chromosome 5q21 genes in FAP and colorectal cancer patients*. Science, 1991. **253**(5020): p. 665-9.
 35. Baarsma, H.A., M. Konigshoff, and R. Gosens, *The WNT signaling pathway from ligand secretion to gene transcription: molecular mechanisms and pharmacological targets*. Pharmacol Ther, 2013. **138**(1): p. 66-83.
 36. MacDonald, B.T., K. Tamai, and X. He, *Wnt/beta-catenin signaling: components, mechanisms, and diseases*. Dev Cell, 2009. **17**(1): p. 9-26.
 37. Angers, S. and R.T. Moon, *Proximal events in Wnt signal transduction*. Nat Rev Mol Cell Biol, 2009. **10**(7): p. 468-77.
 38. Clevers, H., *Wnt/beta-catenin signaling in development and disease*. Cell, 2006. **127**(3): p. 469-80.

-
39. Semenov, M.V., et al., *SnapShot: Noncanonical Wnt Signaling Pathways*. Cell, 2007. **131**(7): p. 1378.
 40. McNeill, H. and J.R. Woodgett, *When pathways collide: collaboration and connivance among signalling proteins in development*. Nat Rev Mol Cell Biol, 2010. **11**(6): p. 404-13.
 41. De, A., *Wnt/Ca2+ signaling pathway: a brief overview*. Acta Biochim Biophys Sin (Shanghai), 2011. **43**(10): p. 745-56.
 42. Aberle, H., et al., *beta-catenin is a target for the ubiquitin-proteasome pathway*. EMBO J, 1997. **16**(13): p. 3797-804.
 43. Kimelman, D. and W. Xu, *beta-catenin destruction complex: insights and questions from a structural perspective*. Oncogene, 2006. **25**(57): p. 7482-91.
 44. Taurin, S., et al., *Phosphorylation of beta-catenin by cyclic AMP-dependent protein kinase*. J Biol Chem, 2006. **281**(15): p. 9971-6.
 45. Vlad, A., et al., *The first five years of the Wnt targetome*. Cell Signal, 2008. **20**(5): p. 795-802.
 46. Tanaka, K., Y. Kitagawa, and T. Kadowaki, *Drosophila segment polarity gene product porcupine stimulates the posttranslational N-glycosylation of wingless in the endoplasmic reticulum*. J Biol Chem, 2002. **277**(15): p. 12816-23.
 47. Willert, K., et al., *Wnt proteins are lipid-modified and can act as stem cell growth factors*. Nature, 2003. **423**(6938): p. 448-52.
 48. Schneider, V.A. and M. Mercola, *Wnt antagonism initiates cardiogenesis in Xenopus laevis*. Genes Dev, 2001. **15**(3): p. 304-15.
 49. Li, X., et al., *Prostate tumor progression is mediated by a paracrine TGF-beta/Wnt3a signaling axis*. Oncogene, 2008. **27**(56): p. 7118-30.
 50. Kurayoshi, M., et al., *Post-translational palmitoylation and glycosylation of Wnt-5a are necessary for its signalling*. Biochem J, 2007. **402**(3): p. 515-23.
 51. Janda, C.Y., et al., *Structural basis of Wnt recognition by Frizzled*. Science, 2012. **337**(6090): p. 59-64.
 52. Hofmann, K., *A superfamily of membrane-bound O-acyltransferases with implications for wnt signaling*. Trends Biochem Sci, 2000. **25**(3): p. 111-2.
 53. Clevers, H. and R. Nusse, *Wnt/beta-catenin signaling and disease*. Cell, 2012. **149**(6): p. 1192-205.
 54. Takada, R., et al., *Monounsaturated fatty acid modification of Wnt protein: its role in Wnt secretion*. Dev Cell, 2006. **11**(6): p. 791-801.
 55. Banziger, C., et al., *Wntless, a conserved membrane protein dedicated to the secretion of Wnt proteins from signaling cells*. Cell, 2006. **125**(3): p. 509-22.
 56. Bhanot, P., et al., *A new member of the frizzled family from Drosophila functions as a Wingless receptor*. Nature, 1996. **382**(6588): p. 225-30.
 57. Yang-Snyder, J., et al., *A frizzled homolog functions in a vertebrate Wnt signaling pathway*. Curr Biol, 1996. **6**(10): p. 1302-6.
 58. Schulte, G., *International Union of Basic and Clinical Pharmacology. LXXX. The class Frizzled receptors*. Pharmacol Rev, 2010. **62**(4): p. 632-67.
 59. Dann, C.E., et al., *Insights into Wnt binding and signalling from the structures of two*

-
- Frizzled cysteine-rich domains.* Nature, 2001. **412**(6842): p. 86-90.
60. Bejsovec, A., *Wnt pathway activation: new relations and locations.* Cell, 2005. **120**(1): p. 11-4.
61. Cadigan, K.M. and Y.I. Liu, *Wnt signaling: complexity at the surface.* J Cell Sci, 2006. **119**(Pt 3): p. 395-402.
62. Dale, T.C., *Signal transduction by the Wnt family of ligands.* Biochem J, 1998. **329 (Pt 2)**: p. 209-23.
63. Bjarnadottir, T.K., et al., *Comprehensive repertoire and phylogenetic analysis of the G protein-coupled receptors in human and mouse.* Genomics, 2006. **88**(3): p. 263-73.
64. Schulte, G. and V. Bryja, *The Frizzled family of unconventional G-protein-coupled receptors.* Trends Pharmacol Sci, 2007. **28**(10): p. 518-25.
65. Kilander, M.B., et al., *WNT-5A stimulates the GDP/GTP exchange at pertussis toxin-sensitive heterotrimeric G proteins.* Cell Signal, 2011. **23**(3): p. 550-4.
66. Jernigan, K.K., et al., *Gbetagamma activates GSK3 to promote LRP6-mediated beta-catenin transcriptional activity.* Sci Signal, 2010. **3**(121): p. ra37.
67. Medina, A., W. Reintsch, and H. Steinbeisser, *Xenopus frizzled 7 can act in canonical and non-canonical Wnt signaling pathways: implications on early patterning and morphogenesis.* Mech Dev, 2000. **92**(2): p. 227-37.
68. Liu, G., A. Bafico, and S.A. Aaronson, *The mechanism of endogenous receptor activation functionally distinguishes prototype canonical and noncanonical Wnts.* Mol Cell Biol, 2005. **25**(9): p. 3475-82.
69. Tamai, K., et al., *LDL-receptor-related proteins in Wnt signal transduction.* Nature, 2000. **407**(6803): p. 530-5.
70. Cong, F., L. Schweizer, and H. Varmus, *Wnt signals across the plasma membrane to activate the beta-catenin pathway by forming oligomers containing its receptors, Frizzled and LRP.* Development, 2004. **131**(20): p. 5103-15.
71. Bilic, J., et al., *Wnt induces LRP6 signalosomes and promotes dishevelled-dependent LRP6 phosphorylation.* Science, 2007. **316**(5831): p. 1619-22.
72. He, X., et al., *LDL receptor-related proteins 5 and 6 in Wnt/beta-catenin signaling: arrows point the way.* Development, 2004. **131**(8): p. 1663-77.
73. Tamai, K., et al., *A mechanism for Wnt coreceptor activation.* Mol Cell, 2004. **13**(1): p. 149-56.
74. Zeng, X., et al., *A dual-kinase mechanism for Wnt co-receptor phosphorylation and activation.* Nature, 2005. **438**(7069): p. 873-7.
75. Niehrs, C. and J. Shen, *Regulation of Lrp6 phosphorylation.* Cell Mol Life Sci, 2010. **67**(15): p. 2551-62.
76. Xu, Y.K. and R. Nusse, *The Frizzled CRD domain is conserved in diverse proteins including several receptor tyrosine kinases.* Curr Biol, 1998. **8**(12): p. R405-6.
77. Hsieh, J.C., et al., *A new secreted protein that binds to Wnt proteins and inhibits their activities.* Nature, 1999. **398**(6726): p. 431-6.
78. Liepinsh, E., et al., *NMR structure of the WIF domain of the human Wnt-inhibitory factor-1.* J Mol Biol, 2006. **357**(3): p. 942-50.

-
79. Xu, Q., et al., *Vascular development in the retina and inner ear: control by Norrin and Frizzled-4, a high-affinity ligand-receptor pair*. Cell, 2004. **116**(6): p. 883-95.
80. Cruciati, C.M. and C. Niehrs, *Secreted and transmembrane wnt inhibitors and activators*. Cold Spring Harb Perspect Biol, 2013. **5**(3): p. a015081.
81. Hoang, B.H., et al., *Expression pattern of two Frizzled-related genes, Frzb-1 and Sfrp-1, during mouse embryogenesis suggests a role for modulating action of Wnt family members*. Dev Dyn, 1998. **212**(3): p. 364-72.
82. Kawano, Y. and R. Kypta, *Secreted antagonists of the Wnt signalling pathway*. J Cell Sci, 2003. **116**(Pt 13): p. 2627-34.
83. Chien, A.J., W.H. Conrad, and R.T. Moon, *A Wnt survival guide: from flies to human disease*. J Invest Dermatol, 2009. **129**(7): p. 1614-27.
84. Malinauskas, T. and E.Y. Jones, *Extracellular modulators of Wnt signalling*. Curr Opin Struct Biol, 2014. **29**: p. 77-84.
85. Mao, B., et al., *LDL-receptor-related protein 6 is a receptor for Dickkopf proteins*. Nature, 2001. **411**(6835): p. 321-5.
86. Brott, B.K. and S.Y. Sokol, *Regulation of Wnt/LRP signaling by distinct domains of Dickkopf proteins*. Mol Cell Biol, 2002. **22**(17): p. 6100-10.
87. Chen, J.Z., et al., *Cloning and identification of a cDNA that encodes a novel human protein with thrombospondin type I repeat domain, hPWTSR*. Mol Biol Rep, 2002. **29**(3): p. 287-92.
88. Kamata, T., et al., *R-spondin, a novel gene with thrombospondin type 1 domain, was expressed in the dorsal neural tube and affected in Wnts mutants*. Biochim Biophys Acta, 2004. **1676**(1): p. 51-62.
89. Kazanskaya, O., et al., *R-Spondin2 is a secreted activator of Wnt/beta-catenin signaling and is required for Xenopus myogenesis*. Dev Cell, 2004. **7**(4): p. 525-34.
90. Kim, K.A., et al., *R-Spondin proteins: a novel link to beta-catenin activation*. Cell Cycle, 2006. **5**(1): p. 23-6.
91. de Lau, W.B., B. Snel, and H.C. Clevers, *The R-spondin protein family*. Genome Biol, 2012. **13**(3): p. 242.
92. de Lau, W., et al., *The R-spondin/Lgr5/Rnf43 module: regulator of Wnt signal strength*. Genes Dev, 2014. **28**(4): p. 305-16.
93. Schuijers, J. and H. Clevers, *Adult mammalian stem cells: the role of Wnt, Lgr5 and R-spondins*. EMBO J, 2012. **31**(12): p. 2685-96.
94. Kim, K.A., et al., *Mitogenic influence of human R-spondin1 on the intestinal epithelium*. Science, 2005. **309**(5738): p. 1256-9.
95. Parma, P., et al., *R-spondin1 is essential in sex determination, skin differentiation and malignancy*. Nat Genet, 2006. **38**(11): p. 1304-9.
96. Vainio, S., et al., *Female development in mammals is regulated by Wnt-4 signalling*. Nature, 1999. **397**(6718): p. 405-9.
97. Tomizuka, K., et al., *R-spondin1 plays an essential role in ovarian development through positively regulating Wnt-4 signaling*. Hum Mol Genet, 2008. **17**(9): p. 1278-91.
98. Nam, J.S., T.J. Turcotte, and J.K. Yoon, *Dynamic expression of R-spondin family genes in*

-
- mouse development*. Gene Expr Patterns, 2007. **7**(3): p. 306-12.
99. Bell, S.M., et al., *R-spondin 2 is required for normal laryngeal-tracheal, lung and limb morphogenesis*. Development, 2008. **135**(6): p. 1049-58.
100. Nam, J.S., et al., *Mouse R-spondin2 is required for apical ectodermal ridge maintenance in the hindlimb*. Dev Biol, 2007. **311**(1): p. 124-35.
101. van Tuyl, M., et al., *Iroquois genes influence proximo-distal morphogenesis during rat lung development*. Am J Physiol Lung Cell Mol Physiol, 2006. **290**(4): p. L777-L789.
102. Cadieu, E., et al., *Coat variation in the domestic dog is governed by variants in three genes*. Science, 2009. **326**(5949): p. 150-3.
103. Kazanskaya, O., et al., *The Wnt signaling regulator R-spondin 3 promotes angioblast and vascular development*. Development, 2008. **135**(22): p. 3655-64.
104. Bergmann, C., et al., *Mutations in the gene encoding the Wnt-signaling component R-spondin 4 (RSPO4) cause autosomal recessive onychia*. Am J Hum Genet, 2006. **79**(6): p. 1105-9.
105. Blaydon, D.C., et al., *The gene encoding R-spondin 4 (RSPO4), a secreted protein implicated in Wnt signaling, is mutated in inherited onychia*. Nat Genet, 2006. **38**(11): p. 1245-7.
106. de Lau, W., et al., *Lgr5 homologues associate with Wnt receptors and mediate R-spondin signalling*. Nature, 2011. **476**(7360): p. 293-7.
107. Hao, H.X., et al., *ZNRF3 promotes Wnt receptor turnover in an R-spondin-sensitive manner*. Nature, 2012. **485**(7397): p. 195-200.
108. Koo, B.K., et al., *Tumour suppressor RNF43 is a stem-cell E3 ligase that induces endocytosis of Wnt receptors*. Nature, 2012. **488**(7413): p. 665-9.
109. Hsu, S.Y., S.G. Liang, and A.J. Hsueh, *Characterization of two LGR genes homologous to gonadotropin and thyrotropin receptors with extracellular leucine-rich repeats and a G protein-coupled, seven-transmembrane region*. Mol Endocrinol, 1998. **12**(12): p. 1830-45.
110. Hsu, S.Y., et al., *The three subfamilies of leucine-rich repeat-containing G protein-coupled receptors (LGR): identification of LGR6 and LGR7 and the signaling mechanism for LGR7*. Mol Endocrinol, 2000. **14**(8): p. 1257-71.
111. Carmon, K.S., et al., *R-spondins function as ligands of the orphan receptors LGR4 and LGR5 to regulate Wnt/beta-catenin signaling*. Proc Natl Acad Sci U S A, 2011. **108**(28): p. 11452-7.
112. Van Hiel, M.B., et al., *An evolutionary comparison of leucine-rich repeat containing G protein-coupled receptors reveals a novel LGR subtype*. Peptides, 2012. **34**(1): p. 193-200.
113. Hsu, S.Y., et al., *Evolution of the signaling system in relaxin-family peptides*. Ann N Y Acad Sci, 2005. **1041**: p. 520-9.
114. Mazerbourg, S., et al., *Leucine-rich repeat-containing, G protein-coupled receptor 4 null mice exhibit intrauterine growth retardation associated with embryonic and perinatal lethality*. Mol Endocrinol, 2004. **18**(9): p. 2241-54.
115. Yi, J., et al., *Analysis of LGR4 receptor distribution in human and mouse tissues*. PLoS One, 2013. **8**(10): p. e78144.

-
116. Barker, N., et al., *Identification of stem cells in small intestine and colon by marker gene Lgr5*. Nature, 2007. **449**(7165): p. 1003-7.
 117. Barker, N., et al., *Lgr5(+ve) stem cells drive self-renewal in the stomach and build long-lived gastric units in vitro*. Cell Stem Cell, 2010. **6**(1): p. 25-36.
 118. Jaks, V., et al., *Lgr5 marks cycling, yet long-lived, hair follicle stem cells*. Nat Genet, 2008. **40**(11): p. 1291-9.
 119. Barker, N., et al., *Lgr5(+ve) stem/progenitor cells contribute to nephron formation during kidney development*. Cell Rep, 2012. **2**(3): p. 540-52.
 120. Huch, M., et al., *Unlimited in vitro expansion of adult bi-potent pancreas progenitors through the Lgr5/R-spondin axis*. EMBO J, 2013. **32**(20): p. 2708-21.
 121. Huch, M., et al., *In vitro expansion of single Lgr5+ liver stem cells induced by Wnt-driven regeneration*. Nature, 2013. **494**(7436): p. 247-50.
 122. Plaks, V., et al., *Lgr5-expressing cells are sufficient and necessary for postnatal mammary gland organogenesis*. Cell Rep, 2013. **3**(1): p. 70-8.
 123. Sato, T., et al., *Single Lgr5 stem cells build crypt-villus structures in vitro without a mesenchymal niche*. Nature, 2009. **459**(7244): p. 262-5.
 124. de Visser, K.E., et al., *Developmental stage-specific contribution of LGR5(+) cells to basal and luminal epithelial lineages in the postnatal mammary gland*. J Pathol, 2012. **228**(3): p. 300-9.
 125. van de Wetering, M., et al., *The beta-catenin/TCF-4 complex imposes a crypt progenitor phenotype on colorectal cancer cells*. Cell, 2002. **111**(2): p. 241-50.
 126. Yamamoto, Y., et al., *Overexpression of orphan G-protein-coupled receptor, Gpr49, in human hepatocellular carcinomas with beta-catenin mutations*. Hepatology, 2003. **37**(3): p. 528-33.
 127. McClanahan, T., et al., *Identification of overexpression of orphan G protein-coupled receptor GPR49 in human colon and ovarian primary tumors*. Cancer Biol Ther, 2006. **5**(4): p. 419-26.
 128. Zucman-Rossi, J., et al., *Differential effects of inactivated Axin1 and activated beta-catenin mutations in human hepatocellular carcinomas*. Oncogene, 2007. **26**(5): p. 774-80.
 129. Zhang, Y., et al., *Dynamic expression of Lgr6 in the developing and mature mouse cochlea*. Front Cell Neurosci, 2015. **9**: p. 165.
 130. Blaas, L., et al., *Lgr6 labels a rare population of mammary gland progenitor cells that are able to originate luminal mammary tumours*. Nat Cell Biol, 2016. **18**(12): p. 1346-1356.
 131. Ren, W., et al., *Single Lgr5- or Lgr6-expressing taste stem/progenitor cells generate taste bud cells ex vivo*. Proc Natl Acad Sci U S A, 2014. **111**(46): p. 16401-6.
 132. Oeztuerk-Winder, F., et al., *Regulation of human lung alveolar multipotent cells by a novel p38alpha MAPK/miR-17-92 axis*. EMBO J, 2012. **31**(16): p. 3431-41.
 133. Gong, X., et al., *LGR6 is a high affinity receptor of R-spondins and potentially functions as a tumor suppressor*. PLoS One, 2012. **7**(5): p. e37137.
 134. Mokarram, P., et al., *Distinct high-profile methylated genes in colorectal cancer*. PLoS One, 2009. **4**(9): p. e7012.
 135. Battle, E., et al., *The transcription factor snail is a repressor of E-cadherin gene expression*

-
- in epithelial tumour cells*. Nat Cell Biol, 2000. **2**(2): p. 84-9.
136. Yang, J., et al., *Twist, a master regulator of morphogenesis, plays an essential role in tumor metastasis*. Cell, 2004. **117**(7): p. 927-39.
137. Hajra, K.M., D.Y. Chen, and E.R. Fearon, *The SLUG zinc-finger protein represses E-cadherin in breast cancer*. Cancer Res, 2002. **62**(6): p. 1613-8.
138. Comijn, J., et al., *The two-handed E box binding zinc finger protein SIP1 downregulates E-cadherin and induces invasion*. Mol Cell, 2001. **7**(6): p. 1267-78.
139. Thiery, J.P. and J.P. Sleeman, *Complex networks orchestrate epithelial-mesenchymal transitions*. Nat Rev Mol Cell Biol, 2006. **7**(2): p. 131-42.
140. Thiery, J.P., et al., *Epithelial-mesenchymal transitions in development and disease*. Cell, 2009. **139**(5): p. 871-90.
141. Eastham, A.M., et al., *Epithelial-mesenchymal transition events during human embryonic stem cell differentiation*. Cancer Res, 2007. **67**(23): p. 11254-62.
142. Ullmann, U., et al., *Epithelial-mesenchymal transition process in human embryonic stem cells cultured in feeder-free conditions*. Mol Hum Reprod, 2007. **13**(1): p. 21-32.
143. Kalluri, R. and R.A. Weinberg, *The basics of epithelial-mesenchymal transition*. J Clin Invest, 2009. **119**(6): p. 1420-8.
144. Chapman, H.A., *Epithelial-mesenchymal interactions in pulmonary fibrosis*. Annu Rev Physiol, 2011. **73**: p. 413-35.
145. Schmidt, J.M., et al., *Stem-cell-like properties and epithelial plasticity arise as stable traits after transient Twist1 activation*. Cell Rep, 2015. **10**(2): p. 131-9.
146. Singh, M., et al., *EMT: Mechanisms and therapeutic implications*. Pharmacol Ther, 2018. **182**: p. 80-94.
147. Scheel, C. and R.A. Weinberg, *Cancer stem cells and epithelial-mesenchymal transition: concepts and molecular links*. Semin Cancer Biol, 2012. **22**(5-6): p. 396-403.
148. Brabletz, T., et al., *Opinion: migrating cancer stem cells - an integrated concept of malignant tumour progression*. Nat Rev Cancer, 2005. **5**(9): p. 744-9.
149. Perez-Moreno, M., C. Jamora, and E. Fuchs, *Sticky business: orchestrating cellular signals at adherens junctions*. Cell, 2003. **112**(4): p. 535-48.
150. Perez-Moreno, M. and E. Fuchs, *Catenins: keeping cells from getting their signals crossed*. Dev Cell, 2006. **11**(5): p. 601-12.
151. Gottardi, C.J., E. Wong, and B.M. Gumbiner, *E-cadherin suppresses cellular transformation by inhibiting beta-catenin signaling in an adhesion-independent manner*. J Cell Biol, 2001. **153**(5): p. 1049-60.
152. Kuphal, F. and J. Behrens, *E-cadherin modulates Wnt-dependent transcription in colorectal cancer cells but does not alter Wnt-independent gene expression in fibroblasts*. Exp Cell Res, 2006. **312**(4): p. 457-67.
153. Onder, T.T., et al., *Loss of E-cadherin promotes metastasis via multiple downstream transcriptional pathways*. Cancer Res, 2008. **68**(10): p. 3645-54.
154. Groden, J., et al., *Identification and characterization of the familial adenomatous polyposis coli gene*. Cell, 1991. **66**(3): p. 589-600.
155. Morris, J.P.t., S.C. Wang, and M. Hebrok, *KRAS, Hedgehog, Wnt and the twisted*

-
- developmental biology of pancreatic ductal adenocarcinoma*. Nat Rev Cancer, 2010. **10**(10): p. 683-95.
156. Al-Aynati, M.M., et al., *Epithelial-cadherin and beta-catenin expression changes in pancreatic intraepithelial neoplasia*. Clin Cancer Res, 2004. **10**(4): p. 1235-40.
157. Ilmer, M., et al., *RSPO2 Enhances Canonical Wnt Signaling to Confer Stemness-Associated Traits to Susceptible Pancreatic Cancer Cells*. Cancer Res, 2015. **75**(9): p. 1883-96.
158. Renz, B.W., et al., *Repurposing Established Compounds to Target Pancreatic Cancer Stem Cells (CSCs)*. Med Sci (Basel), 2017. **5**(2).
159. Nakamoto, M. and M. Hisaoka, *Clinicopathological Implications of Wingless/int1 (WNT) Signaling Pathway in Pancreatic Ductal Adenocarcinoma*. J UOEH, 2016. **38**(1): p. 1-8.
160. Mutlu, P., et al., *Determination of the relationship between doxorubicin resistance and Wnt signaling pathway in HeLa and K562 cell lines*. EXCLI J, 2018. **17**: p. 386-398.
161. Lustig, B., et al., *Negative feedback loop of Wnt signaling through upregulation of conductin/axin2 in colorectal and liver tumors*. Mol Cell Biol, 2002. **22**(4): p. 1184-93.
162. Jho, E.H., et al., *Wnt/beta-catenin/Tcf signaling induces the transcription of Axin2, a negative regulator of the signaling pathway*. Mol Cell Biol, 2002. **22**(4): p. 1172-83.
163. He, T.C., et al., *Identification of c-MYC as a target of the APC pathway*. Science, 1998. **281**(5382): p. 1509-12.
164. Yan, D., et al., *Elevated expression of axin2 and hnkd mRNA provides evidence that Wnt/beta -catenin signaling is activated in human colon tumors*. Proc Natl Acad Sci U S A, 2001. **98**(26): p. 14973-8.
165. Tetsu, O. and F. McCormick, *Beta-catenin regulates expression of cyclin D1 in colon carcinoma cells*. Nature, 1999. **398**(6726): p. 422-6.
166. Salic, A., et al., *Control of beta-catenin stability: reconstitution of the cytoplasmic steps of the wnt pathway in Xenopus egg extracts*. Mol Cell, 2000. **5**(3): p. 523-32.
167. Nusse, R., *WNT targets. Repression and activation*. Trends Genet, 1999. **15**(1): p. 1-3.
168. Walker, F., et al., *LGR5 is a negative regulator of tumorigenicity, antagonizes Wnt signalling and regulates cell adhesion in colorectal cancer cell lines*. PLoS One, 2011. **6**(7): p. e22733.
169. Fukuma, M., et al., *Leucine-rich repeat-containing G protein-coupled receptor 5 regulates epithelial cell phenotype and survival of hepatocellular carcinoma cells*. Exp Cell Res, 2013. **319**(3): p. 113-21.
170. Carmon, K.S., et al., *LGR5 receptor promotes cell-cell adhesion in stem cells and colon cancer cells via the IQGAP1-Rac1 pathway*. J Biol Chem, 2017. **292**(36): p. 14989-15001.
171. McDonald, S.A., et al., *Stem cells and solid cancers*. Virchows Arch, 2009. **455**(1): p. 1-13.
172. Bhagwandin, V.J. and J.W. Shay, *Pancreatic cancer stem cells: fact or fiction?* Biochim Biophys Acta, 2009. **1792**(4): p. 248-59.
173. Sergeant, G., et al., *Role of cancer stem cells in pancreatic ductal adenocarcinoma*. Nat Rev Clin Oncol, 2009. **6**(10): p. 580-6.
174. Barker, N. and H. Clevers, *Leucine-rich repeat-containing G-protein-coupled receptors as markers of adult stem cells*. Gastroenterology, 2010. **138**(5): p. 1681-96.
175. Koo, B.K. and H. Clevers, *Stem cells marked by the R-spondin receptor LGR5*.

-
- Gastroenterology, 2014. **147**(2): p. 289-302.
176. Rao, C.V. and A. Mohammed, *New insights into pancreatic cancer stem cells*. World J Stem Cells, 2015. **7**(3): p. 547-55.
177. Dorado, J., et al., *Pancreatic cancer stem cells: new insights and perspectives*. J Gastroenterol, 2011. **46**(8): p. 966-73.
178. Kasper, M., et al., *Wounding enhances epidermal tumorigenesis by recruiting hair follicle keratinocytes*. Proc Natl Acad Sci U S A, 2011. **108**(10): p. 4099-104.
179. Snippert, H.J., et al., *Lgr6 marks stem cells in the hair follicle that generate all cell lineages of the skin*. Science, 2010. **327**(5971): p. 1385-9.
180. Shah, A.N., et al., *Development and characterization of gemcitabine-resistant pancreatic tumor cells*. Ann Surg Oncol, 2007. **14**(12): p. 3629-37.
181. Jacquemet, G., H. Hamidi, and J. Ivaska, *Filopodia in cell adhesion, 3D migration and cancer cell invasion*. Curr Opin Cell Biol, 2015. **36**: p. 23-31.
182. Jung, D., et al., *The heparan sulfate mimetic PG545 interferes with Wnt/ β -catenin signaling and significantly suppresses pancreatic tumorigenesis alone and in combination with gemcitabine*. Oncotarget, 2015. **6**(7): p. 4992-5004.
183. Yamada, T., et al., *Transactivation of the multidrug resistance 1 gene by T-cell factor 4/ β -catenin complex in early colorectal carcinogenesis*. Cancer Res, 2000. **60**(17): p. 4761-6.
184. Deng, R., et al., *PKB/Akt promotes DSB repair in cancer cells through upregulating Mre11 expression following ionizing radiation*. Oncogene, 2011. **30**(8): p. 944-55.
185. Sjoblom, T., et al., *The consensus coding sequences of human breast and colorectal cancers*. Science, 2006. **314**(5797): p. 268-74.
186. Steffen, J.S., et al., *LGR4 and LGR6 are differentially expressed and of putative tumor biological significance in gastric carcinoma*. Virchows Arch, 2012. **461**(4): p. 355-65.

IV. Acknowledgment

I would like to thank my doctor father, Prof. Dr. Jens Werner, for giving me the opportunity to perform pancreatic cancer research at the Ludwig-Maximilians-University. It is of great importance to me to have such experience. I want to thank my supervisor Prof. Dr. Alexandr Bazhin sincerely for his continuous support. He always guided me whenever I was in difficult situations, both in life and research. He taught me what scientific logic is. Thanks to him for everything he has done for me. I would like to express my sincere gratitude to my scientific advisor Dr. Matthias Ilmer. His motivation encouraged me during all the time of the research and thesis writing. He explained me everything I didn't know and encouraged me to think deeply. He made me know what a researcher should do. He corrected the thesis with great patience. His insightful ideas, advice, and comments are important to my research life.

My sincere thanks go to PD Dr. Jan D'Haese and Dr. Bernhard W. Renz for their insightful comments. I would also like to thank Frau Karin Enderle and Frau Michaela Svihla for their technical support. They helped a lot during the experiments. I am grateful to Frau Dana Dacian for administrative support. I can always get help from her and learn something new about Germany from her. I would like to express my thanks to all my colleagues in Experimental Surgery Division in the Department of General, Visceral and Transplantation Surgery of the Ludwig-Maximilians-University. It was my great pleasure to be here.

Last but not least, I would like to thank my family and my friends, who encouraged me and supported me the whole time. Without their help, it would not have been possible to finish this research.